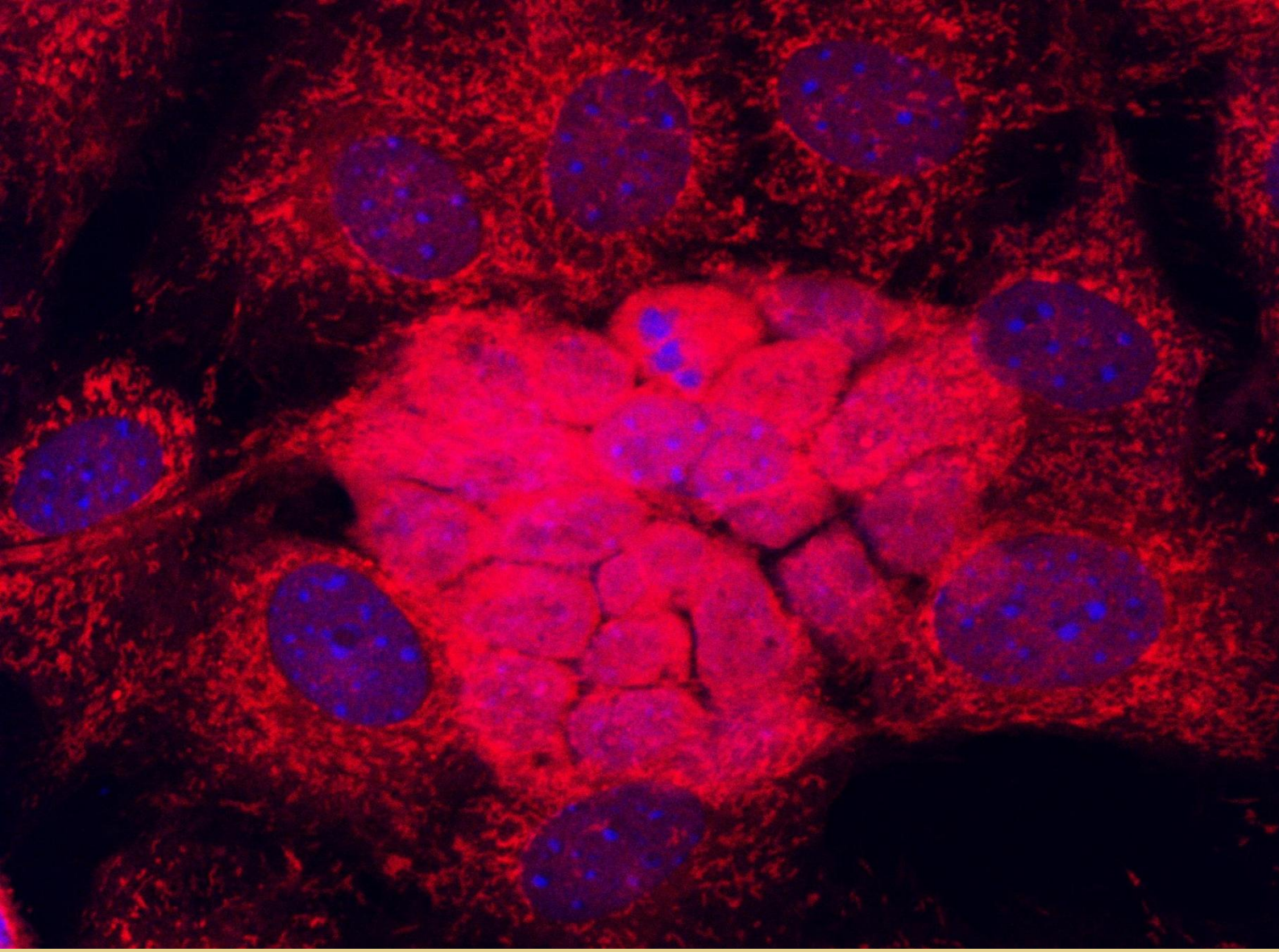

Sandro Lino Cardoso Pereira

A Metabolic Switch for Cell Differentiation

Doctoral Dissertation in Biology with specialization in Cell Biology, under the supervision of Professor João Ramalho-Santos and co-supervision of Professor Rui A.Carvalho and Paulo J. Oliveira, PhD, presented to the Department of Life Sciences, Faculty of Sciences and Technology of the University of Coimbra

February 2013

· U C ·

UNIVERSIDADE DE COIMBRA

A METABOLIC SWITCH FOR CELL DIFFERENTIATION

UNIVERSIDADE DE COIMBRA

Sandro Lino Cardoso Pereira
School of Sciences and Technology
University of Coimbra

Coimbra, February 2013

Cover:

The cover image depicts a colony of mouse embryonic stem cells differentiating on top of PA6 mouse stromal cell line. A coculture system promoting neuronal differentiation Red staining corresponds to mitochondria (MitoTracker Red) and blue (DAPI) to nuclei.

This work was conducted at the Center for Neurosciences and Cell Biology, Department of Life Sciences, University of Coimbra, Coimbra, Portugal, under the supervision of Professor João Ramalho-Santos and the co-supervision of Professor Rui A. Carvalho and Dr. Paulo J. Oliveira and in the Department of Medical Biochemistry & Biophysics Karolinska Institutet, Stockholm, Sweden under the guidance of Dr. Ernest Arenas.

The work included in this thesis was funded by a PhD scholarship (SFRH / BD / 37933 /2007) and research grants (POCI/SAU-OBS/55802/2004, PTDC/QUI/64358/2006, PTDC/EBB-EBI/101114/2008, PEst-C/SAU/LA0001/2011) from Fundação para Ciência e a Tecnologia co-funded by Compete/FEDER/National Funds.

Partilho a concretização desta tese com os **Meus**.

Pai e **Mãe** este é o meu mais sincero reconhecimento por todo o esforço e abnegação que tomaram na vossa vida para nos criarem. Obrigado por compreenderem e por acreditarem em mim. E sobretudo, obrigado por serem meus. **Mana**, desde sempre e uma vez mais estiveste ao meu lado.

Obrigado **Avó** pelas histórias que nos contavas e faziam borbulhar a minha imaginação.

Gisa…pelo silêncio inflexível das horas…pelas ondas que hão-de vir e o sol que há-de ser…
Obrigado por continuares ao meu lado

Agradecimentos:

Agradeço à Fundação para a Ciência e a Tecnologia a bolsa de doutoramento que me foi atribuída (SFRH / BD / 37933 / 2007) e que me permitiu progredir no meu crescimento pessoal e científico. Agradeço de igual modo pelos fundos atribuídos ao nosso laboratório que asseguraram a prossecução do trabalho agora apresentado.

Aproximando-se o momento de concluir esta longa etapa, as minhas primeiras palavras de agradecimento terão necessariamente que ser dirigidas aos meus orientadores, tanto pela amizade, como pelo apoio e orientação.

Ao Professor João Ramalho-Santos, meu orientador principal: sinto-me afortunado por colaborar consigo. Devo agradecer pela liberdade para errar e experimentar, porque o conhecimento cresce e é estimulado pelos equívocos e pelo desconhecido. Obrigado por me ter dado essa liberdade para aprender e igualmente por não ter concordado com tudo o que sugeri. Um agradecimento sentido pelo facto de me ter dado as condições para poder prosseguir nos nossos vários projectos.

Agradeço ao Professor Rui de Albuquerque Carvalho a sinceridade e a contínua disponibilidade para me apoiar sempre e nos diversos projectos/ideias que foram surgindo. Ainda pela sua grande generosidade ao partilhar o seu conhecimento, tanto no laboratório, durante as muitas horas passadas a discutir resultados, como a ajudar-me a perceber um pouco mais sobre o mundo do metabolismo e da ressonância magnética nuclear. Muito obrigado. Devo-lhe o gosto pelo metabolismo.

Ao Doutor Paulo Oliveira, o principal responsável pela minha vinda para Coimbra e pelo facto de que um pequeno treino de laboratório se ter materializado neste percurso de 6 anos, estou inefavelmente grato. É uma honra ter tido a oportunidade de ingressar no seu grupo desde os primeiros tempos e ter testemunhado o seu crescimento coeso. Foi no seu grupo que realmente comecei a "entrar" na investigação. Agradeço por me ter ajudado a criar as condições que possibilitaram o meu projecto de doutoramento sem as quais não estaria com toda a certeza hoje nesta posição. Agradeço, ainda, pela sua permanente e incansável disponibilidade para me apoiar.

I am grateful to my external advisor, Doctor Ernest Arenas, for receiving me in his lab and giving me the possibility to enter in the stem cell research. I thank you for providing me with helpful insights during the first stage of my work in Sweden and with an inspiring environment to start my research.

Quero agradecer ao Doutor Mário Grãos por toda a amizade e por me ter integrado no seu laboratório e grupo. Obrigado pelo contínuo apoio e permanentes discussões e sugestões sempre muito pertinentes e substanciais, que condicionaram positivamente tanto o meu trabalho como o meu crescimento. Obrigado ainda pela sua simplicidade e maneira de ser afável que ajudaram, indelevelmente, nos momentos menos bons da rotina laboratorial, não esquecendo ainda as conversas clubísticas que aqueciam os dias, um período que deu cor ao meu doutoramento.

Agradeço ao Biocant, na pessoa do Professor Carlos Faro, por me ter acolhido sempre da melhor maneira e com máxima hospitalidade. Não vou enumerar nomes porque seria impossível nomear todas as pessoas que desempenharam um papel importante na minha vida diária. Esses meus colegas e amigos especialmente das Unidades de Biologia Celular, da Unidade de Proteómica e da Unidade de Engenharia de Tecidos, sabem que foram e continuam a ser preponderantes para mim. A todos os colaboradores do Biocant que de um modo quase latente com a sua dedicação fazem a máquina funcionar, o meu muito obrigado.

Agradeço à Doutora Evguenia Bekman, a quem reconheço as maiores qualidades e rigor científico, e que talvez sem que tenha plena noção, foi muito importante na resolução de algumas questões durante este período, sempre com a sua enorme simpatia.

Ao Professor António Moreno e à Doutora Sancha, por serem a essência da zoologia e fazerem aparecer dos seus chapéus mágicos todos os recursos mais inusitados de que fui necessitando.

Agradeço aos meus colegas e amigos dos grupos da Zoologia e do IBILI. A vossa amizade e suporte não são esquecidas. To my lab mates at the Karolinska for receiving and teaching me the stem cell basics.

Agradeço ao Gonçalo a amizade mas também o rigor e a objectividade que sustentam o seu sólido conhecimento. Por ter sido um dos pilares edificantes deste meu período de aprendizagem, a minha total gratidão.

Agradeço à minha irmã de laboratório, Susana. Admiro a sua frontalidade e coragem para enfrentar os seus receios como uma "mulher do norte"…sempre com um sorriso que também transporta obrigado por estares presente e por comungares das minhas tristezas e das minhas alegrias e me motivares sempre mais.

Agradeço às "minhas pessoas" de fora do círculo do laboratório que me fizeram acreditar e sorrir perante os obstáculos. Aqueles que apesar da maior ou menor distância sempre estiveram perto. Aos meus manos Rui e à Bea por vos ter sempre presentes. À Joaninha por trazeres contigo os serenos passeios na avenida. Obrigado pela tua paz. Anne for your friendship and always making me laugh and miss my helmet rrrrrr, Andreas dear brother the wine is served

and the guitar is tuned… Catarina por toda a amizade e apoio incondicional e obrigado por me fazeres sempre ver o outro lado. Muito obrigado.

Agradeço aos meus familiares, avós Albertino e Alice. Aos meus primos e tios. Agradeço ao meu irmão Paulo e aos meus pequeninos sobrinhos Gui e Carol, por me fazerem acreditar que os milagres existem.

Resumo:

A aplicação de células estaminais tanto num contexto clínico como em modelos toxicológicos é perspectivada como potencial ferramenta para o desenvolvimento de terapias dirigidas a uma grande variedade de estados patológicos. Consequentemente, um significativo corpo de trabalho tem-se avolumado na tentativa de aprofundar o conhecimento que possa sustentar a exploração deste recurso biológico. Este crescente esforço de investigação tem resultado numa melhor compreensão de mecanismos que actuando a um nível preponderantemente genético, epigenético e transcricional sustentam as características únicas das células estaminais. Contudo, a fisiologia destas células não poderá ser totalmente compreendida se não se atender à dinâmica metabólica que a acompanha. Neste âmbito alguns trabalhos demonstram que o metabolismo terá de ser correctamente regulado tanto no processo de autorenovação e proliferação como durante o processo de diferenciação e especialização celular, de modo a adequar-se à função e manutenção da própria célula. Aqui reside um ponto de convergência entre as células estaminais pluripotentes num estado indiferenciado e as células fundadoras de tumores, edificando no seu conjunto um fenótipo metabólico característico de células com grande capacidade proliferativa. Apesar de relativamente pouco explorado, estudos recentes demonstram que o metabolismo concorre para a própria

identidade das células estaminais, estabelecendo uma relação bidireccional de regulação com os processos genéticos.

Neste âmbito a presente dissertação trata o envolvimento do metabolismo no processo de diferenciação celular. Numa primeira instância visamos a caracterização da reprogramação metabólica inerente ao processo de diferenciação de um modelo mioblástico de rato, amplamente empregue em estudos toxicológicos, a linha celular H9c2. Estes mioblastos indiferenciados, caracterizados por uma grande taxa proliferativa, foram induzidos a diferenciar em células semelhantes a cardiomiócitos ou células musculares esqueléticas com menor proliferação. O estudo comparativo do perfil metabólico destas três populações baseado em ressonância magnética nuclear demonstrou que o processo de especificação celular é acompanhado por uma alteração coesa do metabolismo visando um aumento de eficiência dos processos energéticos. Assim, verificamos que o estado de indiferenciação celular corresponde a uma situação fisiológica mais dependente da via glicolítica e as populações diferenciadas apresentam uma actividade mitocondrial mais elevada, nomeadamente denotando um maior consumo de oxigénio. Será importante referir ainda que verificamos um maior acoplamento entre a via glicolítica e a actividade mitocondrial nas células diferenciadas e uma maior incidência de actividade anaplerótica no ciclo de Krebs nas células indiferenciadas.

Na segunda parte deste trabalho abordamos os efeitos da modelação da actividade da mitocôndria durante a diferenciação neuronal de células

estaminais embrionárias (pluripotentes) de ratinho. Demonstramos que a inibição da actividade mitocondrial subsequente à aplicação de um inibidor específico para o complexo III da cadeia respiratória (Antimicina A) traduz-se numa menor eficiência de diferenciação e curiosamente no aumento da percentagem de colónias positivas para marcadores de pluripotência, mesmo em condições indutoras à diferenciação celular. Esta inibição afectou de modo distinto diferentes populações correspondentes a diferentes fases de maturação celular, sendo que ao nível das células estaminais embrionárias não detectamos um incremento de apoptose, mas discernimos alterações no seu ciclo celular com consequente incidência nas dinâmicas de proliferação. Por fim, demonstramos que a aplicação de Antimicina A em células estaminais embrionárias leva a uma estabilização em condições de normoxia do factor induzido por hipoxia HIF-1α, sobejamente reconhecido como indutor de metabolismo glicolítico e que poderá ser um dos factores a contribuir para os efeitos de manutenção de pluripotência nas células estaminais embrionárias.

No seu conjunto os resultados desta dissertação vêm comprovar que o metabolismo é um factor preponderante durante o processo de diferenciação celular. A realização do potencial terapêutico das células estaminais esta intimamente dependente da nossa capacidade de controlarmos as suas características e processos celulares como pluripotência, autorenovação e diferenciação específica. Os nossos resultados contribuem ainda para a compreensão do metabolismo como substrato plausível para modelação dessas

características, sendo portanto um factor que acreditamos instrumental para a eficaz concretização dos potenciais benefícios das células estaminais.

Palavras-chave: metabolismo, diferenciação celular, células estaminais embrionárias, mitocôndria, antimicina A, efeito Warburg.

Abstract:

The potential application of stem cells as practical *in vitro* models for toxicological and pharmacological studies, or their prospective use in regenerative medicine converts them in a powerful instrument for the development of efficient therapies directed to a large array of pathologies. Responding to the active demand to obtain the necessary knowledge to explore this unique biological resource, a large body of literature has accumulated. This has resulted in a better understanding of some of the mechanisms that regulate stem cell properties, acting predominantly at the genetic, epigenetic or transcriptional levels. However, an often-disregarded element without which the physiology of stem cells cannot be truly comprehended is the cell metabolism. In this context relatively few works show that in order to support cell function metabolism must be appropriately regulated during different cell processes, such as stem cell self-renewal, proliferation and differentiation. This metabolic adaptation is a meeting point between stem and cancer founding cells, as these present a common metabolic phenotype characteristic of actively proliferating cells. Albeit not widely explored some evidences suggest that metabolism is fundamental for stem cell identity, establishing a bidirectional regulatory dialogue with the genetic processes.

The topic of the present dissertation is therefore the study of metabolic involvement in cell differentiation in two distinct biological models. We hypothesize that metabolic remodeling must accompany the process of cell differentiation.

We first focused on the characterization of metabolic remodeling inherent to the differentiation of a rat myoblast cell line profusely used as a model in toxicological studies, the H9c2 cell line. The parental undifferentiated myoblasts, which have a characteristically high proliferation rate, were induced to differentiate towards skeletal muscle-like or cardiomyocytes-like cells, with restricted proliferation. The comparative study of the metabolic profiles from these three distinct populations was based on nuclear magnetic resonance and convincingly confirmed that a marked metabolic shift accompanied the cell specification process. The differentiating cells employed a more energy-efficient metabolism associated with higher mitochondrial oxygen consumption whereas the undifferentiated cells present a higher reliance on glycolysis. Importantly, we have demonstrated that the parental cells have relatively increased anaplerosis in the Krebs cycle and the differentiated cells present a better coupling between glycolysis and the mitochondrial oxidative machinery.

In the second part of the thesis, our approach was to evaluate the effects of an active metabolic modulation during neuronal differentiation of mouse embryonic stem cells (mESC). Here, we demonstrated that the inhibition of the normal mitochondrial electron transport chain activity, particularly due to the

application of Antimycin A (AA; a specific inhibitor of mitochondrial complex III), translates into a lower differentiation efficiency. Remarkably, AA treatment was able to maintain pluripotency marker expression on colonies grown for prolonged periods under differentiation-inducing conditions. AA affected distinct population of cells with different maturation states differently. Specifically for mESC, AA did not cause apoptosis but did alter the cell cycle with implications in terms of the proliferation rates. Lastly, we demonstrate that AA treatment stabilized the hypoxia inducible factor HIF-1α in mESC grown in normoxic conditions. HIF-1α is acknowledged to work as an inducer of a metabolic shift favoring increased glycolysis, namely in cancer cells, thus contributing to the Warburg effect, and might be an influential factor for pluripotency maintenance acting downstream of AA in our model.

In sum the results presented in this relevant scientific thesis add substance to the notion that a metabolic remodeling is a central element during cell differentiation. The concretization of the stem cell therapeutic potential is intimately dependent on our ability to tame stem cells and efficiently control their properties such as pluripotency, self-renewal and specific differentiation. Our results further contribute to the understanding of metabolism as a credible substrate for modulating stem cell properties, and therefore identify metabolism as an instrumental factor for the attainment of the stem cells promise.

Keywords: metabolism, cell differentiation, embryonic stem cells, mitochondria antimycin A, Warburg effect.

List of Publications Included in the Thesis:

Pereira, S. L., Ramalho-Santos, J., Branco, A. F., Sardão, V. A., Oliveira, P. J., & Carvalho, R. A. (2011). **Metabolic remodeling during H9c2 myoblast differentiation: Relevance for *in vitro* toxicity studies**. Cardiovascular toxicology, 11(2), 180-190.

Sandro L. Pereira, Mário Grãos, Sandra I. Anjo, Rui A. Carvalho, Paulo J. Oliveira, Ernest Arenas, João Ramalho-Santos (2013) Modulation of Mitochondrial Activity by Antimycin A Blocks Neuronal Differentiation and Maintains Embryonic Stem Cell Pluripotency. (submitted)

Index

List of Abbreviations

Δp	proton motive force
$\Delta\psi$	mitochondrial transmembrane electric potential
AA	antimycin A
ACL	ATP-citrate lyase
ADP	adenine diphosphate
AMP	adenine monophosphate
ATP	adenine triphosphate
BDNF	brain-derived neurotrophic factor
bFGF	basic fibroblast growth factor
BMP4	bone morphogenetic protein 4
BrdU	bromodeoxyuridine
CCCP	Carbonyl cyanide m-chlorophenylhydrazone
ChIP	chromatin immunoprecipitation
CM	cristae membrane
DA	dopaminergic neurons
EB	embryoid body

EC	embryonal carcinoma
EGC	embryonic germ cells
ELISA	enzyme-linked immunosorbent assay
EpiSC	epiblast stem cell
ESC	embryonic stem cell
ETC	electron transport chain
FAD	flavin adenine dinucleotide
FAO	fatty acid oxidation
FCCP	carbonyl cyanide 4-(trifluoromethoxy)phenylhydrazone
FGF8	fibroblast growth factor 8
FMN	flavin mononucleotide
GAPDH	glyceraldehyde-3-phosphate dehydrogenase
GDN	glial cell-derived neurotrophic factor
GSH	glutathione reduced form
GSK3	glycogen synthase kinase 3
GSSH	glutathione oxidized form
HAT	histone acetyltransferases
HDAC	histone deacetylase
hESC	human embryonic stem cell

HIF	hypoxia inducible factor
HIF-1α	hypoxia inducible factor 1 alpha
HRP	horseradish peroxidase
IBM	inner boundary membrane
ICC	immunocytochemistry
IDH	isocitrate dehydrogenase
ICM	inner cell mass
IL6	interleukin 6
IMM	internal mitochondrial membrane
iPSC	induced pluripotent stem cell
LDH	lactate dehydrogenase
LIF	leukemia inhibitor factor
mESC	mouse embryonic stem cell
MF-20	cardiac myosin heavy chain
mitoKATP	ATP sensitive potassium channels
MLC2v	cardiac myosin light chain
MMP	mitochondrial membrane potential
MnSOD	manganese superoxide dismutase
mtDNA	mitochondrial DNA

NAD^+	nicotinamide adenine dinucleotide oxidized form
NADH	nicotinamide adenine dinucleotide reduced form
NADPH	nicotinamide adenine dinucleotide phosphate reduced form
NMR	nuclear magnetic resonance
Oct4	octamer 4
OMM	outer mitochondrial membrane
OXPHOS	oxidative phosphorylation
PCA	perchloric acid
PDK	pyruvate dehydrogenase kinase
PGC	primordial germ cell
PHD	prolyl hydroxylase
PHGDH	phosphoglycerate dehydrogenase
PI	propidium iodide
PI3K	phosphoinositide 3-kinase
PPP	pentose phosphate pathway
PSC	pluripotent stem cell
PTM	Post-translational modification
RA	retinoic acid
RET	reverse electron transfer

ROS	reactive oxygen species
SAM	S-adenosylmethionine
Shh	sonic hedgehog
SOD	superoxide dismutase
Sox2	sex determining region Y box 2
SRB	sulforhodamine B
SSEA	stage specific embryonic antigen
STAT3	signal transducer and activation of transcription 3
TCA cycle	tricarboxylic acid cycle
TH	tyrosine hydroxylase
TUJ1	β III Tubulin
UCP	uncoupler protein
UQ	ubiquinone
$UQ^{\cdot-}$	semiubiquinone
UQH_2	ubiquinol
VDAC	voltage-dependent anion channel

Chapter 1

General introduction

1.1) Stem cells Biology

Before any profound considerations about stem cell biology, a clarification of some key concepts regarding cell potentiality is due. A stem cell is characterized essentially by self-renewal, the replicative capacity to produce new stem cells, and the ability to differentiate into a number of lineages. It is the extension of this differentiation capacity that structures the hierarchical classification of stem cells, even though precise and sharp distinctive classifications are often error prone as biological concepts usually form a continuum.

The mammalian development process is believed to be unidirectional entailing a progressive restriction in development capacity. It starts with the unicellular zygote, considered to be an archetype of *totipotency* (as it originates the embryo proper and the extra-embryonic tissues, with the exception of the maternal contribution to the placenta), and culminates with the generation of hundreds (ca. 220) of distinct differentiated cell types in adult organisms (*1*). However, undifferentiated stem cell populations are still present in most tissues. Totipotency is rapidly lost as the zygote undergoes cleavage and morula formation. The following blastocyst stage is characterized by the presence of two distinct cell types, the outer throphoectoderm cells (originating the outer layers of the placenta) and the inner cell mass (ICM) that contains the cells that will give rise to the embryo (Fig. 1.1). Because they have the ability to form any of the cell

types from the adult organism ICM cells are called *pluripotent*. Embryonic stem cells are the *in vitro* counterparts of ICM cells and thus are also pluripotent. Progression of development, with subsequent implantation of the embryo in the uterine endometrium, will involve the delamination of the blastocoel-contacting layer of cells from the ICM. This will allow the distinction of 2 groups of cells, the epiblast potentially giving rise to the embryo proper and comprising the bulk of ICM and the delaminating layer named hypoblast or primitive extra-embryonic endoderm cells with a differentiation capacity that is restricted to the extra-embryonic tissues such as the lining of the primary yolk-sac (*2*–*4*). Epiblast cells are still considered pluripotent, but this differentiation ability will be narrowed with further development as these cells differentiate into each one of the primordial germ layers (endoderm, mesoderm and ectoderm) and some extra-embryonic structures (*5*). Cells composing these embryo layers are *multipotent* and their developmental capacity is thought to be constrained to cells from a single lineage. Adult stem cells such as hematopoietic and neural stem cells are included in this group. Further development will progressively result in the differentiation of progenitors and more differentiated precursors that will ultimately lead to terminally differentiated cells. Throughout development, each one of these hierarchical cell populations is thought to have a characteristic epigenetic pattern that supports their differentiation potential (*1*). Nevertheless, this epigenetic-exerted control can be experimentally challenged by nuclear reprogramming that potentially, but not necessarily, results in a transgression in the route of normal development by yielding cells with a broader differentiation

capacity than the parental cells (e.g. Induced pluripotent cells), or even by giving rise to differentiated cells belonging to a completely distinct lineage.

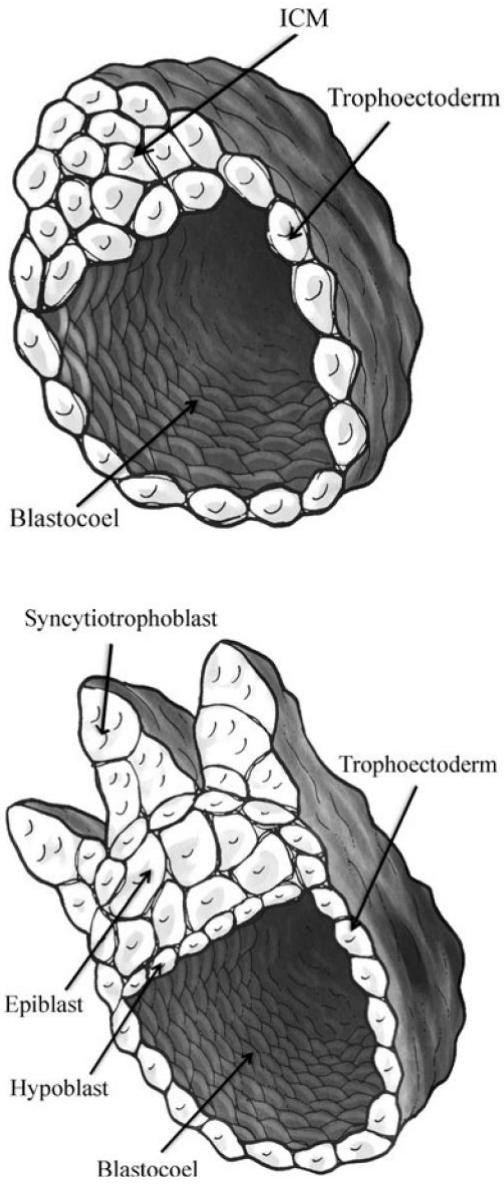

Fig. 1.1 - Drawing representing a mammalian embryo at the early (upper) and bilaminar (lower) blastocyst stages. ICM: Inner cell mass. Adapted from (2)

1.2) Stem cells –Recalling their origins

The growing interest that stem cells evoked in the general public over the last one and half decades, boosted by the report of the first isolation of human embryonic stem cells in 1998 (*6*) and probably originating from their *quasi* fictional potential applications in regenerative medicine, does not often pay adequate homage to the previous efforts that paved the way for stem cells research. Indeed, stem cells studies rooted from the pioneer work developed on mouse teratocarcinomas and teratomas started in the middle of the last century.

The establishment in 1954 by Stevens and Little (*7*), of an inbred strain of mice with a high prevalence of testicular teratocarcinomas was instrumental to perceive that these tumors could be transplanted repeatedly and in their genesis were primordial germ cells in the fetal testis. Teratocarcinomas are characterized by the presence of chaotic masses of differentiated cells belonging to the different germ cell layers. Of utmost significance was the demonstration by Kleinsmith and Pierce, that a single cell derived from a tumor was able to regenerate the entirety of the tumoral mass (comprising all the distinct phenotypes observed in the original tumor) when injected intraperitoneally(*8*). These findings clearly proved the existence of pluripotent tumor stem cells that were later to be called embryonal carcinoma cells (EC). Subsequent technical developments and further studies revealed evident similarities between embryonal carcinoma cell-derived tumors and normal embryonic development. Of particular importance was the finding that *in vitro* EC differentiation yielded embryoid bodies (EB) that would,

in initially steps, follow normal development pathways. A paradigm shift was set as cells formerly regarded as malignant were shown to be essentially embryonic cells out of their biological context. Moreover, when injected into the mouse blastocoel EC have been shown to contribute, albeit modestly, to chimeric mice. However no contribution to the germline was consistently seen, and most reports refer that chimeras would develop tumors (*3*, *9*).

The invaluable background knowledge and the technologies gained studying EC cells formed the basis for future stem cell ventures. Indeed the attempt to derive embryonic cells similar to EC but directly isolated from the embryo (without an intermediate tumor step) and possessing germline competence in chimeras, resulted in the isolation of mouse embryonic stem cells (mESC), in 1981 (*10*, *11*).

Despite the pre-existing technical knowledge that would enable the isolation of human embryonic stem cells (hECS), the first report of their derivation only occurred in 1998 (*6*), most probably hindered by constraints in obtaining suitable human material due to the fundamental moral and ethical dilemma underlying the use of human embryos. In 2006, however, a new door was opened thanks to a new pluripotent player, the induced pluripotent stem cell (iPSC) (*12*). These cells resulted from the direct reprogramming of adult differentiated cells to a pluripotent state comparable to ESC, relying on ectopic transcription factors, but without the inherent ethical concerns or material limitations. iPSC could also conceivable serve as a tool for possible autologous regenerative therapies or applications, thus eliminating histocompatibility issues.

And the journey for a deeper understanding of stem cell biology, pluripotency regulation and directed specification, the *sine qua non* knowledge needed to fulfill stem cell promises, is just in the beginning.

1.3) Pluripotency and Pluripotent Stem Cells

In this review we will mainly focus our attention on the pluripotent stem cells (PSC), their different types and characteristics. As mentioned in section (1.1) pluripotency can be described as the ability of the cell to generate progeny from the three primordial germ layers, endoderm, mesoderm and ectoderm, which is to say that pluripotent cells are potentially capable of originating any of the cells present in the embryonic and adult organism (*13*). This functional pluripotency is intimately supported by a set of molecular factors underlying the properties of pluripotent cells (*5*).

1.3.1) Pluripotent Stem Cells

Pluripotent stem cells have been isolated at different stages of the development, and constitute four discernible groups: embryonal carcinoma stem cells (EC), embryonic germ cells (EGC), embryonic stem cells (ESC) and induced pluripotent stem cells (iPSC).

Embryonal carcinoma stem cells were the first PSC population to be derived and characterized. As mentioned in section 1.1 they are the stem cells from primordial germ cell-induced teratocarcinomas, and were of extreme usefulness to set the basic conditions for future isolation of the remaining pluripotent populations. However with the advent of embryonic stem cells and maybe due to

limitations in their pluripotency, with most studies revealing no germline contribution in chimeras and some EC lines showing lineage-restricted differentiation, the interest in the application of EC as a pluripotent model decreased drastically(*3*, *9*, *14*).

Embryonic germ cells are directly derived from the *in vivo* primordial germ cells (PGC), the stem cells that give rise to gametes. Even though PGC are unipotent cells (their differentiation is restricted to either sperm or oocytes) when isolated and cultured in the presence of specified factors they yield the pluripotent EGC, in a process thought to involve nuclear reprograming (*15*). EGC do present normal and stable karyotypes and mouse EGC generate chimeras with efficient transmission to the germ line (*2*).

Embryonic stem cells were firstly derived from the pre-implantation mouse blastocyst in 1981, by two independent groups, as stated previously (*10*, *11*). Contrary to their *in vivo* analogues (ICM cells) that persist only transiently in the embryo, the explanted ESC are intrinsically immortal, with robust self-renewal partially grounded in their high telomerase activity and abbreviated cell cycle. ESCs have a high nucleus/cytoplasm volume ratio in accordance with their epigenetic status establishing extensive transcription-permissive euchromatin regions. ESCs are the paradigm for pluripotency and besides their putative applications for *in vitro* toxicology or regenerative medicine, these cells prove to

be a unique tool for addressing embryonic development. Most particularly, their stable karyotype and germ line transmission originating new viable organisms, empowered transgenesis creating a route to genetic manipulation from "culture to creature"(*3*). Besides sharing several of the same properties, mouse and hESC do present some dissimilarities. Morphologically mESC grow as tree-dimension dome-shaped colonies (Fig. 1.2) while hESC normally proliferate as thin flat colonies. Female mESC lines present a characteristic activation of both X chromosomes (XaXa), a process that resembles the *in vivo* X activation which occurs transiently, and restricted to the pluripotent lineage in the pre-implantation embryo (*16*). On the contrary, the majority of hESC lines invariably display complete or partial inactivation of one of the X chromossomes (XaXi) (*17*). Most strikingly, mESC and hESC resort to different extrinsic factors to maintain their pluripotency in feeder free cultures (Fig. 1.3). mESC require the presence of leukemia inhibitor factor (LIF) an IL6 family member cytokine and bone morphogenetic protein 4 (BMP4). LIF (which is also secreted by the trophoectoderm *in vivo*) signals through the heterodimerization of its receptor LIFR and gp130. The intracellular domain of gp130 will activate a recruited JAK (janus activated-kinase) protein that subsequently activates/phosphorylates Stat3 (signal transducer and activator of transcription 3). Stat3 is a transcription factor that upon activation will translocate to the nucleus and regulate the expression of genes interacting with the pluripotency transcription factor network. A second LIF signaling pathway, involves the PI3K (phosphoinositide 3-kinase) activation by JAK, what results in the downstream activation of AKT and consequent

inactivation of glycogen synthase-kinase 3 (GSK3) ultimately leading to elevated levels of c-myc and Nanog (*18*). BMP4 (normally present in serum) exerts its pro-pluripotency action by inhibiting pro-differentiation signaling pathways either by activating Id (inhibitors of differentiation) gene expression through smad proteins or by blocking p38 MAP-kinase (*19*). These same factors LIF and BMP4 have distinct effect on hESC. While the former is incapable of supporting hES pluripotency, the later actively induces trophectodermal differentiation (*20*). Instead, hESC is believed to rely on a combination of Activin/Nodal and basic fibroblast growth factor bFGF (or FGF2). Activin/Nodal signaling acts through Smad2/3 activation. And Activin and Nodal belong to the same protein family of BMP, the transforming growth factor β superfamily. Parallel to BMP Activin/Nodal signaling involves the activation of Smad proteins, in this case Smad 2/3, which directly regulate Nanog. Despite not being completely unraveled the mechanism of bFGF seems to simultaneously involve direct and indirect mechanisms. Firstly, FGF2 acts through activation of FGF receptors (FGFRs), stimulating the mitogen-activated protein kinase (MAPK) pathway and secondly bFGF has been shown to act on feeder cells elevating the secretion of activin by those cells (*21*). An extra element emerging as crucial for hESC self-renewal is PI3K, the action of which is partially justified by inhibition of GSK3 (*19*).

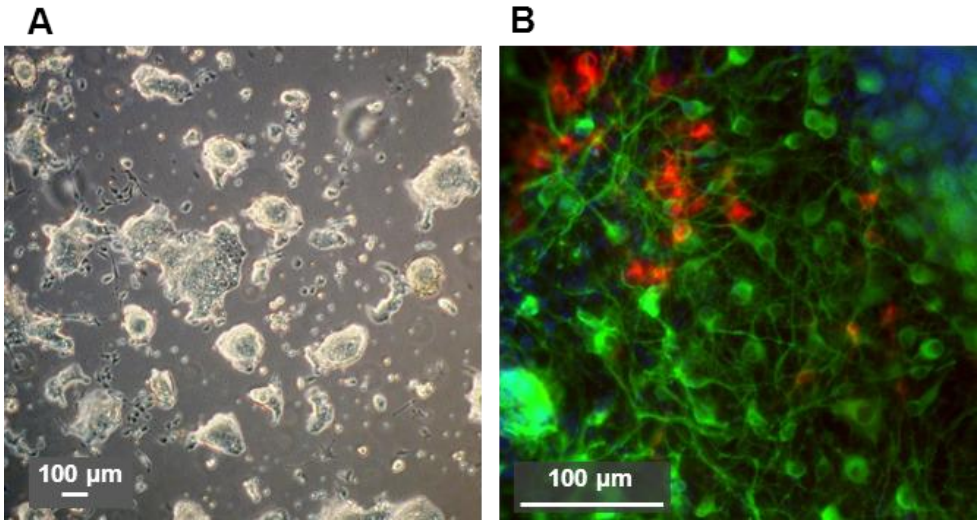

Fig. 1.2 – Microscopy images of undifferentiated and differentiated cells. (A) Typical morphology of mouse embryonic stem cells (R1 cell line) growing in dome-shaped 3D colonies. (B) Epifluorescence microscopy images of neurons differentiated for 14 days from R1 mouse embryonic stem cells. Green: Tuj1 (neurons), Red: TH (dopaminergic neurons), Blue: DAPI (nuclei).

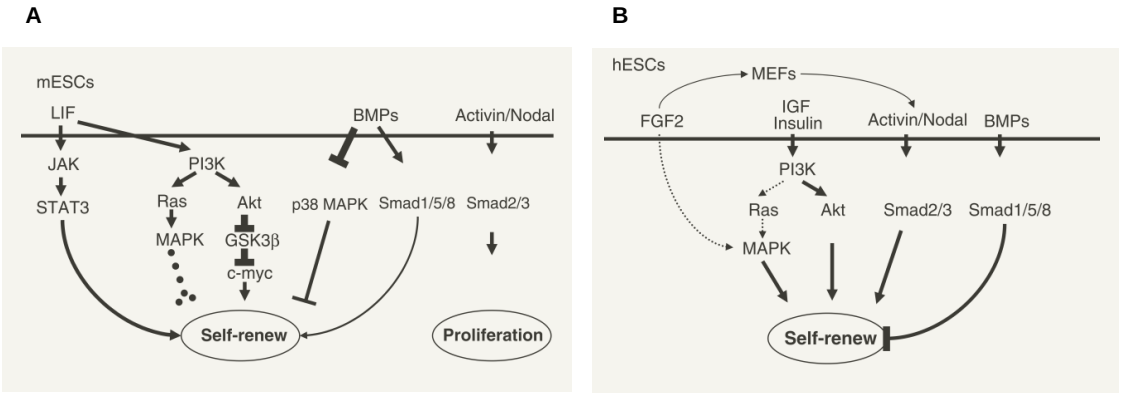

Fig. 1.3 – Schematic representation of the key signaling pathways required for maintaining pluripotency of (A) mESCs and (B) hESCs (see text for detail). (A) LIF signaling activates JAK–STAT3 to induce target genes essential for pluripotency, such as c-myc, which is also regulated negatively by glycogen synthase kinase-3 (GSK3)β via inhibitory phosphorylation. LIF also induces MAP kinase activation, which antagonizes self-renewal. BMP signals potentially function in two ways: (i) activation of Smad1/5/8-Id gene and (ii) suppression of p38 MAP kinase. Activin A has been shown to contribute mESCs proliferation but not pluripotency. (B) Fgf2 is an essential factor for hESCs self-renewal and functions in part by inducing Activin secretion from MEFs. Activin/Nodal signaling is essential to support hESCs self-renewal via activation of Smad2/3, resulting in upregulation of Nanog and Oct3/4 transcription. In contrast to mESCs, BMP promotes hESCs differentiation toward trophectoderm. PI3K–Akt pathway is also essential for hESC self-renewal although down-stream effectors and targets have not been defined. BMP: bone morphogenetic protein; Fgf: fibroblast growth factor; LIF: leukemia inhibitory factor; MEFs, mouse embryonic fibroblasts. Adapted from (*19*)**.**

These differences between mouse and hESC nurtured the hypothesis that both cell types would represent different stages of embryonic development. In 2007 the explant of epiblast cells from post-implantation mouse embryos resulted in the successful isolation of epiblast stem cells (**EpiSC**) (*22*). Recent experiments were also able to isolate EpiSC from pre-implantation mouse embryos. Mouse EpiSC, do share some pluripotent traits with mESC as the shared expression of

the pluripotency core transcriptional factors (Oct4, Sox2 and Nanog), however other factors are not similarly expressed in both cells and their epigenetic pattern is dissimilar. Conspicuously, mouse EpiSC rely on the same extrinsic factors used by hESC and human induced pluripotent stem cells (see below) to maintain pluripotency in culture such as Activin/Nodal and bFGF (*2*, *16*, *23*). Mouse EpiSC display X chromosome inactivation (as hESC) and despite giving rise to distinct cell lineages upon differentiation and being teratoma competent, they do not possess the ability of originating high-grade chimeras as mESC, the definitive functional criterion for ESC identity. As the contribution to blastocyst chimeras evaluation cannot be applied in humans, some concerns regarding the true pluripotency of hESC were therefore raised. Moreover it is now accepted that PSC may exist as two distinct, stable pluripotent states: *naïve* and *primed* (*16*). mESC are considered to be the standard of *naïve* pluripotency while mouse EpiSC and hESC represent orthologues of a primed pluripotent stem cells. Interest is now focused on the possible derivation of truly *naïve* pluripotent human stem cells.

Induced pluripotent stem cells, similarly to EGC, are originated from a cell with a narrower developmental capacity. But in this case nuclear reprogramming is induced intentionally through the forced expression of genes or exposure to certain proteins. Underlying the cell identity shift is the remodeling of the original epigenetic pattern resultant from the developmental restrictions imposed

during the differentiation process. This epigenetic barrier has to be overcome in order for the cell to re-adopt a pluripotent phenotype (*1*). The basis for this artificially-induced nuclear reprograming came from studies trying to reprogram a mature cell nucleus by changing its environment, as seen in somatic cell nuclear transfer or cell fusion strategies (*5*). The original report of iPSC derivation identified a combination of 4 genes (Oct4, Sox2, c-Myc and Klf4) that upon introduction in mouse fibroblasts could transform them into ESC-like cells (*12*). Follow-up studies have since used distinct factors and delivery methods (*24*, *25*). iPSC is an exceptional tool for the derivation of disease-specific stem cells from affected patients, with which molecular etiology and prospective treatments can be identified. These cells are also of great significance for furthering the knowledge in pluripotency regulatory mechanisms, allowing for the study of the factors that endow a differentiated somatic cell with PSC properties. However the epigenetic status of IPSC in relation to ESC has also been the subject of some discussion.

1.3.2) Evaluation of Functional Pluripotency

Functional pluripotency can be demonstrated by different approaches: 1) *in vitro* directed or spontaneous differentiation, namely by the formation of EB and identification of cells from the 3 germ layers; 2) injection of cells into immune-compromised mice that can lead to the formation of teratomas; 3) proof that cells can functionally replace all cell types in the developing organism (the true gold

standard for pluripotency), which can be attained by producing germ line competent chimeras or by tetraploid complementation generation of a new organism. The referred assays can only be completely performed for non-human cells; due to logical ethical concerns chimera formation and tetraploid complementation is not possible in humans. Therefore assessment of pluripotency in human pluripotent stem cells must be based in less stringent surrogate standards.

1.3.3) Molecular Pluripotency

Molecular pluripotency comprises not only the phenotypic markers that are characteristic of pluripotent stem cells, and instrumental for their identification, but also the molecular factors that play a role in stem cell biology. Although some of these markers are not specific to PSC, when included in a panel with other markers they are vital to distinguish pluripotent stem cells from other somatic cells.

1.3.3.1) Markers and Cell Surface Antigen Expression

Technical resources developed for the identification and isolation of EC cells from teratocarcinomas were later found to be viable tools for the study of other PSC namely mESC and hESC. The first marker used for this purpose was alkaline phosphatase activity. Soon, the establishment of new specific monoclonal

antibodies allowed for the identification of characteristic surface markers as the stage specific embryonic antigen-1 (SSEA1) present in undifferentiated mouse PSC. However, SSEA1 was demonstrated not to be highly present in undifferentiated human PSC, but its expression would rather increase with cell differentiation in those cells. Conversely, undifferentiated hESC and hEC (human embryonal carcinoma cells) present high reactivity for the stage specific embryonic antigen-3 and 4 (SSEA3 and SSEA4 respectively), curiously, markers for early differentiation in mouse PSC. Human PSC additionally express the keratan sulfate tumor recognition antigens TRA-1-60 and TRA-1-81(*9*, *13*, *19*). For a more detailed review see reference (*2*).

1.3.3.2) Transcription Factors and Regulators

Innumerable transcription factors and regulators have been identified to be active in maintaining pluripotency, with a core transcriptional network proposed to maintain pluripotent stem cell identity. This core consists of a troika of Oct4, Sox2 and Nanog, whose expression patterns and roles during development account for their pivotal function in pluripotency.

Oct4 that is encoded by the *Pou5f1* gene belongs to the POU family of transcription factors that contact DNA in 2 specific domains (4 bp each and hence the name *octamer*) (*26*). During embryo development its expression is restricted to the totipotent blastomeres, pluripotent ICM, epiblast and primordial germ cells

(*27*). This protein is implicated in the first fate decision in the embryo since Oct4-deficient embryos develop to the blastocyst stage but their ICM developmentally leans towards the trophoblast fate and is not pluripotent (*27*). Importantly, Oct4 expression must be fine-tuned, because either its overexpression or repression result in the differentiation of ESC into mesodermal and endodermal or trophoectodermal lineages respectively (*28*, *29*).

Sox2 is a member of a protein superfamily presenting a single high mobility group (HMG) DNA binding domain and similarly to Oct4 it is expressed in the ICM, epiblast, and germ cells. However, Sox2 is also expressed in the multipotential cells of the extraembryonic ectoderm and in uncommitted dividing stem and precursor cells of the developing central nervous system (*30*). Sox2-null embryos did not form pluripotent ICMs as *in vitro* these ICM cells gave rise to trophoblast giant cells. The same result was obtained while studying Sox2-null mES (*31*), a respecification similar to the one described for Oct4. This resemblance in phenotypes for Sox2 and Oct4 loss and their expression patterns is attributed to the cooperative action of Oct4/ Sox2 in controlling several ESC-specific genes, including themselves.

Indeed, ectopic Oct4 expression was found to be sufficient in rescuing the differentiation phenotype of Sox2-null mESCs, supporting the notion that Sox2 also acts by ultimately stabilizing Oct4 expression (*31*).

Nanog has a single homeodomain DNA-binding region and was discovered through functional screening of an ESC cDNA library, with the goal to find

factors capable of maintaining mESC self-renewal in the absence of the usually crucial factor leukemia inhibitor factor (LIF) (*32*, *33*). Nanog expression appears as a temporal wave with maximal levels between the late morula and the mid blastocyst and downregulation just prior to implantation, a pattern coincidental with the transient potential for ES cell generation, which arises in the ICM and is lost around the time of implantation. Nanog expression is also present in primordial germ cells (*33*). Disruption of Nanog results in the differentiation of ICM and ES into extra-embryonic endoderm (*32*, *33*), a phenotype comparable to the exerted by Oct4 overexpression.

To better elucidate the importance of these three proteins for pluripotency, two studies using chromatin immunoprecipitation (ChIP) followed by sequencing or DNA microarrays analysis have been applied to map the genomic-binding loci of these core factors both in mESCs and hESCs (*34*, *35*). Oct4 had been previously shown to cooperate with Sox2 to control the expression of several genes. Notably these two studies did not only confirm this, but also reported that these three factors (Oct4, Sox2 and Nanog) extensively co-occupied the promoter of a large population of genes. This cooperation was found for both transcriptionally active and inactive genes. Furthermore the promoter regions of these three factors were also involved in auto-regulation by the combined factors.

In conclusion, the core transcription factors Oct4 Sox2 and Nanog serve to establish a pluripotent state by activating the expression of additional

pluripotency-associated factors while concomitantly repressing lineage-specific genes (Fig. 1.4). Furthermore this core also regulates their own gene expression and that of each other in complex regulatory feedforward loops (*34*, *35*). Subsequent studies applying large-scale RNAi knockdown strategies or via the coupling of affinity purification methods with protein identification by mass spectrometry contributed significantly to the identification of new important players in the pluripotency regulatory circuitry. To the core pluripotency network, an extensive list of factors and co-factors has been added, such as Esrrb, Tbx3, Tcl1, SetDB1, Tip60-p400,Cnot3 and Trim28, Paf1C, among others, further complicating the intricate pluripotency regulatory system. These new studies exposed an extensive protein-protein interaction network comprised of other ESC transcription regulators, chromatin remodeling and modifying factors, DNA methyltransferases and Polycomb group proteins (PcG). Remarkably, it was made clear that the core pluripotency factors may also regulate gene expression by modifying chromatin states (*36*).

Further studies analyzing possible interaction between particular sets of these factors uncovered a broad combinatorial binding at many common pluripotency-related targets (*37*, *38*). Kim et al. suggested a direct correlation between the number of bound factors and the likelihood that the target gene is expressed (*37*). The authors conceive that the pluripotency factors individually serve as weak activators, and that multi-factor binding augments activator function and promotes expression of the target gene. This study also provided some evidence

for the distinction of two independent modules to which factors could be bound, the core Oct4- centered module or the c-Myc module. The Myc module encompassing c-Myc, n-Myc, Rex1, Zfx and E2f1, is now known to be involved in self-renewal and cell metabolism (*36*).

Moreover, adding an extra layer to the regulatory capacities of the ESC transcriptional core, evidences show that the core transcriptional network is capable of regulating micro RNA expression (*36*).

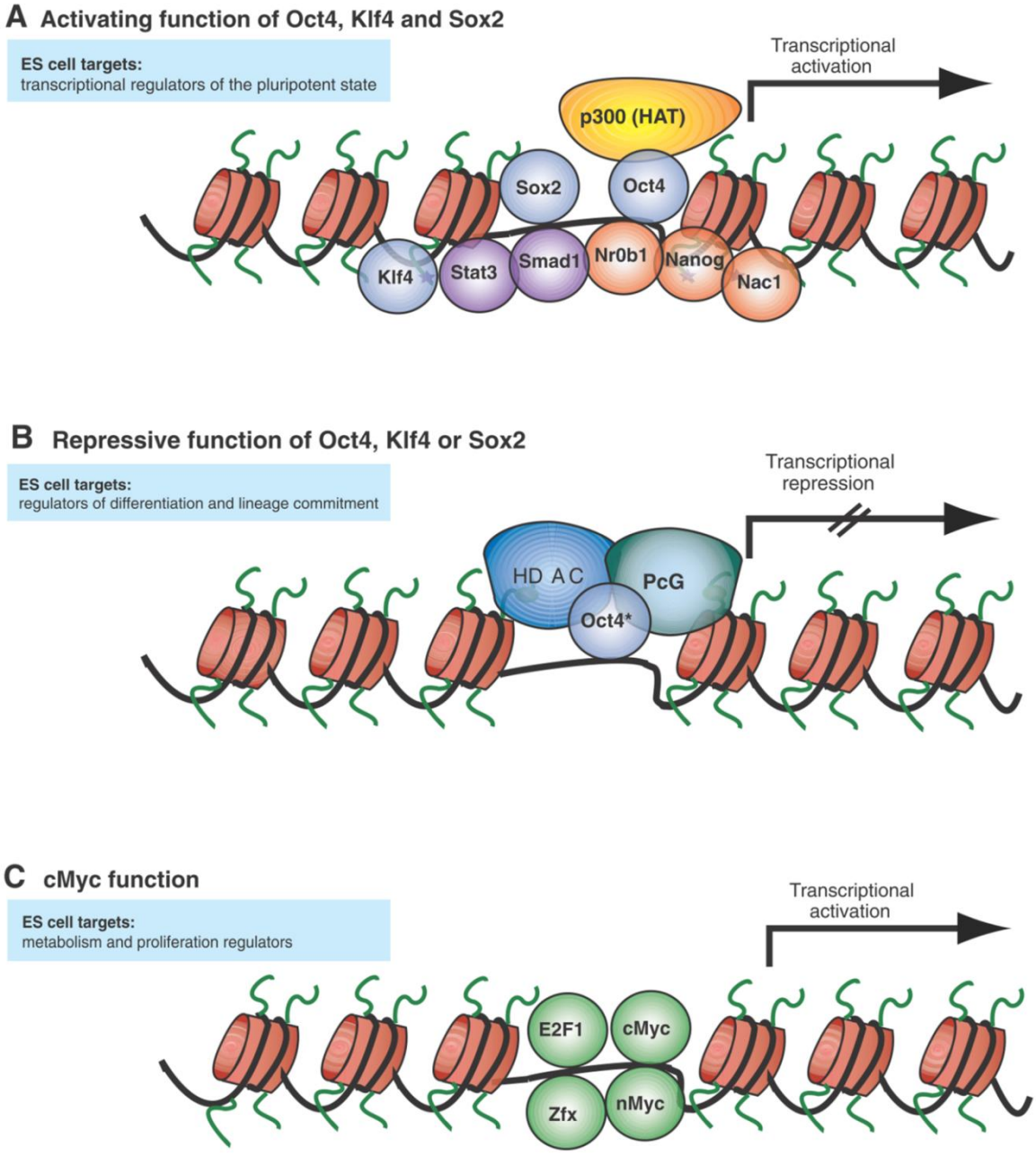

Fig. 1.4 – Pluripotent cell transcription factor network and target groups. (A) The reprogramming factors Oct4, Sox2 and Klf4 often co-bind promoter regions with other transcription factors including Nanog. The recruitment of co-activators, such as the histone acetyltransferase (HAT) p300 is often observed. This binding pattern is found in transcriptionally active genes in embryonic stem cells. (B) In ESC, genes bound by either Oct4, Sox2 or Klf4 are often repressed, potentially through the recruitment of Polycomb group (PcG) proteins or histone deacetylases (HDACs), but become activated upon differentiation. (C) cMyc representing another transcriptional axis is proposed to bind and activate independent sets of genes in collaboration with other transcription factors. Nr0b1: nuclear receptor subfamily 0, group B, member 1; Esrrb: estrogen-related receptor, beta; Zfp281: zinc finger protein 281; Nac1: nucleus accumbens associated 1; Stat3: signal transducer and activation of transcription 3. Adapted from *(1)*.

1.4) Mitochondria

"Life did not take over the globe by combat, but by networking…"

Margulis and Sagan

1.4.1) Evolution

Revamped considerations regarding the endosymbiotic theory, substantiated on relatively new studies have led to the emergence of the symbiotic association hypothesis, which consider mitochondria to have evolved from a α-proteobacteria ancestor that was associated with a basal anaerobic archeobacteria host, rather than with a defined eukaryotic cell. From this cellular merger a new breed of complex cellular organization was generated, still defined as proto-eukaryotes, as it is speculated that this new entity probably still lacked a membrane-bounded nucleus (*39*). Various conjectural reasoning lines point to protection and symtrophy interactions as credible justifications for the perennial symbiosis between the referred cells. Indeed in a context of a rising oxidative environment due to the accumulation of O_2 resulting from the photosynthetic activity of cyanobacteria, the ability of the aerobic symbiont to detoxify the host cytoplasm by decreasing O_2 concentration, serves as a significant advantage for the host, endowing it with the capability to survive or even colonize otherwise inaccessible niches. On the other hand the by-products from the fermentative metabolism of archeobacteria could serve as organic nutrients for the α-

proteobacteria symbiont (*40*). Therefore the two entities undergoing symbiogenesis engaged an unceasing co-evolutionary process that resulted in an intimate and interactive structural, genomic and metabolic integration. This integrative process with a consequential reduction of redundant structures and genes in the proto-mitochondria was so extensive that it rendered the new constituted organelle incapable of an independent existence (*41*). On the other hand, the co-evolutionary process also attributed new functions and regulatory properties to mitochondria, which became essential for life in the cell and later in the organism, reinforcing mitochondria as a key organelle.

1.4.2) Structure

Classical conception of mitochondria depicts them as defined and stiff ellipsoidal organelles with two membranes, an internal membrane (IMM) and an outer membrane (OMM). These two membranes circumscribe two specific compartments, the mitochondrial matrix and the intermembrane space, respectively. The outer membrane has a high abundance of specific proteins called porins (also known as the voltage-dependent anion channels, VDAC), which form transmembrane aqueous channels, rendering this membrane permeable to all small molecules (≤5000 daltons) (*42*). This sieve-like structure of the OMM conditions the composition of the intermembrane space milieu. On the other hand, the inner mitochondrial membrane has a particularly high protein/lipid content (~75/25) and is rich in the phospholipid cardiolipin, which

may account for the stabilization of protein complexes, to confer the IMM impermeable to ions and for defining the shape of the IMM (*43*). Selective IMM permeability also results from the presence of specific transport proteins. Protein complexes that compose the electron transport chain (ETC) and the ATP synthase are responsible for the generation of chemical energy in the form of adenosine triphosphate (ATP) and are also embedded in the IMM, (*vide infra)*. The IMM presents two distinct regions, the inner boundary membrane (IBM) that is adjacent to the outer membrane and the cristae membrane (CM) that lies around the cristae.

Initial studies of mitochondria using electron microscopy in the 1950s resulted in the elucidation of their ultrastructure, demonstrating the existence of both membranes and particularly noting that the inner membrane presented a highly convoluted organization (which accounts for an increased surface area). Different perspectives were suggested in an attempt to explain the configuration of the inner mitochondrial membrane. A model presented by George Palade, while prevailed for more than 40 years, depicted the inner mitochondrial membrane with simple invaginations forming the cristae (*44*). Technological developments particularly related to substantial advances in 3D-microscopy imaging (including electron tomography and laser confocal microcopy) and the advent of new staining techniques and novel selective fluorescent dyes have helped deconstruct this classical notion (*44*, *45*). Not only was it shown that mitochondrial shape and size is mutable and diverse, with some organelles presenting a dynamic reticular

morphology characterized by continuous fusion and fission processes (*44*, *45*) (Fig. 1.5), but also the cristae organization was demonstrated to be more fluid, and its total area has been shown to positively correlate with ATP production (*43*). Instead of the invaginations with wide openings linking the intercristal space to the intermembrane space, cristae are now accepted to possess a tubular or lamellar morphology, presenting distinct topological domains, with constricted narrow segments (cristae junctions) as the links to the inner boundary membrane (*44*). These distinct topological regions may be of great importance for the physiology of the organelle itself, as they may translate into diverse functional domains due to differential distribution of intermembrane poteins and lipids or even creating ionic or molecular gradients between the intercristal and the remaining intermembrane space (*44*, *45*). More recently, cristae junction has been suggested to be controlling cytochrome C release from the intercristal space where it is majorly stored, during apoptosis (*43*).

As referred, the mitochondrion is not regarded as a static organelle anymore. Its dynamics can be seen in terms of size, morphology, cristae complexity and relative distribution within a cell and may be modulated in response to pathological states but also physiological events during the lifetime of the cell (*43*). Of major interest are the modifications occurring in mitochondria during the course of cells differentiation and development (*46*).

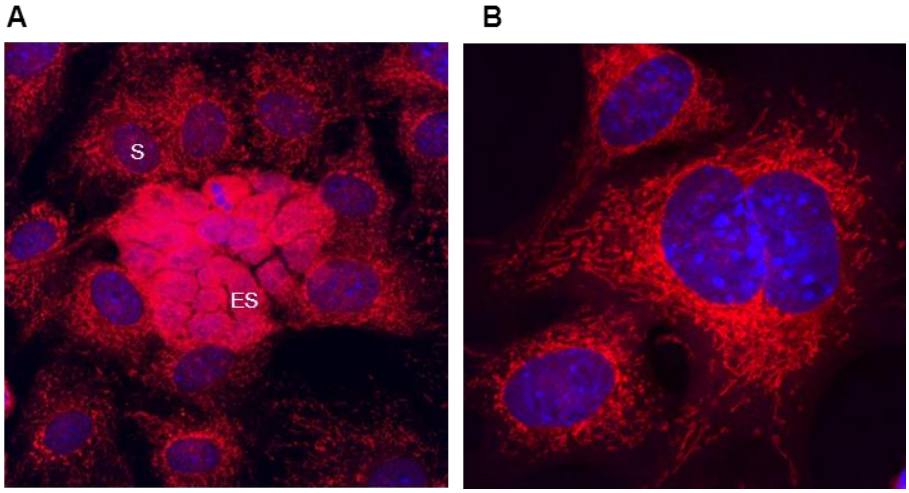

Fig. 1.5 – Epiflurescence microscopy depicting mitochondria (red) in distinct cells. (A) A colony of mouse embryonic stem cells (ES) differentiating over PA6 stromal cells (S). (B) Detail of the complex mitochondrial network present in PA6 stromal cells. Red: MitoTracker Red (mitochondria), Blue: DAPI (nuclei).

Together with chloroplasts mitochondria are unique organelles within the eukaryotic cell, as they possess their own genome, a remnant from their evolutionary background. This genome is organized as a closed circular molecule with ~16.5 kb and harbor the coding capacity for 13 protein subunits for the mitochondrial complexes I, III, IV and V, 22 tRNAs and 2 ribossomal RNA essential for the translation of the referred subunits in the mitochondrial matrix (*47*). All the remaining subunits of mitochondrial complexes and further proteins acting within the mitochondria are coded by the nuclear DNA and must be imported from the cytosol, which emphasizes the need for a complex crosstalk between the nuclear and mitochondrial genomes. Mitochondrial genes do not present introns, and are arranged end on end with relatively few intergenic regions (*47*, *48*).

1.4.3) Functions

Mitochondria are immediately associated to their energetic function as a major ATP supplier in the cell, but several other roles have been attributed to this organelle. Besides oxidative phosphorylation (OXPHOS) and the Krebs cycle, mitochondria have further distinct metabolic and bioenergetic activities, such as heme biosynthesis, the metabolism of amino acids, and β-oxidation of fatty acids (*49*). Also, thousands of studies imply mitochondria in the apoptotic process and in the synthesis of the iron/sulfur clusters (*43*). Mitochondria are also involved in the process of nonshivering thermogenesis, active in brown adipose tissue, through the presence of specialized proteins called uncoupling proteins (UCPs) (*50*).

In the present review we will mainly focus and explore the energetic contribution of mitochondria, which is being increasingly associated with the regulation of stem cell pluripotency/differentiation mechanisms.

1.4.4) Oxidative Phosphorylation

The core of the mitochondrial energetic machinery is composed by a set of multiprotein complexes (Complex I – NADH:Ubiquinone oxireductase; Complex II – Succinate:Ubiquinone oxireductase; Complex III – Ubiquinol:Cytochrome C oxireductase; Complex IV – Cytochrome C oxidase) and two transporter molecules (ubiquinone or Coenzyme Q10 and Cytochrome C) structuring the

electron transport chain (ETC), which is embedded in the IMM This machinery will enable the organelle to produce an electrochemical gradient across the IMM, which will then be majorly converted into chemical energy in the form of ATP by the ATP synthase. This gradient is also used for powering selective transport across the IMM or to generate heat by UCPs, stimulating thermogenesis. Electrons originating from reducing equivalents species as NADH (reduced nicotinamide adenine dinucleotide) directly formed at the Krebs cycle or indirectly, through defined shuttles, from the glycolytic pathway, and those from the succinate dehydrogenase-associated $FADH_2$ (reduced nicotinamide adenine dinucleotide) are transferred to complexes I or II respectively. These electrons will further traverse ETC transporters and complexes with increasing redox potential, finally reaching Complex IV where oxygen is reduced to water. The progressive flowing of electrons through the ETC complexes is coupled to the pumping of H^+ from the mitochondrial matrix to the intermembrane space, at defined sites of the ETC (Complexes I, III and IV), creating the mitochondrial proton motive force (Δp). The thermodynamic favorable inflow of protons through the ATP synthase leads to consecutive conformational changes in this protein, resulting in the formation of ATP from ADP (adenosine diphosphate) and inorganic phosphate (Pi).

1.4.5) Feeding mitochondria: the glycolytic pathway

The glycolytic process lies at the heart of cellular energetic metabolism. This pathway was one of the first metabolic pathways to be elucidated and is virtually universal. The inexistence of O_2 in the primitive Earth atmosphere, supports the notion that anaerobic glycolysis might have served as the primordial metabolic mechanism to extract energy from organic compounds in primitive living forms. Furthermore, the significance of this pathway endured the evolutionary time that brought life from primitive forms to modern forms, as its principles have been significantly conserved throughout the three domains of life (*51*). Moreover, glycolysis is still in function in aerobic organisms, being in fact the prelude for the Krebs cycle and the oxidative phosphorylation in mitochondria, as pyruvate is channeled to mitochondria to be catabolized by the Krebs cycle.

The detailed study of the steps involved in glycolysis is beyond the scope of this introduction (for that purpose we address the reader for technical textbooks), as we will mostly focus on the biological significance of the pathway in the context of cell physiology.

Glycolysis entails sequential reactions through which one molecule of glucose is converted into two molecules of pyruvate with partial conservation of the energy in the form of ATP. The pathway may be divided in two phases, a preparatory phase where glucose is activated and subsequently cleaved into two triose phosphate molecules (glyceraldehyde 3-phosphate and dihydroxyacetone phosphate) with an obligatory investment of 2 ATP molecules and a second

"payoff" phase where each one of the two molecules of glyceraldehyde 3-phosphate (dihydroxyacetone phosphate is readily converted to glyceraldehyde 3-phosphate by an isomerase) is converted to pyruvate incurring in the energy-conserving phosphorylation steps that capture some of the free energy of glucose in the form of ATP. Accordingly, each glucose molecule will generate two molecules of pyruvates and 4 ATPs, but as 2 ATP had been antecedently invested during the preparatory phase, only 2 ATPs should be considered as the net yield of glycolysis (*52*). Importantly, glycolysis also leads to the generation of 2 NADH molecules.

Pyruvate is completely oxidized to carbon dioxide the mitochondrial Krebs cycle, originating also NADH and succinate which will then be oxidized by the respiratory chain. Under aerobic conditions, these pyruvate-derived NADH molecules and those deriving from the cytoplasmic NADH molecules generated in glycolysis may then be oxidized back to NAD^+ passing on its electrons to the electron transport chain, leading to the formation of ATP through oxidative phosphorylation. Under anaerobic conditions however, the unavailability of O_2 as a final electron acceptor in ETC hampers the regeneration of NAD^+ from glycolysis-derived NADH molecules at this level, what would consequentially inhibit the glycolytic flux. In those situations cells use a fermentation strategy, with pyruvate originating either lactate (as in mammalian cells) or ethanol (as in yeast and other microorganisms) and incurring in reactions that will regenerate the cytoplasmic NAD^+ pool.

1.4.6) Reactive Oxygen Species

Within the cell, mitochondrial electron transport chain harboring potential loci for single reduction reactions, accounts for a significant source of reactive oxygen species (ROS). However, the widespread perception of mitochondria as the prime source of cellular ROS, is unlikely to be true as many other quantitatively important sites capable of ROS production, (e.g., endoplasmic reticulum, peroxisomes, cytosol, plasma membrane and extracellular space), have been reported (*53*).

Nevertheless, mitochondrial ROS generation is important not only due to their etiological relation to several pathological conditions, but also for their possible contribution to retrograde redox signaling from mitochondria to the cytosol and the nucleus (*54*).

ROS are unavoidable molecules in cells and their capacity to serve antithetical (pathological versus physiological) functions requires a fine tune regulation of their production and detoxification processes, in order for the cell physiology to be maintained. Moreover, disturbing this equilibrium can rapidly cause the cell to enter into an oxidative stress status, with potential harmful consequences.

1.4.7) Reactive Oxygen Species: Nomenclature

Radical is the designation given to any atom or molecule with one or more unpaired electrons, irrespectively of its net charge (*55*). As an example O_2 has two

unpaired electrons in antibonding orbitals with parallel spins, making it prone to accept one electron at a time (*54*). From the first monovalent reduction of O_2 the superoxide anion ($O_2^{\bullet-}$) is formed. This reactive species can be readily disproportionated (dismutated) either spontaneously or, more significantly, by the enzyme superoxide dismutase (SOD) to the more stable hydrogen peroxide (H_2O_2). Albeit not being a radical, H_2O_2 is considered a ROS (*56*), and in the presence of metal irons, particularly ferrous iron (Fe^{2+}) it may undergo the Fenton reaction generating the perniciously reactive hydroxyl radical ($HO^{\bullet}$). The hazardous effects of ROS are intimately related to their half-life and range of action, with the hydroxyl radical as the less stable, and highest reactive species. On the other hand, the membrane-permeant H_2O_2 is relatively stable, modestly reactive and highly diffusible (*57*). Superoxide anion is assumed not to significantly cross membranes, due to both its charge and the fact that its membrane-permeant protonated form, the hydroperoxyl radical, is insignificantly present at physiological pH (*53*). In terms of reactivity, stability and half-life, $O_2^{\bullet-}$ lies in between the other two ROS focused here (*57*).

1.4.8) Mitochondrial Sources of Reactive Oxygen Species

The redox activity-rich mitochondrial environment harbors several documented enzymatic sources of ROS, namely the flavoproteins acyl-CoA dehydrogenase and glycerol phosphate dehydrogenase, aconitase, monoamine oxidase,

dihydroorotate dehydrogenase and the pyruvate and α-ketoglutarate dehydrogenases (*58*). However, we will specifically focus our attention on the ROS production sites integrated in the ETC, as they have been shown to be more significant (*58*). The set of protein complexes and carriers constituting the ETC, house an extensive number of potential places for one-electron reduction of O_2. However, the physical protection conferred by bulky proteins that maintain O_2 at a secure distance, results in only some of these spots actually accounting for meaningful ROS generation. This is the case of Complex I and Complex III.

Complex I

NADH-derived electrons first enter the ETC by flowing to the FMN cofactor of Complex I. Within this complex, electrons are then passed through a chain of seven FeS (iron–sulfur) centres to the UQ reduction site. Conceptually there are two mechanisms for ROS production in Complex I. The first one is related to the formation of $O_2^{\bullet-}$ by the reaction of the fully reduced FMN with O_2. $NADH/NAD^+$ ratio is important in setting the proportion of reduced FMN and increased ROS production by inhibition of Rotenone (at the UQ reduction site) is explained by this model, as it would lead to the accumulation of electrons at the FMN site and to the subsequent $O_2^{\bullet-}$ production. Factors increasing $NADH/NAD^+$ ratio (e.g., inhibition of the respiratory chain by damage, mutation, ischemia, loss of cytochrome c or low ATP demand) will favor this mechanism. Nonetheless, ROS

production by this route is considered insignificant in physiological situations where NADH/NAD^+ ratio is relatively low (*59*).

The second way for $O_2^{\cdot-}$ formation at Complex I engages the reverse routing of electrons and is therefore named RET (reversed electron transport). It is instrumental for the highest ROS generation in the ETC and it occurs for mitochondria energized with succinate (through Complex II) when electron supply reduces the UQ pool. If in the presence of a high protonmotive force (Δp) electrons are thermodynamically forced back from reduced ubiquinone into complex I, reducing NAD^+ to NADH at the FMN site. RET-derived ROS generation is inhibited by Rotenone, and its biological significance might not be extensive since Complex II is not the main entry of electrons in the ETC and the Δp is normally not sufficiently high to drive an electron back flow (*54*, *60*).

Complex III

Mitochondrial complex III is another major source of superoxide anion, which is generated in two well-defined sites of its structure, the Qo and Qi sites (Fig. 1.6). Redox reactions at this level of the electron transport chain are initiated by the binding of ubiquinol (UQH2) to the Qo site of the complex III, which faces the intermembrane space. UQH2 initially donates one electron to the Reiske protein which will further reduce cytochrome C, leading to the formation of the semiubiquinone radical (UQ.-) at the Qo site. The remaining electron from UQ.- is then transferred to the Qi site of the Complex III where a ubiquinone (UQ) molecule is bound, reducing it to UQ.-. The ubiquinone in the Qo site is then

released and another molecule of ubiquinol then binds it, transferring one electron to the Reiske protein and a second electron to the semiubiquinone radical in the Qi site, thus generating UQH2 at this level (for a review see (*58*)). It is the generation of the semiubiquinone radical within the context of these reactions that mostly accounts for the ROS formation potential of Complex III. $UQ^{\bullet -}$ is capable of promptly reducing O_2, forming the superoxide anion, at both the Qo and Qi sites. Although accessibility to O_2 is considered increased at the Qo site, rendering it a more substantial site of superoxide generation, the Qi site has also been demonstrated to be an active ROS source (*61*). Some studies have referred that during normal function of the ETC, complex III ROS production is negligible when compared to the one found for Complex I (*54*, *57*).

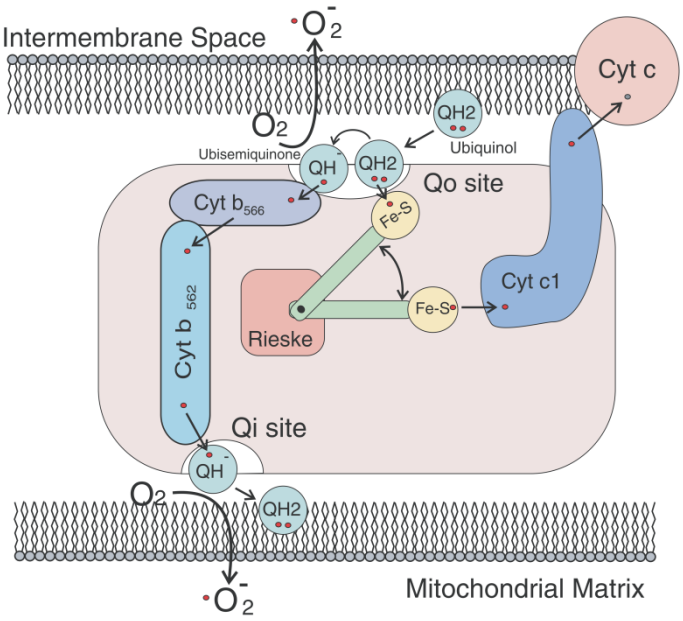

Fig. 1.6 – Schematic representation of the function of mitochondrial complex III, with possible sites for reactive oxygen species production. For detailed explanation see text. Cyt c: cyctochrome c; Cyt b: Cytochrome b; QH2: ubiquinol; QH: ubisemiquinone; Rieske, iron sulphur protein. Adapted from (*62*).

However, it is easily predicted that reactions that affect $UQ^{\bullet -}$ generation, and its net concentration and lifetime during the quinone cycle in complex III, may consequently modulate superoxide anion production, so both stimulation of the ETC (with faster $UQ^{\bullet -}$ generation) and its inhibition in locations distal to the sites of $UQ^{\bullet -}$ formation accounts for the regulation of superoxide anion generation, as well as that of further reduced species (*63*). Antimycin A is an established chemical inhibitor of the ETC complex III, known to act by inhibiting electron transfer from the Qo to the Qi site, resulting in this case in the accumulation of semiquinone radical, and thus substantially enhancing the overall production of reactive superoxide anion (*58*, *64*).

1.4.9) Countering Reactive Oxygen Species actions – Cell Antioxidant Defenses

The noxious attributes of ROS are substantiated by their ability to oxidize proteins, lipids, DNA and RNA, which in a mitochondrial context may lead, for instance, to the inactivation of ETC components, to peroxidation of membrane lipids and to the mitochondrial DNA damage, rendering the organelle dysfunctional. In order to elude this situation mitochondria have developed a complex array of enzymatic and non-enzymatic protective strategies. One of the non-enzymatic defense mechanisms accounting for a decreased ROS generation

by the ETC is named mild mitochondrial uncoupling, which encompasses a small and beneficial decrease in the mitochondrial transmembrane electric potential ($\Delta\psi$). This mild uncoupling is believed to be mediated by uncoupling proteins and the mitochondrial potassium ATP-sensitive channels (mitoK$_{ATP}$) as these entities have been showed to be activated under oxidative insults, resulting in a sophisticated negative feedback system, controlling mitochondrial ROS formation (*58*, *64*). Uncoupling stimulates ETC activity, promoting a range of factors that may contribute to diminished ROS generation, namely a slight decrease in O_2 tensions, lower NADH and a reduced semiubiquinone half-life (*58*, *63*).

The non-enzymatic mitochondrial antioxidant array repository is considerable extensive, including ascorbic acid (vitamin C), membrane soluble-tocopherol (vitamin E) with an important role in preventing membrane-lipid peroxidation, retinol (vitamin A), flavonoids and lipoid acid (*57*). Besides being the electron carrier from complexes I and II to complex III Coenzyme Q has been recognized as a non-enzymatic antioxidant, not only preventing lipid peroxidation due to its liposolubility and IMM integration but also by preventing oxidation of proteins at that level. Of foremost importance is glutathione (GSH), a tripeptide with its thiol group of cysteine serving as an electron donor. Indeed the GSH (reduced form) / GSSH (oxidized form) ratio is accepted as a good determinant of the thiol redox state of the cell, given that under physiological conditions the former state is the prevalent form. GSH is recruited at several levels in the antioxidant

response serving as cofactor of antioxidant enzymes (glutathione peroxidase), directly neutralizing $HO^{\bullet}$, and by regenerating vitamins C and E to their reduced active forms (*57*).

For enzymatic-driven defenses, mitochondrial possess the mitochondrial-specific manganese-SOD (MnSOD) (fundamental to rapidly dismute mitochondrial $O_2^{\bullet-}$ to H_2O_2), enzymes catalyzing the removal of H_2O_2 to water and O_2 (catalase, glutathione peroxidase, peroxiredoxins and thioredoxins) cytochrome c, glutathione reductase (essential to regenerate reduced GSH pools in the mitochondria using NADPH), and the phospholipid hydroperoxide glutathione peroxidase (responsible for the reduction of phospholipid hydroperoxides, H_2O_2, cholesterol peroxides and thymine peroxide), among others (*57*, *58*, *65*).

1.5) Metabolism - Where Stem Cells Meet their Cancer Counterparts

"*The era in which the fermentation of the cancer cells or its importance could be disputed is over, and no one today can doubt that we understand the origin of cancer cells if we know how their large fermentation originates...*"(*66*)

These words originally delivered in 1955 by Otto Warburg (*66*), one of the founding fathers of the metabolic theory of cancer, albeit unheeded for decades by the inattentive scope of cancer biologists are disconcertingly regaining notoriety. In the light of modern evidence, metabolic matters are increasingly vivid now, not only in cancer but also in stem cell biology. Indeed, what to a distracted mind could appear as an odd connection between stem and cancer cells, could have been anticipated considering the basis underlying the seminal attempts to derive stem cells (in fact, embryonal carcinoma cells were the first plutipotent cells to be isolated (*3*)) and following the undisputed demonstration for the existence of cancer stem cells in different tumor types (*67*, *68*). Cancer founding cells and stem cells do share innumerable properties and characteristics, such as self-renewal, some cell markers and the reliance on similar signaling pathways (*69*). Additionally and despite the necessary constraints when drawing general considerations about broad groups due to the

existence of many "oncogenotypes" and stem cell types, it is notable that both cell groups employ a unique conceptual metabolic phenotype, one that lays the foundations for active proliferating cells. In the 1920's, Warburg reported that tumor cells growing as ascites would grow mostly supported by a robust fermentation of glucose (glycolysis with the subsequent conversion of pyruvate to lactate). Extraordinarily this metabolic trait was observed when cells were cultured in aerobic conditions. This enhanced glycolysis in aerobiosis was later named the "Warburg effect". Warburg's first rationalizations on the unexpected metabolic phenotype pointed to an "irreversibly damaged respiration" as the cause of the metabolic shift. Contrary to such metabolic profile, normal somatic cells in an adult organism (excluding adult stem cells and remaining progenitors) are in a state of terminal differentiation executing their specific roles and not enrolling in proliferation. The metabolic infrastructure of differentiated cells is adapted in a lineage-specific fashion to their energetic demands, but it is accepted that these cells mostly rely in mitochondrial respiration to fabricate the bulk of their ATP.

Stem cells, namely ESC and iPSC, with their inherent unlimited self-renewal, proliferate at extremely high ratios and also present the Warburg effect, with consistently elevated lactate production and diminished O_2 consumption rates (*70*, *71*). Indeed, strategies to up-regulate the glycolytic pathway in detriment of a majority of ATP production via OXPHOS is beneficial to maintain stem cell identity while hampering differentiation processes (submitted, (*72*–*74*)). The

opposite is also verified, and this metabolic regulation was shown to be instrumental in the reprogramming efficiency of iPSC (*75*, *76*). Inversely to the differentiation process, reprogramming engages the oxidative to glycolytic metabolic shift, and this metabolic reprogramming was shown to precede the genetic reprogramming process, underscoring the importance of metabolic status for stem cell identity (*75*). Moreover, the induced overexpression of specific glycolytic enzymes was reported to be sufficient to bypass senescence in mouse embryonic fibroblast, while depletion of such enzymes had the reverse effect shortening cellular life span (*77*).

When considering the peculiar metabolism of proliferating cells, it may seem challenging to find the rationale behind what might seem an energetically-unfavorable choice. Whereas the glycolytic process yields 2 ATP molecules, the complete oxidation of a single glucose molecule through glycolysis and the Krebs cycle, and subsequent oxidative phosphorylation will result in at least 15 times more ATP produced. Furthermore, enhanced glycolysis imposes an immediate conversion of the glycolytic-derived pyruvate into lactate, which despite being an energetic valuable molecule is promptly discarded by the cell. Why would then an active proliferating cell in need of a significant energetic supply, waste such a metabolic asset and shift from mitochondrial respiration towards glycolysis? To understand this paradox, one should comprehend the dynamic regulation of metabolism. Metabolism results from the integration of the cellular internal needs with external cues present in the niche (morphogens, substrates, oxygen,

etc). Cancer cells have become relatively independent from some of such external signals to maintain their growth. This integrative regulation makes metabolism pliable, with cells adopting distinct metabolic modes. If a cell is terminally differentiated as we have discussed before, it will adopt a catabolic mode where its metabolism is adjusted for maximal energetic efficiency, and substrates completely oxidized to feed the mitochondrial energetic machinery with sufficient reducing equivalents for ATP production in aerobiosis. This catabolic mode provides the cells with appropriate energetic charge to sustain their functions; this is particularly true for high energy-requiring phenotypes, such as cardimyocytes.

On the other hand, if a cell is committed to rapid proliferation, ATP and NADH are not its only required commodities. Pathways such as glycolysis and the Krebs cycle do not operate as strict unidirectional metabolic avenues serving energetic purposes. They rather serve as metabolic hubs closely communicating with several other metabolic branches engaged in the production of distinct molecules some of which serve as molecular precursors for the synthesis of biological structuring molecules including lipids, proteins, DNA and RNA (*78*, *79*). A proliferating cell will then adopt an anabolic state assuming a compromise between energy production and the synthesis of molecular precursors necessary for cell growth and subsequent cell division. Nevertheless, glycolysis is a much faster process to obtain energy and sufficient energy loads are generated through it if sufficient amounts of glucose are present, such is the case of *in vitro* stem cell

cultures. An elevation of ATP levels and a decrease in AMP/ATP ratios would be detrimental for glycolytic fluxes, as it would lead to AMPK inactivation and cells would slow down the glycolytic process. Adding to this, ATP is also a known direct allosteric inhibitor of glycolytic enzymes so its levels should not rise uncontrollably, and must be balanced by ATP consumption. Moreover, a metabolic shift towards glycolysis has also been proposed as a mechanism to protect the cell from increased reactive oxygen species produced in mitochondria (*77*, *80*).

1.5.1) Metabolic pathways conferring anabolic advantages to the Warburg effect

In the cytosol, glucose that is transported into the cells is rapidly activated by hexokinase-mediated phosphorylation, rendering the molecule usable by subsequent enzymes and hampering its removal from the cell. Resulting glucose-6-phosphate can be isomerized to fructose-6-phosphate or serve also as a substrate for another catabolic process, the Pentose Phosphate Pathway (PPP) (Fig 1.7). This set of reactions branching from glycolysis yields the important production of ribose-5-phosphate and NADPH. While ribose-5-phosphate is necessary for *de novo* synthesis of nucleotides, the NADPH electron donor is equally vital for the reductive synthesis of lipids or for the regeneration of reduced glutathione, a major antioxidant in the cell. The importance of the PPP for cell growth is well established, as seen for example in the fact that human fibroblasts deficient for glucose-6-phosphate dehydrogenase (the first enzyme in

the PPP and responsible for catalyzing one of the steps yielding NADPH) proliferated less and evidenced early senescence when compared to control cells, a phenotype related to an increment in oxidative stress (*81*).

Recently, the hexosamine biosynthetic pathway has been shown to be necessary for cell growth and survival (*82*). This pathway recruits fructose-6-phosphate from glycolysis and yields N-acetylglucosamine in a glutamine and acetil-CoA-dependent fashion. N-acetylglucosamine is the substrate for protein glycosylation and was shown to benecessary to maintain growth factor receptor expression, which in turn would enable cell growth and integration of glutamine and glucose metabolism.

For the increased glycolytic flux to be maintained, cytosolic NAD^+ pools must be rapidly regenerated to serve as cofactors for glyceraldehyde-3-phosphate dehydrogenase (GAPDH). In cells reliant on mitochondrial oxidative phosphorylation, the NADH reducing equivalents are indirectly transferred to the mitochondria via the malate-aspartate shuttle or the glycerol-3-phosphate shuttle resulting in NAD^+ recycling. However under hypoxic conditions or in aerobic glycolysis the bulk regeneration of NAD^+ occurs through the lactate dehydrogenase (LDH)-catalyzed reaction converting pyruvate into lactate, which is ultimately excreted by the cell, a pattern identified in actively proliferating cells such as cancers and stem cells (*66*, *70*, *83*).

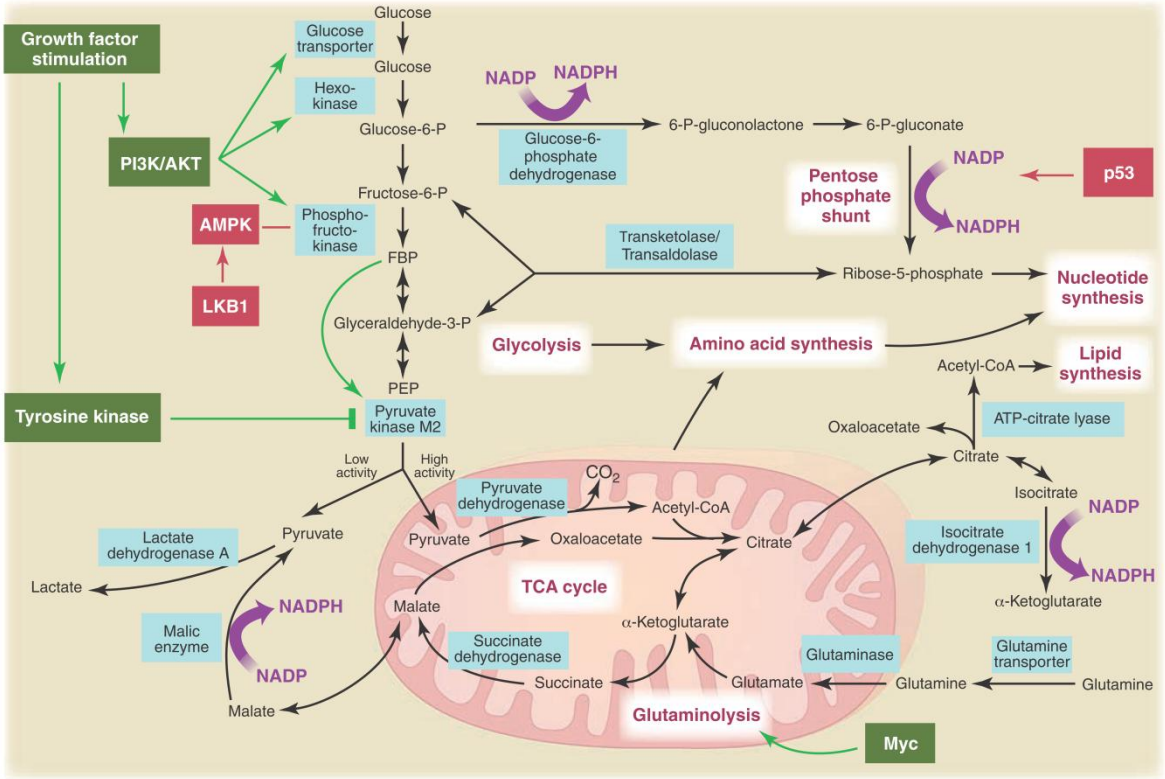

Fig. 1.7 – Metabolic pathways active in proliferating cells are directly controlled by signaling pathways involving known oncogenes and tumor suppressor genes. This schematic shows the complex interconnection between glycolysis, oxidative phosphorylation, the pentose phosphate pathway, and glutamine metabolism in proliferating cells. Tumor suppressors are shown in red, and oncogenes are in green. Key metabolic pathways are labeled in purple with white boxes, and the enzymes controlling critical steps in these pathways are shown in blue. Adapted from (*78*)**.**

Some of the glycolytic intermediates may also serve as carbon sources for the synthesis of macromolecule precursors. Pyruvate can be converted to alanine and phosphenolpyruvate can originate tyrosine. Of extreme importance is the ability of phosphoglycerate dehydrogenase (PHGDH) to remove 3-phosphoglycerate from the glycolytic route redirecting it to serine synthesis, which in turn originates glycine and cysteine. The conversion of serine to glycine leads to the

donation of a carbon to the folate pool (tetrahydrofolate). Derivatives of tetrahydrofolate serve as versatile carriers of the received carbon, which can then be donated in a variety of biosynthetic processes including the synthesis of purines, thymine and for example the regeneration of methionine (*84*, *85*). Recent studies have shown that PHGDH is recurrently over-expressed in certain cancers and that the serine and glycine pathways are necessary for the proliferation of such cells. The shunting of 3-phosphoglycerate away from glycolysis would benefit cancer cell growth namely by limiting ATP production, by influencing the redox status and by promoting α-ketoglutarate generation from glutamate (*86*).

The mitochondrial Krebs cycle is an amphibolic hub to which major catabolism and anabolism related reactions converge. Despite old assumptions probably rooted on Warburg's ideas that the aerobic glycolysis was caused by an irreversible damage to the mitochondria, we now know that this is not the case, as cancer cells may present an active Krebs cycle (*87*). Many of the metabolites involved in this cycle can serve as substrates for biosynthesis (Fig. 1.7); for example α–ketoglutarate and oxaloacetate can be transaminated into the aminoacids glutamate and aspartate respectively, which are precursors for other amino acids and nucleotides. Succinyl-CoA can be used in the synthesis of the porphyrin ring of the heme group. Conspicuously, citrate can be shunted to the cytosol were it can be converted back to acetyl-CoA by ATP-citrate-lyase (ACL) and be used for the necessary synthesis of lipids or to serve other purposes (see below). These reactions are critical for cell proliferation as the inhibition of ACL

causes cell growth arrest in cancer cells *in vitro* and *in vivo* (*88*). The voluminous cataplerotic reactions removing intermediates from the Krebs cycles in proliferating cells must be counterbalanced by anaplerosis that will replenish those pools. Glucose is made of carbon, hydrogen and oxygen atoms and so other molecules must be incorporated in biosynthetic events to supply other required elements, such as nitrogen. Consequently, glutamine is considered a major anaplerotic substrate. Studies in glioblastoma cells grown in aerobic conditions and presenting the Warburg effect revealed that glucose-derived carbon is the major source of carbon skeleton to be incorporated in lipogenesis through citrate (*87*). Under those conditions glutamine, known to be highly consumed by glutaminolysis, mostly served as an anaplerotic substrate, contributing significantly for the lactate and alanine pools (60% of all glutamine consumed) and less notably to lipogenesis. Glutaminolysis also yielded oxaloacetate to replenish intermediate pools and especially resulted in a robust NADPH production that was used to support biosynthesis (*87*). Glutamine has similarly been shown to be essential for mouse ESC proliferation (*89*). Non-canonical reactions in the Krebs cycle have been observed as cancer mechanisms to support cell growth. The oxidation of isocitrate to α-ketoglutarate is catalyzed by isocitrate dehydrogenase (IDH) and requires the presence of NAD^+. Three isoforms of IDH has been identified, and IDH 3 is accepted to be responsible for the canonical conversion of isocitrate. The other two isoforms exist in the mitochondrial matrix (IDH2) or in the cytosol (IDH1), and are NADPH dependent and capable of facilitating the reductive reverse conversion of α-

ketoglutarate to isocitrate (*90*). Certain cancers have been shown to have a significant flux through the reductive pathway especially when growing under hypoxic conditions or when challenged with mitochondrial poisons (*90*–*92*). This adaptation does not merely reflect isotopic exchange between metabolite pools but functions to supply the cell with sufficient carbon precursors to enable a robust lipogenesis. Aerobic glycolysis, hypoxia and the inhibition of the mitochondrial OXPHOS all result in the decrease of glucose-derived carbon entrance in the Krebs cycle with the glucose-derived carbon being mostly transformed into lactate. Glutamine is then exploited as the major *de novo* lipogenic precursor, and the reductive reaction is an elegant adaptation of the cell to boost the rapid conversion of glutamine-derived carbons to citrate, supporting cell growth (*90*–*92*). However more insights in the regulation of these reactions are needed and it would be interesting to understand if stem cells are akin to cancer cells in using this reductive pathway.

1.5.2) Shared molecular basis of the Warburg effect.

As referred before, despite many differences, cancer cells and stem cell populations share regulatory pathways, some of which are influential for their identity and regulate their metabolic profiles. In the present overview we are not thoroughly exposing the molecular factors conceivably implicated in the Warburg effect as its complete regulation is still elusive but we will rather give a brief overview on some of such factors acting both in stem cells and cancer.

1.5.2.1) HIF

One of the most consensual and documented factors related to aerobic glycolysis is the hypoxia inducible factor (HIF) (*93*, *94*). HIF transcription factors establish the primary instrument mediating a cellular adaptation and consequent survival to hypoxic conditions. The spectrum of activated responses is broad, including a pro-angiogenic action, the control of gene methylation and notably the active promotion of the metabolic shift from oxidative phosphorylation towards an oxygen independent glycolysis (*93*, *95*). This could render the cell metabolically independent from O_2 and reduce the risk of cellular damage due to oxidative stress. HIF-mediated metabolic reprogramming occurs via the upregulation of genes encoding critical enzymes for glucose uptake and the glycolytic pathway, as well as the repression of genes related to OXPHOS. Particularly, HIF-1α was shown to directly activate the expression of pyruvate dehydrogenase kinase (PDK), which inhibits the pyruvate dehydrogenase complex, the enzyme responsible for condensing pyruvate and acetyl-CoA in the first step of the Krebs cycle. This diverts pyruvate away from the mitochondria, thus reducing mitochondrial O_2 consumption and enhancing cytosolic lactate production (*96*, *97*). Biosynthetic pathways branching from glycolysis have been suggested to be elevated due to the HIF-1a-favored expression of a less active pyruvate kinase isoform (*85*). HIF-1α also activates genes responsible for mitochondrial autophagy (*93*). HIF-1α and HIF-2α are broadly expressed in several cancers and are fundamental at distinct stages of tumorigenesis (*93*, *98*). Similarly, HIF

participate in the maintenance of stem cell identity, namely by interacting with pluripotency core transcriptional factors (*99–103*). Stem cells and cancer stem cells reside in niches that will influence their physiology (*99*). The Warburg effect has been justified as a cellular adaptation to hypoxia that is present in solid tumors and in some stem cell niches. But this notion is not coherent with the fact that these cells maintain enhanced glycolysis under nearly 20% O_2, or with the generation of cancers appearing in well oxygenated tissues as leukemia or lung cancers (*78*). The HIFs are now known to be controlled by multiple genetic factors including for instance oncogenes, tumor suppressing factors, and signaling kinases (*98*). Most importantly an increasing number of factors that stabilize HIF proteins under normoxia is being reported, some of which could serve as good tools for metabolic reprograming control by stem cells and cancers (see below).

1.5.2.2) c-myc

The transcription factor c-myc belongs to the Myc family of proto-oncogenes and more than one thousand of its target genes have been identify, accounting for 15% of all genes in the genome (*104*). C-myc regulates and integrates cell proliferation, cell cycle control and metabolism and its altered expression is implicated in a myriad of cancers. This transcription factor has regulatory functions in stem cells and is necessary for instance for the self-renewal of mouse embryonic stem cells (*105*), establishing an axis with other factors to regulate

genes related to pluripotency (*36*). C-myc was also one of the 4 factors originally described to induce nuclear reprogramming during the derivation of iPSC. This factor is known to induce the expression of enzymes involved in glycolysis, biosynthetic pathways as the PPP, amino acid metabolism. Interestingly, c-myc also upregulates mitochondrial biogenesis while decreasing O_2 consumption in proliferating cells, probably to promote Krebs cycle anabolic-oriented functions (*106*). Moreover, this protein favors glutamine oxidative pathways, once again most likely to serve anabolic purposes, endorsing the use of glutamine as a carbon and nitrogen source (*106*).

1.5.2.3) Uncoupling Protein 2

Recently, the idea that increased glycolysis results not from a permanent and irreversible damage to mitochondria but instead from the inability of this organelle to use the mitochondrial proton gradient to produce ATP, gained significance with studies demonstrating the action of uncoupling protein 2 (UCP2) in cancers and stem cells (*107–109*). UCP2 is an inner mitochondrial protein and serves as a shunt dissipating the mitochondrial proton gradient, hence uncoupling energy production from O_2 consumption. In a general way, UCP2 has been shown to decrease glucose-derived pyruvate oxidation in the mitochondria, while promoting the use of other substrates as glutamine in the Krebs Cycle(*107*). UCP2 must be repressed during the differentiation process to allow metabolic maturation (*109*).

1.5.3) When metabolism takes over

Mounting evidences substantiate that metabolism is not a mere foot soldier subordinated to the signaling pathways and transcriptional dynamics regulating stem cell/cancer physiology. The analysis of metabolism and the identification that some resulting metabolites and cofactors themselves have regulatory roles, either at the metabolic level or by interfering in signaling and transcriptional processes strengthen this notion. Therefore, it is conceivable to envisage that metabolism can take advantage of these mechanisms to control cell state, particularly by influencing the molecular decision-making processes as those involved in tumorigenesis or stemness versus differentiation.

Much of the control exerted in HIF signaling is related to the stability of the HIF-1α and HIF-2α subunits. In order to perform their function, HIF-α monomers heterodimerize with the HIF-1β subunit. Alpha and beta subunits are constitutively expressed, but in normoxic conditions HIF signaling is suppressed by the degradation of the alpha subunit. This degradation is dependent on the hydroxylation of proline residues of the alpha subunit carried out by prolyl hydroxylases (PHD), which will promote interaction with the von Hippel-Lindau protein and subsequent targeted degradation by the proteasome (*110*). PHD protein activity requires O_2 and α-ketoglutarate as substrates and non heme iron as a cofactor (regenerated by ascorbate); hence hypoxia inactivates PHD and leads to the stabilization of HIF enabling its transcriptional regulatory function (*62*). Normoxic stabilization of HIF can occur downstream the activity of growth

factors (*111*, *112*) and nitric oxide (*110*). It is then equally reasonable to say that events disrupting PHD function through changes in α-ketoglutarate levels and binding would render HIF signaling active, even in normoxic conditions. This is what occurs for example with the metabolites succinate and fumarate, which inhibit PHD activity by competing with α-ketoglutarate for the catalytic center of the enzyme, as seen in some cancers (*110*). Interestingly, pyruvate and lactate are similarly capable of stabilizing HIF-1α in normoxia, establishing a feed-forward loop between HIF signaling and the glycolytic products that might be important in malignant progression of cancer or for the metabolic status of stem cells (*111*, *113*).

Post-translational modification (PTM) of proteins is a mean to ultimately regulate protein function and downstream cellular processes. Most of these modifications make use of metabolic substrates, serving as an ingenious way for the cell to sense metabolic fluctuations and allow the integration of metabolic fluxes with cellular programs (*114*). Phosphorylation, glycosylation, prenylation, methylation and acetylation are possible PTMs (*114*). Importantly epigenetic modifications change global gene expression and modulate transcriptional networks involved for instance in pluripotency, differentiation, and tumorigenesis. Through the following examples, metabolism can control chromatin organization influencing the cellular transcriptional landscape. Epigenetics is based in specific acetylation and methylation reactions of histones and DNA. Histone acetylation normally associated with gene expression is mediated by histone acetyltransferases (HAT)

which require cytosolic acetyl-CoA as a substrate and are therefore dependent on its availability. The cytosolic acetyl-CoA pool can be fed by the mitochondrial citrate through a mitochondrial shunt and subsequent ACL conversion of this cytosolic citrate to acetyl-CoA. Acetylcarnitine, another mitochondrial-derived molecule has also been shown to serve as an additional substrate for nuclear acetylation of histones (*115*). Opposing the action of HATs are histone deacetylases (HDAC), comprised of several protein families one of which includes the NAD^+-dependent sirtuins, enzymes that respond to the intracellular redox state (*116*). Histone and DNA methylation are also intrinsically linked with metabolism. Firstly the activity of histone and DNA methylases depends upon the availability of S-adenosylmethionine (SAM) that serves as a methyl group donor, and is regenerated through the methionine cycle that communicates with the folate cycle (involved in the synthesis of glycine from serine) and with the reaction regenerating glutathione (*117*). Secondly, some of the histone demethylases (JmjC superfamily) and enzymes contributing for DNA demethylation (TET1) are equally reliant on α-cetoglutarate, oxygen and ascorbate akin to what was discussed for PHD (*114*, *116*).

These are just some examples of converging points between metabolism and other cellular programs within the intricate regulatory network supporting the execution of cellular processes (growth, self-renewal and differentiation).

1.6) Aims and hypothesis of the present thesis

For the present thesis, our general hypothesis is that metabolic remodeling and cell differentiation are mutually interconnected, i.e., manipulating one factor will also lead to alterations in the other.

In order to test the general hypothesis, we will investigate two distinct specific aims, which are presented separately in chapters II and III.

Chapter II

The objective of this specific aim is to demonstrate that the differentiation of myoblasts (muscle progenitors) is associated with a remodeling of metabolism.

H9C2 myoblasts are recurrently used as a model for cardiomyocytes in toxicological studies (*118–120*). Despite of the existence of well-established protocols to differentiate these cells into either cardiac-like or skeletal muscle-like cells the vast majority of studies do not take into account the specific differentiation state of these cells (*121*, *122*). We believe that this must pose an incorrect determination of the real toxicity of studied toxicants as the differentiation of H9c2 may result in differential susceptibility to drugs. A process that may underlie this phenomenon is a remodeling in cell metabolism, supporting cell differentiation. We therefore pretend to use this model to gain some insights of the modeling of metabolism occurring with muscle cell differentiation.

In this specific aim, we will evaluate putative metabolic shifts during cell differentiation by comparatively studying the metabolic profiles of parental H9c2 myoblasts and their differentiated counterparts. NMR-based isotopomer analysis will be applied to get detailed understanding of the utilization of glycolytic and mitochondrial pathways.

Chapter III

In this specific aim, we will aim at modulating mitochondrial metabolism to control the process of cell differentiation.The influence of mitochondria and metabolism in stem cell differentiation has not been appropriately addressed. Recent studies suggest that metabolism is indeed a crucial factor in the stem cell equation, potentially affecting cell physiology and functions such as self-renewal, proliferation and differentiation (*85*). Pluripotency one of the major embryonic stem cell's asset may also be influenced by metabolism. To study the importance of metabolism to the cell differentiation we will modulate mitochondrial metabolism during *in vitro* neuronal differentiation of mouse embryonic stem cells. We will use antimycin A, a recognized specific inhibitor of mitochondrial complex III at different stages of the differentiation protocol and evaluate any change in the differentiation efficiency and in cell physiology. As some previous studies describe a progressive mitochondrial maturation accompanying stem cell differentiation (*71*, *123*) we hypothesize that antimycin A treatments may differently affect distinct cell populations simultaneously present in culture.

This is a **relevant** work which will contribute to increase the knowledge regarding

Chapter 2

Metabolic Remodeling During H9c2 Myoblast Differentiation: Relevance for *In Vitro* Toxicity Studies

---

Abstract:

H9c2 cells, derived from the ventricular part of an E13 BDIX rat, possess a proliferative and relatively undifferentiated phenotype, but can be readily directed to differentiate under reduced serum conditions originating cells presenting muscle features. Skeletal or cardiac phenotypes can be originated depending on whether or not serum reduction is accompanied by a daily treatment with *all-trans*-retinoic acid. In the present study, we aimed to characterize and compare the metabolic profile of H9c2 cells at various differentiation states, correlating the differences between different populations with muscle-specific development. We determined that H9c2 myoblasts remodel their metabolism upon differentiation, with undifferentiated cells more reliant on glycolysis, as demonstrated by higher lactate production rates. Differentiated cells adopted a more oxidative metabolism with better coupling between the glycolytic and oxidative pathways, which is indicative of a metabolic evolvement towards a higher energetic efficiency state. Our findings emphasize the metabolic differences between differentiated and undifferentiated H9c2 cells, and raise caution on how to adequately select the H9c2 differentiation state that will act as the better model for the design of experimental studies.

Keywords: H9c2 myoblasts; differentiation; metabolism; NMR isotopomer analysis**;** cardiotoxicology

2.1) Introduction

Mammalian cardiomyocyte differentiation is a complex process, and throughout the different stages of cardiac development the evolving transcriptome must intimately and dynamically adjust to external stimuli, leading to the adaptation of cell structures to their specific biological developmental context (*124*). Cardiac bioenergetics are a good example, being progressively altered in order to simultaneously adapt to environmental cues and meet cell metabolic requirements (*125*, *126*). Accordingly, the metabolic phenotype of cardiac cells is altered during differentiation/maturation with a parallel shift in the preferred substrates for ATP production (*127*). Fetal cardiac cells are exposed to relatively hypoxic conditions and consequently their metabolism is more adapted to the use of substrates such as glucose and lactate (*125*, *126*, *128*). Adding to this, the nature of the available substrates in the fetal environment may also account for this metabolic phenotype outcome. Circulating fetal levels of lactate are high (*129*, *130*), and although glucose levels are similar to those encountered in adults, the free fatty acid quantity in fetal blood is lower (*131*), contributing to an increased reliance in the glycolytic pathway and lactate oxidation, with fatty acid oxidation accounting only for less than 15% of fetal myocardial ATP production in newborn rabbits (*132*).

Although cardiac cells in the early newborn still use glycolysis to supply around half of the total ATP produced (*128*, *132*), the metabolic profile is rapidly shifted in a period of days and mitochondrial fatty acid oxidation (FAO) appears as the

prevalent energy source with glycolysis providing only 10% of the total ATP produced (*125*, *126*, *128*). The switch may result from the integration of external stimuli such as increased oxygen tension and diet alterations as mammalian newborns are fed on high fat breast milk (*126*, *133*). Adult heart maintains a predominantly mitochondrial oxidative metabolism, and even considering the variety of substrates the heart can use (*134*), fatty acids are still the preferred fuel during normal physiological conditions.

The H9c2 cell line was isolated from the ventricular part of a thirteenth-day rat embryo and presents a myoblastic proliferative phenotype while maintained in normal 10% fetal bovine serum (FBS) containing culture media (*135*). Since its derivation, H9c2 cells have been extensively applied as a model for cardiac cells in a multiplicity of studies intending to address not only the mechanisms of cardiac differentiation (*136*) but also cardiac hypertrophy (*137*), cardiotoxicology (*118*, *119*, *138*) ischemia/reperfusion injury (*122*), and oxidative stress (*122*, *139*), among others.

An advantageous peculiarity of H9c2 myoblasts is the ability to differentiate into adult muscle cells. On the other hand, addition of retinoic acid (RA) during serum reduction favors a cardiac phenotype at the expense of skeletal muscle transdifferentiation, resulting in an increase in cardiac-like cells in the overall population (*140*). Despite the straightforwardness of the differentiation process, the vast majority of the studies using H9c2 cells do not take into account their differentiation state (*121*, *122*), disregarding possible differentiation-related

effects. Indeed, our own experience has shown dissimilar susceptibility of differentiated and undifferentiated H9c2 cells to some cardiotoxicants including isoproterenol. Thus, a better knowledge of the biochemical alterations during H9c2 differentiation is very important in the context of the reliability of the model in toxicological, pharmacological or other studies. The goal of the present study was to investigate whether H9c2 metabolism is altered during cell differentiation.

Our results demonstrated metabolic changes induced by the differentiation protocol, which were in accordance with *in vivo* muscular development, further stressing the need for using a proper differentiation state when applying this cell model to various toxicological or pharmacological studies.

2.2) Materials and Methods

2.2.1) Materials

D_2O (99.9%) and uniformly ^{13}C enriched glucose ([U-^{13}C]glucose) (98%) were obtained from Cambridge Isotope Laboratories (CIL), Inc (Andover, MA). For cell culture, if not further described in respective section, reagents were obtained from Gibco-Invitrogen (Barcelona, Spain). All other chemicals used were of the highest purity available and were purchased from Sigma-Aldrich (Barcelona, Spain).

2.2.2) Cell culture and differentiation procedure

H9c2 cell line, originally derived from embryonic rat ventricle through the method of selective serial passages, was purchased from America Tissue Type Collection (CRL-1446) (Manassas, VA). Cells were maintained in a proliferative state by culture in high glucose DMEM (Sigma, D5648) supplemented with 3.7 g/L sodium bicarbonate, 10% fetal bovine serum, 100 U/mL of penicillin and 100 μg/mL of streptomycin, at 37°C in a humidified atmosphere of 5% CO_2. Medium was changed every 2–3 days, and cells were split once they reached 70–80% confluence. Differentiation was initiated by changing the medium to high glucose DMEM (same supplementation) but with 1% FBS. In some differentiation conditions, media was daily supplemented with 10 nM retinoic acid (Sigma, R2625) in order to improve cardiomyocyte yield. Culture in 1% FBS containing

medium was continued for a period of 6 days and the medium was changed on the third day.

2.2.3) Western blot analysis

Total cellular extracts from differentiated and undifferentiated H9c2 cells were obtained as previously reported (*118*). After protein denaturation at 100°C for 5 min in Laemmli buffer (BioRad, Barcelona, Spain), 15 μg of protein from each sample was separated by electrophoresis on 12% SDS-polyacrylamide gels (SDS-PAGE) and electrophoretically transferred to a polyvinylidene difluoride membrane. After blocking with 3% BSA, for cardiac myosin light chain II (MLC2v) antibody, or 5% milk (for cardiac troponin T antibody) in PBS supplemented with 0.1% of Tween 20 (PBST) for 1 hours at room temperature, membranes were incubated overnight at 4°C with antibodies directed against MLC-2v (rabbit anti-MLC-2v; 1:1600, Abcam, Cambridge MA, USA) and Troponin T (mouse anti-Troponin T; 1:1000, Abcam, Cambridge MA, USA). Membranes were further incubated with secondary antibodies goat anti-rabbit IgG (for anti- Phospho-troponin I and anti-MC-2v antibodies; 1:20000) or goat anti-mouse (for anti-troponin T antibody; 1:20000), HRP-conjugated, for 1 hours at room temperature. Secondary antibodies were obtained from Jackson immunoResearch (West Grove, PA, USA). Chemiluminescence detection was carried out using the FluorChem™ system (Alpha Innotech, San Leandro, CA, USA). Membranes were also stained with Ponceau reagent to confirm equal

protein loading in each lane. This technique was used instead of "house-keeping" proteins, since the differentiation process may alter their intra-cellular content.

2.2.4) Immunocytochemistry

After differentiation processes, H9c2 cells (35,000 cells/mL) were seeded on glass coverslips in 6 well plates and allowed to recover for 24 hours in respective differentiation media. For the detection of Cardiac Myosin Heavy Chain (MF-20 Antibody, Developmental Studies Hybridoma Bank, Iowa City, IA), the cell incubation media was removed and cells were fixed and stored at -20°C in ice-cold absolute methanol. Following rehydration with PBST during 5 minutes for 3 times, cells were incubated in blocking solution (PBST supplemented with 1% nonfat powdered milk) for 30 minutes at 37°C, probed with specific primary antibody (MF-20) during 2 hours at 37°C and stained with TexRed-conjugated secondary antibody (goat anti-mouse, dilution 1:50, Jackson ImmunoResearch Laboratories, Inc.), containing 5μg/mL of Hoechst 33342 (Invitrogen), for an additional 2 hours at 37°C. Between labeling with primary and secondary antibodies, cells were rinsed 3 times with PBST during 5 minutes each.

2.2.5) NMR analysis

For metabolism assays, cell culture was performed on 150 mm dishes to yield sufficient cell numbers for NMR analysis. Cells were expanded and differentiated

as described above. Following the differentiation process or when cells reached 70% confluence (undifferentiated cell conditions), cells were washed with phosphate-buffered saline (PBS), and incubated for 48h with 30 mL of freshly made DMEM without phenol red, supplemented as referred above but this time by replacing normal glucose with uniformly ^{13}C enriched ([U-^{13}C]) glucose.

To quantify glucose consumption and lactate production, 200 μL of the incubation medium was sequentially collected and immediately frozen at different time points (0, 1, 4, 8, 24 and 48 hours). At the final endpoint and after medium collection, cells extracts were prepared. To this end cells were trypsinized following PBS-EDTA washing. The cell pellets were then rigorously weighed and a volume of a 7% perchloric acid (PCA) solution was added at the ratio of 2 mL of PCA solution per 1 g of cells pellet. The homogenate was then centrifuged (9,000xg for 10 min at 4ºC) and the supernatant collected. Supernatant was neutralized (~pH 7) with a minimum volume of KOH. The supernatant resulting from a new centrifugation was freeze-dried. PCA extracts were subsequently dissolved in 200 μL D_2O for proton (^1H-) and carbon 13 (^{13}C-) NMR analyses.

NMR samples of cell media for ^1H NMR analyses were prepared by mixing 160 μL of media with 40 μL of a sodium fumarate solution (10 mM, 99%D_2O), used as internal standard. ^1H NMR spectra were acquired in a 14.1 Tesla Varian NMR spectrometer using a 3-mm NMR probe. ^1H NMR spectral parameters included a 30º radiofrequency pulse, an interpulse delay of 10 s and 32k points covering a

9.0 kHz spectral width. Spectra deconvolution to quantify the metabolites was performed using the PC-based NMR program NUTSpro™ (Accorn Inc., Freemont, CA).

^{13}C NMR spectra were acquired using the same spectrometer and probe and acquisition parameters included a 45º radiofrequency pulse a 3s interpulse delay to ensure full relaxation of glutamate aliphatic carbons and 131,000 points defining a spectral width of 40 kHz. Deconvolution of ^{13}C multiplets for ^{13}C NMR isotopomer analysis was also made using NUTSpro™.

2.2.6) Metabolic analysis

Metabolic analyses of H9c2 cells were based on measures of rates of lactate appearance in the culture medium, as a measure of glycolysis (24), and on quantification of ^{13}C enrichments of intermediate metabolites, namely lactate, alanine and glutamate, as well as on the correlation between Krebs cycle turnover (glutamate ^{13}C isotopomers (24, 25)) and oxygen consumption measurements.

2.2.7) Oxygen consumption assessment

Oxygen consumption rates were evaluated for the three distinct experimental groups: undifferentiated cells, and differentiated cells both with and without 10 nM retinoic acid. The 96 well BD (San Jose, CA) Oxygen Biosensor System plate

was used according to the protocol previously described elsewhere (*141*) and has been positively validated against the Clark-type oxygen electrode (*142*). Summarizing, cells were trypsinized and plated at a density of 200,000 cells/well, and the volume was corrected to achieve 200 μL/well. To avoid interference during readings, plating procedure and O_2 consumption assays were performed using DMEM without phenol red (Sigma, D5648). This medium was supplemented with 4.5 g/L glucose, 3.7 g/L sodium bicarbonate, 0.584 g/L of L-glutamine and 100 U/mL of penicillin/100 μg/mL of streptomycin to meet the same specifications of regular DMEM. No FBS was added to the medium. Cells were incubated for 30 minutes at 37ºC and 5% CO_2 in a humidified atmosphere. Maximal mitochondrial respiration was obtained by using carbonyl cyanide 4-(trifluoromethoxy) phenylhydrazone (FCCP) at a final concentration of 10 μM. After the incubation period, FCCP was added to the corresponding wells and readings were immediately initiated in a SectraMax Gemini EM (Molecular Devices, Sunnyvale, CA). Plates were bottom scanned at a stable temperature (37ºC) with an excitation wavelength of 485 nm and an emission wavelength of 630 nm. Specificity of the assay was confirmed by a decrease in O_2 consumption using rotenone (2.5 μM) or antimycin A (2 μM) mitochondrial complex I and III inhibitors, respectively. Raw data was submitted to a two-step normalization protocol, comprising two sequential divisions. First, the fluorescence intensity obtained for a given well was divided by the pre-blank reading (empty well) for the same well, reducing both the machine drift and probe concentration induced variations. This value was subsequently divided by the fluorescence of the

ambient control (DMEM with no cells). Maximal O_2 consumption rates were calculated from the maximal slope of fluorescence plots. Experiments were repeated for a total of n=6 for the undifferentiated cells and n=4 for the differentiated cells.

2.2.8) Statistical analysis

Data analyses were performed using Microsoft Office Excel as a platform for data treatment and using both GraphPad Prism 4 and JMP 8 statistical softwares. Normality and homoscedasticity tests were performed. Statistical differences found by one or two way ANOVA were considered significant when $p<0.05$. Data is presented as means ± SD.

2.3) Results

Differentiation of H9c2 cells was performed through the reduction of fetal bovine serum content from 10% to 1% in the cell culture medium. As described in the literature (*140*), this protocol preferentially induces a myogenic differentiation yielding multinucleated cells harboring a skeletal muscle phenotype. Alternatively, concomitant serum reduction with a daily addition of 10 nM RA forces cells to adopt a cardiac-like phenotype, with the appearance of branched multinucleated cells, presenting lineage specific markers. Cell differentiation was confirmed through optical and epifluorescence microscopy and western blotting analysis (Fig. 2.1 and Fig. 2.2). Morphology evaluation of the three different cell populations revealed striking differences. Undifferentiated H9c2 cells appear generally as small mononucleated and irregular spindle shaped cells (Fig. 2.1A), while differentiated cells are recognized for being either long multinucleated myotubes typical of skeletal muscle cells (cells differentiated in 1% FBS) (Fig. 2.1A, middle panel) or long branched multinucleated cells in the case of the cardiomyocyte differentiation protocol (Fig. 2.1A, bottom panel). Immunocytochemistry for the sarcomeric myosin heavy chain protein (Fig. 2.1B), a protein present in both cardiac and skeletal striated muscle cells, demonstrates that about 25-30% of H9C2 cells show a strong labeling of this marker of adult muscle cells (Fig.2.1C). Many other cells showed a weaker MF20 labeling but were not considered in the counting. Fig. 2.1B shows the distinct labeling pattern of the three distinct H9c2 cells populations. Cardiac troponin T plays an

important role in the contractile system and although it may also be transiently present in a confined stage of fetal skeletal muscle development (*143*), it is normally used as a specific marker for cardiac cells (*144*). Fig. 2.2, left panel, shows increased troponin T in the RA-treated group, confirming the acquisition of a cardiac identity by those cells. Another cardiac marker used in the present study was cardiac myosin light chain 2 (Mlc2v) (*145*), which was more present in H9c2 cells differentiated with RA in low serum media. Interestingly, although troponin T was mostly present in RA-differentiated cells, a smaller amount of Mlc2v protein was also present in 10% and 1% FBS (no RA) grown cells (Fig. 2.2, left panel). In fact, the process of H9c2 differentiation is very dependent on the initial cell confluence and how cells were maintained in terms of confluence until the differentiation process begins (Oliveira et al., unpublished data). The proportion of Mlc2v and cardiac troponin T in the three experimental groups is thus variable, although the RA-treated group has always the highest amount of the two specific cardiac markers (Oliveira et al., unpublished data). Regardless of these considerations, differences in terms of both muscle markers and cell phenotype were always very clear between undifferentiated and differentiated cells. Also, and as expected, cell differentiation also resulted in decreased cell proliferation and decreased DNA synthesis (data not shown).

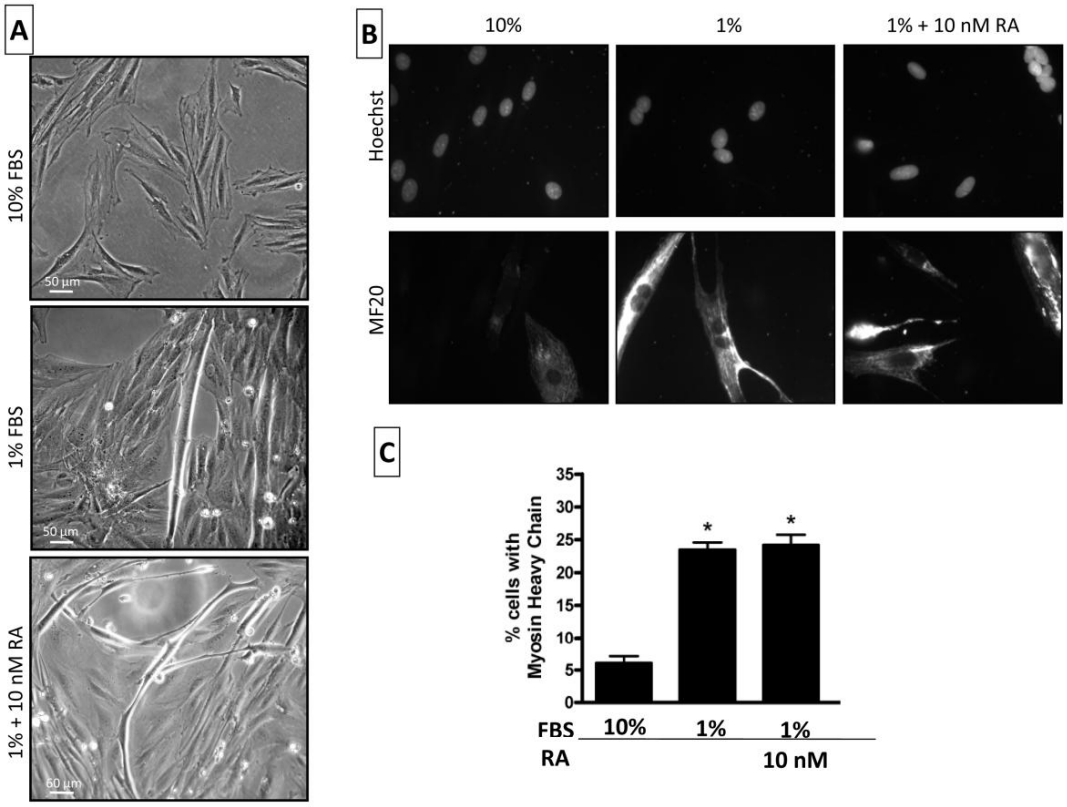

Fig. 2.1 – H9c2 cells differentiation characterization. (A) Left panels depict the typical morphology of undifferentiated mononucleated and small spindle shaped myoblasts. Decrease of serum to 1% leads to the appearance of multinucleated long skeletal muscle myotubes, while concomitant daily addition of 10 nM retinoic acid (RA) induces differentiation into long and multinucleated cardiomyocytes. (B) epifluorescence images of H9c2 myoblasts in the diverse differentiation protocols fixed and labeled with myosin heavy chain antibody (MF20) and counterstained with Hoechst. Images and quantification of cell showing strong MF20 labeling (C) show an increase in the number of cells expressing myosin heaving chain after serum withdrawal or serum withdrawal plus retinoic acid (n=4 separate experiments from independent cell cultures).

Metabolic profile assessments were performed on differentiated and undifferentiated H9c2 cells using NMR. ^{1}H NMR spectra allow the assessment of total metabolite levels in the analyzed sample i.e. labeled and unlabeled species. ^{13}C enriched and unenriched metabolites are distinguished on the basis of the ^{1}H-^{13}C heteronuclear scalar coupling. Rates of glucose consumption throughout 48 hours were relatively low and removal of glucose from the medium was too

small to allow adequate determination by ^{1}H NMR analysis. As for lactate, levels of unlabeled (^{12}C) and uniformly labeled ([1,2,3-$^{13}C_3$]lactate) were easily determined throughout the entire 48 hours. ^{12}C lactate levels were in general low and constant throughout the entire time period of the assay (data not shown). Contrasting with this, [1,2,3-$^{13}C_3$]lactate produced by the cells and excreted to the medium accumulated consistently in all conditions, but more notably in undifferentiated cells, especially at later time points (Fig. 2.3). This fact is predictive of a higher glycolytic rate in undifferentiated cells as lactate is a direct by-product of glycolysis, and the conversion of pyruvate to lactate is essential for sustaining glycolysis.

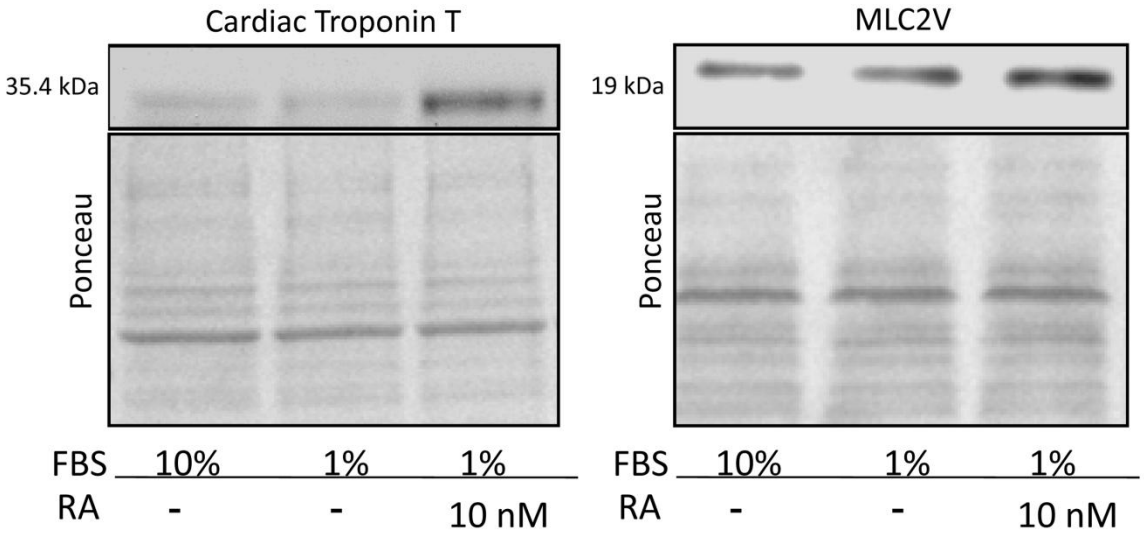

Fig. 2.2 - Western blot analysis of cardiac troponin T and cardiac myosin light chain (Mlc2v) revealed an increase in protein resulting from the differentiation protocol, which is particularly evident in cells treated with RA (n=4 separate experiments from independent cell cultures) for troponin T. The lower image present a section of the membrane stained with Ponceau Red, for equal protein loading confirmation.

For further metabolite quantification, cells were submitted to PCA extractions and analyses by 1H and 13C NMR. Fig. 2.4A shows representative 1H NMR spectra for the three conditions, focusing on the methyl resonances of lactate and alanine. The alanine pool in the cytoplasm is in fast exchange with the pyruvate pools and by being more stable and consequently easier to quantify, is often used as an indirect quantification of pyruvate. In fact, the lactate to alanine ratio is a good indicator of the cytosolic redox state, since the interconversion of pyruvate to lactate catalyzed by lactate dehydrogenase (LDH) is one of the major regulators of cytosolic NADH/NAD^+ levels (*146*). Spectra analysis showed that undifferentiated cells (10% FBS) presented higher levels of total lactate (unlabeled and labeled lactate as perceived from the greater relative height of both the doublet (d) and multiplet (c) components, respectively) which were not accompanied by similar increases in total alanine levels, resulting in significantly higher lactate/alanine ratios (Fig. 2.4B). This is compatible with higher NADH/NAD^+ ratios in undifferentiated myoblasts than in their differentiated counterparts.

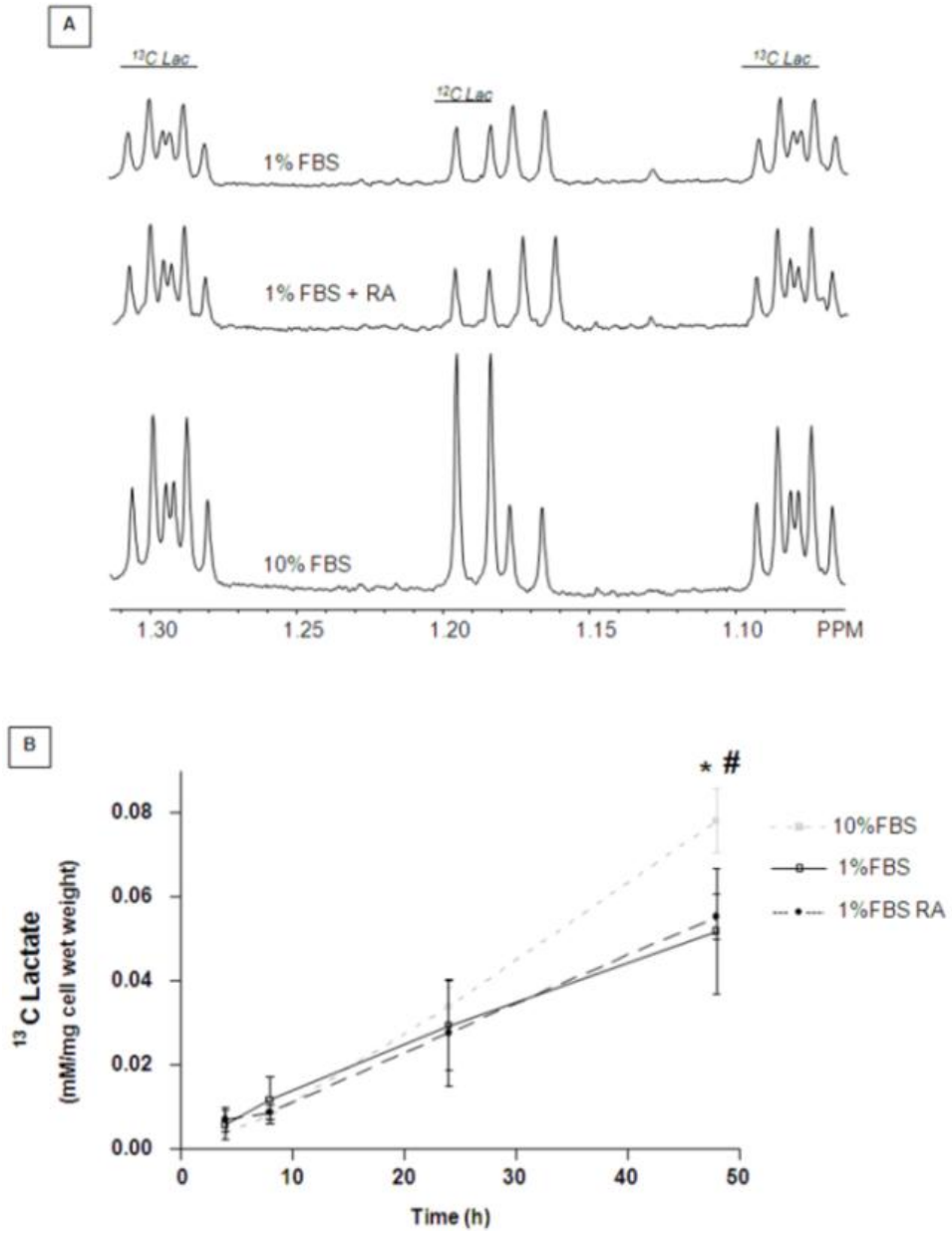

Fig. 2.3 – Accumulation of lactate in the cell medium. (A) Shows expansions of lactate resonances (^{13}C Lac and ^{12}C Lac) from representative ^{1}H NMR spectra of cell medium samples collected at 48 h. Unlabeled lactate (^{12}C Lac) resonance originates essentially from FBS, reason why it is approximately 10 fold more intense in undifferentiated cells. Lactate concentrations (B) were corrected for volume variations due to sample collection, and normalized by cell wet weight. Two way ANOVA was performed for 8, 24 and 48 h. Highly significant differences in concentrations were encountered for 48 h when comparing undifferentiated cells (10% FBS) vs. skeletal muscle cells (1% FBS) (* $p<0.001$) and undifferentiated cells (10% FBS) vs. cardiomyocytes (1% FBS plus RA) (# $p<0.01$). Data was normal and homoscedastic. Two way ANOVA was followed by a Bonferroni's post hoc test. Error bars indicate SD (n=4-7 separate experiments from independent cell cultures).

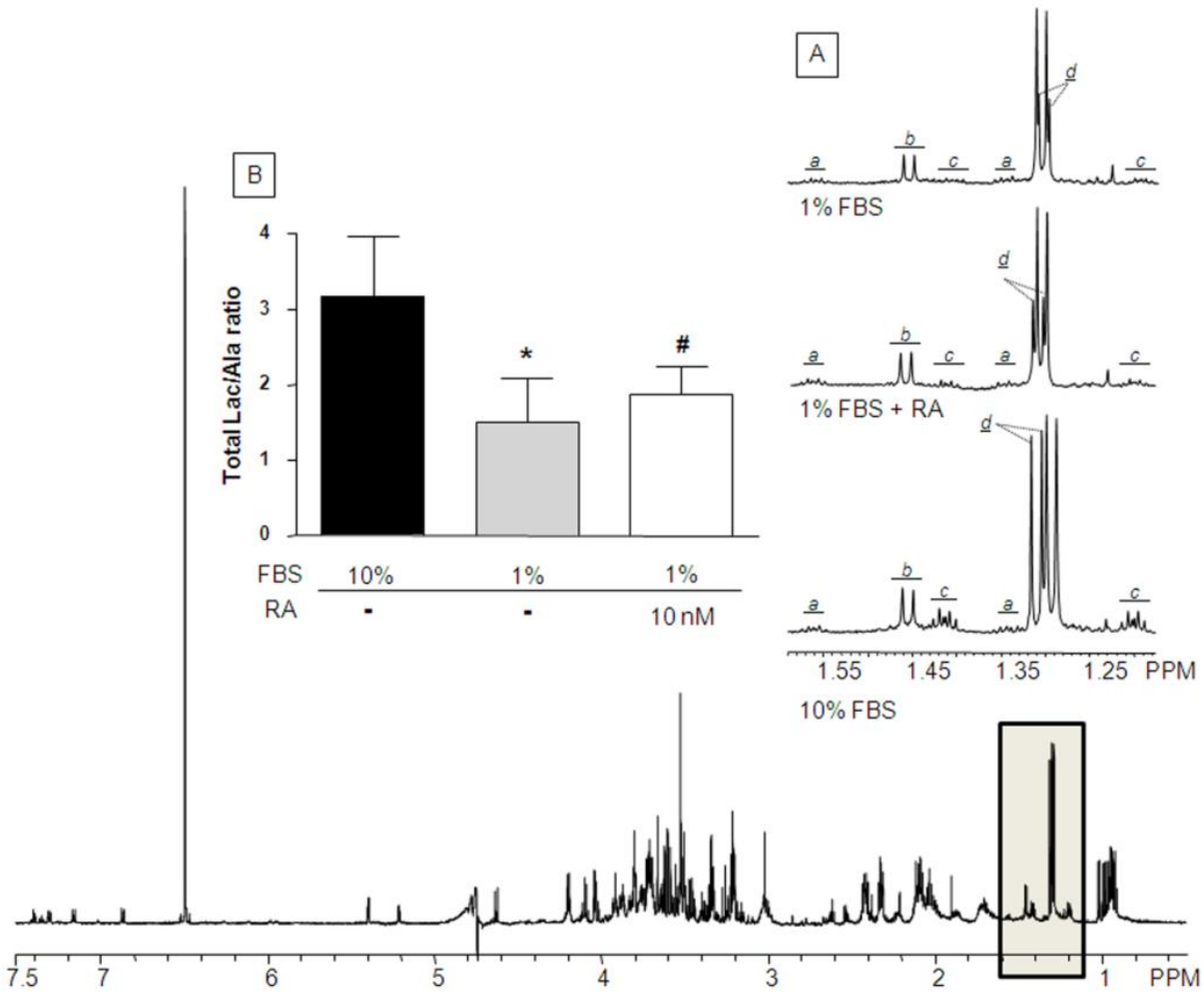

Fig. 2.4 – Representative ^{1}H NMR spectra of neutralized PCA cell extract from undifferentiated cells.

Box corresponds to the region containing methyl peaks from lactate and alanine, which were further highlighted by the corresponding spectral sections from the three groups of cells, depicted above (A). Peaks were analyzed for the estimation of total (^{13}C + ^{12}C) lactate/alanine ratios (B), indicative of the cytosolic redox state. Lactate levels were higher in myoblast but alanine levels did not follow such increase, resulting in higher lactate/alanine ratios in undifferentiated cells. *a*: labeled alanine multiplet; *b*: unlabeled alanine doublet; *c*: labeled lactate multiplet; *d*: unlabeled lactate doublet. Data was normal and homoscedastic, and was analyzed by one way ANOVA followed by a Dunnett's post hoc test. Highly significant differences are present when comparing undifferentiated cells *vs.* skeletal muscle cells (* $p<0.01$) and undifferentiated cells *vs.* cardiomyocytes (# $p<0.05$). Error bars indicate SD (n= 4-6, separate experiments from independent cell cultures).

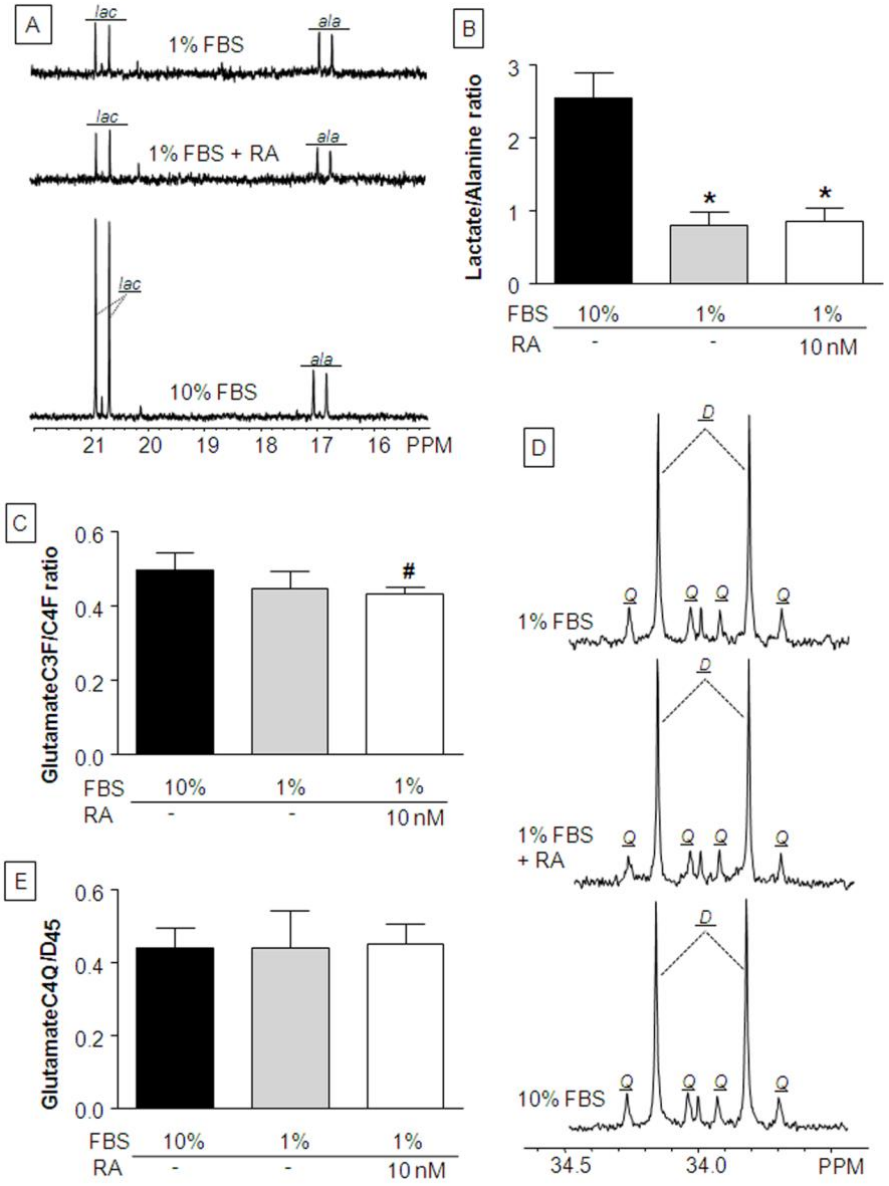

Fig. 2.5 – ^{13}C NMR analysis of neutralized PCA cell extracts. (A) Spectral sections containing lactate and alanine C3 peaks, revealing a marked decrease in ^{13}C lactate quantities in both types of differentiated cells compared to undifferentiated myoblasts. Accordingly, those differences were significantly reflected in ^{13}C lactate/alanine ratios as showed in (B). Anaplerosis contributions to the Krebs cycle, analyzed through glutamate C3F/C4F ratios, were decreased in both differentiated cells, being significantly different from myoblasts in the case of cardiomyocytes (C). (D) Shows the expanded glutamate C4 resonances for the extracts of cells from the three groups. (E) Depicts glutamate C4Q/D45 ratios which are informative of the TCA cycle turnover, revealing no difference between the three groups of cells. Data was normal and homoscedastic, and was analyzed by one way ANOVA followed by a Dunnett's post hoc test. In B highly significant differences are present when comparing differentiated *vs.* undifferentiated cells (* p<0.01). In C, significance is only observed in cardiomyocytes *vs.* myoblasts (# p<0.05). Error bars indicate SD (n= 4-6 separate experiments from independent cell cultures). *Lac*: lactate; *Ala*: alanine; *D*: doublet D45; *Q*: quartet.

Lactate to alanine ratios were also determined using only the labeled isotopomers of the two metabolites ([1,2,3-$^{13}C_3$]lactate and [1,2,3-$^{13}C_3$]alanine), species directly formed from glycolysis. This analysis made use of ^{13}C NMR spectra of the cellular PCA extracts (Fig. 2.5A). As depicted in Fig. 2.5B, this ratio was particularly different when comparing both populations of undifferentiated and differentiated cells, being significantly reduced in the last ones. This data corroborates the idea inherent to Fig. 2.3 that the glycolytic rate was higher in undifferentiated cells. A higher rate of glycolysis with subsequent reduction of pyruvate to lactate by LDH allows a more extensive exchange of intracellular lactate pools and higher ^{13}C fractional enrichment. This warrants close lactate/alanine ratios in undifferentiated cells (approximately 2.5) using either total pools or enriched pools but much smaller ratios (ap. 0.85) in differentiated cells (Fig. 2.4B vs. Fig. 2.5B).

^{13}C NMR spectra from the cells extracts were also used to evaluate Krebs cycle activity in these cells through the study of relative incorporation of ^{13}C in their intermediates. We focused on glutamate, a metabolite that is in constant exchange with α-ketoglutarate pools and is sufficiently abundant for a proper quantification. Fractional enrichment of glutamate C4 (C4F) is a direct measure of the ^{13}C enrichment of the acetyl-CoA being oxidized. On the other hand, incorporation of ^{13}C in glutamate C3 (or C2) is dually dependent, reflecting simultaneously Krebs cycle turnover and activity of anaplerotic pathways. Therefore, a C3F/C4F ratio is an informative measure of the anaplerotic

contribution to the Krebs cycle. Fig. 2.4C refers to the glutamate C3F/C4F ratios for the populations of cells under study. Results expose a statistically significant ($p<0.05$) decrease in more cardiac-like cells (1% FBS-RA) ratios comparing to undifferentiated cells. More skeletal-like muscle cells (1% FBS) also demonstrated a decrease in C3F/C4F ratios but not sufficiently to be significant. The above data describes a clear tendency for a higher C3F/C4F ratio in undifferentiated cells, when compared with differentiated cells. Glutamate isotopomers can provide additional information, namely related to the turnover of the Krebs cycle. For example, if referring to the glutamate C4 peaks, ^{13}C spectra can prove informative in discriminating between [4-^{13}C] (singlet, S), [4,5-$^{13}C_2$] (doublet, D45), [3,4-$^{13}C_2$] (doublet, D34) and [3,4,5-$^{13}C_3$] (quartet, Q) glutamate isotopomers. The use of [U-^{13}C]glucose in the present study allows the formation of only one form of labeled acetyl-CoA isotopomer, the [1,2-$^{13}C_2$] acetyl-CoA, and consequently incorporation of this labeling pattern in the Krebs cycle will necessarily incur in the formation of [4,5-$^{13}C_2$] glutamate in its first turn. Appearance of the C4Q from [3,4,5-$^{13}C_3$] is only possible by C3 positional enrichment in the following turns of the cycle. Thereafter C4Q/C4D45 ratio serves as an evaluator of the turnover of the cycle. A comparison of the C4 resonances (Fig. 2.5D) for the three cell groups revealed no significant differences between undifferentiated and differentiated cells (Fig. 2.5E), which may indicate that the Krebs cycle turnover is not majorly affected by the differentiation process.

Oxygen consumption rates were evaluated for the three groups of cells, using the 96 well BD Oxygen Biosensor System. As demonstrated in Fig. 2.6, both types of differentiated cells presented elevated values of maximal oxygen consumption rate when compared to myoblasts, but are undistinguishable from each other. Oxygen consumption rates are higher in the RA-treated group (p=0.02), and even though we cannot consider the increased oxygen consumption rate in more skeletal muscle-like cells as being significant (p=0.06), we can certainly affirm that there is a trend for an increased maximal respiration during the differentiation process in general.

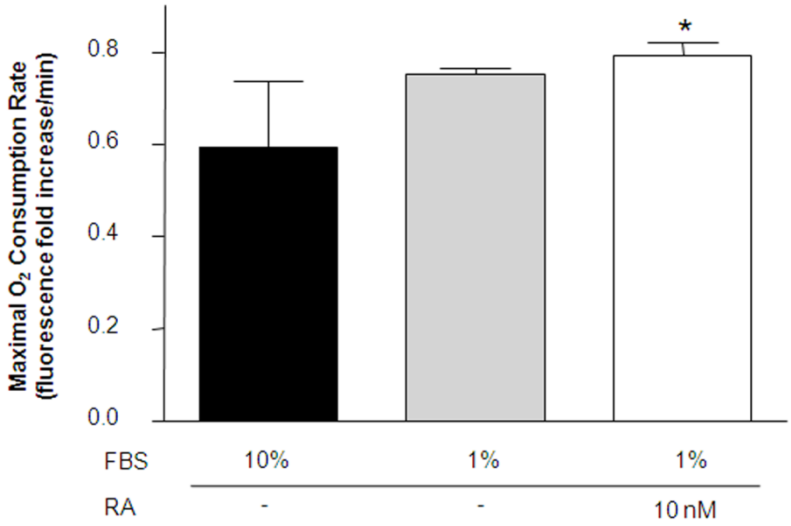

Fig. 2.6 – Maximal O_2 consumption rate as assessed by fluorescence increase using the 96 well BD Oxygen Biosensor System plate. 200,000 cells per well in a total 200 µL of DMEM without FBS or phenol red were used. Respiration was stimulated by the mitochondrial uncoupler FCCP (10 µM). Experiments were conducted in a stable temperature (37ºC), and plates were bottom read (Exc.485 nm/Em.630 nm) for approximately 40 minutes. Maximal slope, corresponding to the maximal O_2 consumption was taken from each graph. Data was normal and homoscedastic, and was analyzed by one way ANOVA followed by a Dunnett's post hoc test. Significant differences were encountered when comparing undifferentiated cells grown under 10% FBS and cardiomyocytes differentiated with 1% FBS and 10 nM RA ($^{\#}$ $p<0.05$). Although also elevated, skeletal muscle cells (1% FBS) O_2 consumptions are not considered significantly different from the undifferentiated cells (p=0.06). Error bars indicate SD (n= 4-6 separate experiments from independent cell cultures).

2.4) Discussion

Metabolic phenotypes for the three cell groups originated from the H9c2 cell line were analyzed throughout this work. The data described in Fig. 2.1 and 2.2 confirms that the three culture conditions yield three different cell populations, two of them containing a majority of adult, differentiated, muscle cells. [U-^{13}C]glucose was used as a substrate in order to isotopically trace the intermediary metabolic pathways of those cells. Simultaneously, [U-^{13}C]glucose can provide information about glycolysis and lactate fermentation (throughout the analysis of lactate in incubation media), and Krebs cycle kinetics plus anaplerotic fluxes (by the evaluation of ^{13}C incorporation in Krebs cycle intermediates or metabolites in fast exchange with these) (*147*).

In the present work, we clearly demonstrated that undifferentiated cells were characterized by increased glycolytic fluxes, higher lactate/alanine ratios, consistent with increased cytosolic redox state (*146*), higher glutamate C3F/C4F, identical glutamate C4Q/C4D45 and lower oxygen consumption. All these metabolic parameters are consistent with cells possessing high proliferative capacity, a characteristic of immature cardiomyocytes present in fetal or immediate postnatal heart (*146*). In this study, we have not encountered major metabolic differences between the two populations of differentiated cells, although one contained a higher proportion of cells with putative cardiac characteristics.

Resembling what was reported as the Warburg effect in several tumor cells, highly proliferating cells also rely upon a predominantly glycolytic pathway (*78*). This fact could apparently pose a paradox, particularly in immature proliferating cells in which the oxidative machinery might still be incompletely established (*46*, *148*), as glycolysis is "energetically inefficient" when compared to oxidative metabolism. This paradox can be easily deconstructed, if one assumes that: i) most malignant tumors (as other cells) parallel to the raise in glucose uptake also maintain constant respiration levels (*149*): ii) the energy restrictions inherent to glycolysis are only materialized in the presence of limited resources, which normally is not the case *in vivo* (*78*) and in normal *in vitro* culture conditions such as the ones reported here. More importantly, increased glycolysis is capable of supplying the cell with building blocks for fast cell proliferation (*78*). This metabolic phenotype is present in myoblastic cells, where an increased lactate production is not associated with higher oxidative metabolic rates.

Higher glycolysis and lower oxygen consumption reveal an inadequate coupling between non-oxidative and oxidative metabolic machinery, in that pyruvate produced in glycolysis is not adequately coupled to pyruvate transport and oxidation in mitochondria. This is readily seen by comparing total (Fig. 2.4B) and ^{13}C enriched (Fig. 2.5B) lactate/alanine ratios. In all cell groups, fractional ^{13}C enrichments of alanine are higher than those of lactate and this difference is more noticeable in differentiated than in undifferentiated cells. This is consistent with a more generalized exchange between lactate and pyruvate/alanine pools in

undifferentiated cells than in differentiated ones. This compartmentalized model of cell metabolism has been discussed thoroughly in literature both in cell cultures (*150*, *151*) and in isolated perfused organs (*152*). The pool of oxidizable pyruvate is more accurately defined by the pool of alanine, and an increase in alanine fractional enrichment in differentiated cells denotes a targeting of [U-^{13}C]glucose for oxidative metabolism in detriment of lactate production. Similar uncoupling mechanisms had been demonstrated to be present in highly proliferative tumor cells, being not only a consequence of decreased pO_2 but also edifying an active molecular regulatory mechanism. This process might result in protection against oxidative stress in the cells (*79*).

Distinct fractional enrichments between alanine and lactate could also be explained by distinct metabolic rates in the cell groups, with the differentiated cells being farther from metabolic and isotopic steady state. This would not be noticeable in the C4Q/C4D45 since the acetyl-CoA pool, derived from the "oxidizable" pyruvate in exchange with alanine pools, would possess a higher fractional enrichment.

The ratio of glutamate C3F/C4F was higher in undifferentiated cells. This observation can have several explanations: i) Krebs cycle flux is faster; ii) anaplerotic flux from enriched substrates is elevated; iii) anaplerotic flux from unenriched sources is reduced. Which of this is the adequate answer requires further evaluation of other metabolic parameters analyzed, namely O_2 consumption and size and enrichment of lactate pools. A faster Krebs cycle flux

would imply higher O_2 consumption, although we observe exactly the opposite in undifferentiated cells. Also, the size and enrichment of the lactate pool is higher in these cells. These two aspects in conjunction, point for more pronounced contribution of [1,2,3-$^{13}C_3$]lactate for anaplerosis, relatively to other provided unenriched substrates, giving rise to higher glutamate C3 enrichment (Fig. 2.5C). Krebs cycle in proliferating cells will not be specifically committed to the generation of reducing equivalents for the mitochondrial electron transport chain, but will specially serve as a hub communicating with different biosynthetic pathways. Since a significant reduction in Krebs cycle's intermediaries pools could be deleterious for mitochondrial physiology (*79*), replenishing mechanisms need to take action and proliferating myoblasts have higher anaplerotic rates than differentiated cells.

In summary, undifferentiated H9c2 cells promote their proliferation by increasing glycolytic flux and anaplerosis while differentiated cells increase their metabolic efficiency by better coupling between glycolysis and Krebs cycle, whatever the nature of this differentiated phenotype in this particular case, i.e. whether the final cellular fate is ultimately a skeletal or cardiac muscle cell. Also, there is an emerging interest in the role of metabolism in cell differentiation (*153*), which demonstrates the opportunity and interest of these type of studies.

H9c2 cells have been profusely used as a model for cardiomyocytes (*118–120*, *138*, *154*), but little emphasis has been given to their differentiation state. In accordance with our observations concerning the distinctive metabolic nature of

differentiated vs. undifferentiated, and their analogy to different *in vivo* developmental stages, a proper differentiation state should be used when toxicological or pharmacological studies are performed in this *in vitro* system. As stated, the main distinction of the present work is between undifferentiated cells versus cells that have been clearly differentiated to a more adult phenotype, whether this be ultimately a skeletal or cardiac muscular fate. Both populations show clear metabolic changes, which also implies that compounds that interact and modulate cell metabolism will have different effects according to the target cell population.

2.5) Acknowledgments

The authors thank Gonçalo Pereira, Dr. Mario Grãos and Dr. Anabela Rolo for their assistance in the different phases of the work.

2.6) Financial Support

SLP is the recipient of a PhD fellowship (SFRH/BD/37933/2007). The present work was funded by research grants POCI/SAU-OBS/55802/2004, PTDC/QUI/64358/2006 and PTDC/EBB-EBI/101114/2008 from the Portuguese Foundation for Science and Technology. We acknowledge the National NMR Network for access to the facilities. The Varian VNMRS 600 MHz spectrometer is part of the National NMR Network and was purchased in the framework of the National Program for Scientific Re-equipment, contract REDE/1517/RMN/2005, with funds from POCI 2010 (FEDER) and Fundação para a Ciência e a Tecnologia (FCT).

Inhibition of mitochondrial complex III blocks neuronal differentiation and maintains embryonic stem cell pluripotency

Chapter 3

Abstract:

The mitochondrion is emerging as a key organelle in stem cell biology, acting as a regulator of stem cell pluripotency and differentiation. In this study we sought to understand the effect of mitochondrial complex III inhibition by antimycin A during neuronal differentiation of mouse embryonic stem cells (mESC). mESC exposed to antimycin A failed to differentiate into dopaminergic neurons, maintaining high Oct4 levels even when subjected to a specific differentiation protocol. Antimycin-A-induced mitochondrial inhibition affected distinct populations of cells present in culture, inducing cell loss in differentiated cells, but not inducing apoptosis in mESC. A reduction in overall proliferation rate was observed, corresponding to a slight arrest in S phase. Also, antimycin A treatment induced a consistent increase in HIF-1α protein levels which correlates with glycolytic metabolism and pluripotency maintenance in stem cells. The present work demonstrates that mitochondrial metabolism is critical for neuronal differentiation and emphasizes that modulation of mitochondrial functions through pharmacological approaches can be useful in the context of controlling stem cell maintenance/differentiation.

Key words: Mouse embryonic stem cells, neuronal differentiation, mitochondria, Antimycin A, HIF-1α

3.1) Introduction

Although mitochondrial involvement in stem cell biology is far from being completely understood, the possible use of mitochondrial modulation to improve stem cell culture, differentiation and, more recently, reprogramming, has raised interest in recent years (*46*, *76*, *155–158*). Embryonic stem cells (ESCs) and induced pluripotent stem cells (iPSCs) are characterized by unlimited self-renewal and pluripotency. ESCs are derived from the inner cell mass (ICM) of the pre-implantation embryo (*6*, *11*) the former physiologically existing in a relatively hypoxic environment (1.5-5.3% O_2) (*159*). Accordingly, ESCs present a prevalent glycolytic metabolism and human ESC have been shown to be better maintained under hypoxic culture conditions (*160*, *161*). Interestingly these cells are capable of robustly growing under normoxia, while maintaining the same metabolic pattern (*77*, *160*). Seminal studies comparing ESCs and iPSCs showed that even though some dissimilarity may exist, the latter embrace a metabolic shift from aerobic oxidative phosphorylation (OXPHOS) towards glycolysis to complete reprogramming from an initial differentiated somatic state, thereby acquiring a metabolism that is comparable to ESCs (*70*, *162–164*). Indeed complete reprogramming of somatic cells to iPSCs apparently involves a metabolic shift towards glycolysis (with the related metabolic architecture restructuring), which reportedly precedes the onset of endogenous pluripotency markers expression (*75*). Furthermore, hypoxic conditions favor the cell reprograming process, both for mouse and human cells (*165*).

Aerobic glycolysis is a recurrent metabolic pattern in rapid proliferating cells including cancer cells, first described by Otto Warburg in what is now known as the Warburg effect (*66*). Despite apparently representing a less efficient metabolic process than aerobic mitochondrial OXPHOS, glycolysis does endow rapidly proliferating stem cells with a few advantages: a) fast ATP generation; b) decreased mitochondrial oxidative stress, as a consequence of reduced reactive oxygen species (ROS) generation in mitochondria, and increased NADPH formation, a substrate for antioxidant defenses regeneration in the pentose phosphate pathway; c) fast production of precursors compounds used for the synthesis of biomolecules (*78*, *79*, *166*).

The metabolic architecture of ESCs is in accordance with what is observed during embryonic development, particularly concerning mitochondria. Throughout initial embryo cleavage a reported bottleneck effect restrains mitochondrial DNA (mtDNA) replication and mitochondrial biogenesis, resulting in a drastic reduction in mitochondrial mass per ICM cell (*46*). Furthermore, mitochondria in ICM cells at this stage, exhibit the shape of small organelles with translucent matrix and few cristae, which is typical of an immature morphology (*46*). Specific patterning in mitochondrial localization was also identified during distinct phases of embryonic development with some stages denoting a characteristic mitochondrial perinuclear localization (*167*). In accordance, both ESC and iPSC are reported to share these mitochondrial properties (*123*, *162–164*, *168*, *169*).

As noted, somatic cells reprogramming via iPS involves an OXPHOS to glycolysis conversion. Contrariwise, conversion of pluripotent stem cells (whether ESCs or iPSCs)

into differentiated phenotypes involves the opposite metabolic remodeling, accompanied by a coordinated genetic and metabolic restructure. This is especially evident if the resulting cells correspond to an active cell type with large energetic requirements, such as neurons (*71*, *74*, *170*, *171*). Although some contradictory results have been reported (*172*), the emerging trend assumes that ESC differentiation involves an increment in mitochondrial mass, with a concomitant increase in more mature mitochondrial morphology (*123*, *169*, *171*). This increased mitochondrial mass is accompanied by a rise in O_2 consumption and ATP production, as well as a decreased lactate production, as expected in a metabolic shift from glycolysis to OXPHOS. The requisite of mitochondrial and metabolic maturation for differentiation was further validated by the fact that mtDNA or nuclear mutations affecting mitochondrial proteins precluded the completion of cell differentiation (*173*).

Mitochondrial function remodeling during pluripotent stem cell self-renewal, differentiation and reprogramming, suggests that modulation of mitochondrial functions may serve as a plausible tool to control both processes. In fact, treatment of both human ESCs (hESCs) and mouse ESC (mESCs) with mitochondrial complex III inhibitors antimycin A (AA) or myxothiazol, or uncoupling of the mitochondrial membrane potential (MMP) with CCCP, increases the expression of pluripotency markers and enhances cell pluripotency (*72*, *73*). The uncoupler CCCP also inhibited spontaneous stem cell differentiation (*73*).

Information on the effects of mitochondrial modulation during the differentiation of stem cells into neurons is scarce. A suggestive work of Vayssiére and colleagues using

clonal cell lines with neuroblastoma origin showed that MMP uncoupling, the inhibition of mitochondrial translation and the inhibition of DNA, RNA and protein synthesis, all had a negative impact on cell maturation (*174*). Interestingly the observed effect did not seem to result from the cells being energetically compromised, thus suggesting alternative mitochondrial functions in the differentiation process.

AA is an established chemical inhibitor of the electron transport chain complex III, known to act by inhibiting electron transfer from the Qp to the Qn site of that complex, resulting in the accumulation of the semiquinone radical, thus also enhancing the possibility for reactive oxygen species formation (*58*).

The objective of the present work was to evaluate if inhibition of mitochondrial functions by AA limits specific differentiation of mESC into neurons and maintains the pluripotency state of the former.

3.2) Material and Methods:

3.2.1) Cell culture and differentiation procedure

Mouse embryonic stem cell lines E14Tg2a and R1 were maintained and propagated in 0.1% gelatin treated plates in ES-Serum Replacement Media (SRM), composed of KnockOut-DMEM (#10829-018; Invitrogen), 15% KnockOut serum replacement (#10828-028; Invitrogen), 1% non-essential amino acids (#11140-035; Invitrogen), 0.1 mM mercaptoethanol (#M-7522, Sigma-Aldrich), 200 mM L-glutamine (#25030-024; Invitrogen) and 100 U/ml penicillin/streptomycin (#15140-122; Invitrogen), with Leukemia inhibitory factor (LIF) (#ESG1107; Chemicon - Millipore) supplementation.

Dopaminergic (DA) neuron differentiation was accomplished by co-culturing mouse embryonic stem cells (mESCs) with PA6 stromal cells according to previously described protocols (*175*, *176*), with adaptations. Briefly, mESC (R1 and E14 cell lines) were seeded (65 cells/cm^2) on mitomycin-treated PA6 cells and cultured in SRM without LIF. After 5 days, the medium was changed and supplemented with 200 ng/ml Shh (#461-SH; R&D Systems) and 25 ng/ml FGF8 (#423-F8; R&D Systems). From day 8 to day 12 cells were cultured in N2 medium consisting of a F12 (#21765-029; Invitrogen) and MEM (#21090-022; Invitrogen) mixture 1:1, N2 supplement (#17502-048; Invitrogen), 15 mM HEPES, 1mM glutamine, 3 mg/ml ALBUMAX (#11020-021; Invitrogen) supplemented with 250 ng/ml sonic hedgehog (Shh), 25 ng/ml fibroblast growth factor 8 (FGF8) and 20 ng/ml basic FGF (bFGF) (#233-FB; R&D Systems). On day 11 the medium was replaced with N2 medium supplemented with 30 ng/ml brain-derived neurotrophic factor (BDNF) (#248-BD; R&D Systems), 30 ng/ml glial-derived

neurotrophic factor (GDNF) (#212-GD; R&D Systems), and 200 mM ascorbic acid (#A-7506; Sigma-Aldrich). The mitochondrial inhibitor antimycin A (50 nM, #A8674; Sigma-Aldrich) was added to the cultures at days 2, 3.5, 5, 6.5, 8, 9.5, 11 and 12.5 following media replacement. Monolayer differentiations were conducted as described elsewhere (*177*, *178*). mESCs were seeded in gelatin-coated plates at a density of 10,000 cell/cm^2 in ES-SRM. 24 hours later, the medium was changed to a N2/B27 mixture. Medium was renewed at days 5 and 8 of differentiation or preceding every antimycin/vehicle (ethanol) treatment. Areas from the colonies were evaluated by processing optical microscopy photographs using the open-source image analysis software Image J.

3.2.2) Immunocytochemistry/High resolution ELISA.

At the end of the differentiation protocols (day 14) or at the referred time points (see Results) cells were fixed with 4% paraformaldehyde (PFA) and submitted to immunocytochemistry (ICC) or high-resolution ELISA, to monitor the presence of Oct4 (pluripotency marker), βIII-tubulin (TuJ1, neuronal marker) and tyrosine hydroxylase (TH, dopaminergic neuron marker). Briefly, cells were blocked in PBS containing 3% bovine serum albumin (BSA) and 0.25% Triton X-100 for one hour at room temperature (RT) and stained overnight at 4 ºC with the following primary antibodies: mouse monoclonal anti-βIII-tubulin (1:500, #G712A; Promega), rabbit polyclonal anti-tyrosine hydroxylase (1:500, #P40101-0; Pel-Freeze) and rabbit monoclonal anti-Oct4a (1:200, #C30A3; Cell Signaling). Secondary antibodies were incubated for one hour at RT. For ICC FITC-AffiniPure goat anti-mouse IgG (1:500, #115-095-146; Jackson

Immunoresearch) and Texas Red-X goat anti-rabbit IgG (1:200, #T6391; Molecular Probes) were used, and nuclei counterstained with Hoechst 33342 (#H1399; Molecular Probes)

The numbers of total and TuJ1 and TH immunoreactive colonies were manually counted based on the presence of integral neural structures, using duplicates for each experimental condition within each experiment. High resolution ELISA was adapted from a protocol described elsewhere (*179*). The procedure was similar to the one described above for ICC with some modifications. Prior to the blocking step, cells were permeabilized with 0.1 % Triton X-100 in PBS and endogenous peroxidase activity was quenched by treatment with 3% H_2O_2 solution in PBS for 5 minutes. Secondary antibodies used were conjugated to horseradish peroxidase: anti-rabbit IgG (1:500, #7074; Cell Signaling) and HRP linked anti-mouse IgG (1:500, #7076; Cell Signaling). HRP activity was detected by incubation with the chromogenic substrate tetramethylbenzidine (1-step Ultra TMB-ELISA, Thermo Scientific) and the reaction was stopped with 1 M H_2SO_4 after a 10 to 15 minute incubation depending on the protein to be detected. Signal quantitation was obtained by determining the optical density at 450 nm in a Microplate Spectrophotometer PowerWave XS, (BioTeK). To define the target protein relative concentration optical density values were first normalized by total cell mass (as assessed by the sulforhodamine B assay, see below) and then to the respective control.

Relative total cell mass quantification using sulforhodamine B (SRB) (#S1402; Sigma-Aldrich) was performed with some adjustments to the protocol previously reported

(*180*). After HRP reaction cells were thoroughly washed with PBS and dried at room temperature (RT). Cells were then stained with 0.5% (w/v) SRB in 1% acetic acid for 1 h at 37 ºC. Unbound dye was removed with 1% acetic acid. SRB bound to cell proteins was extracted with 10 mM Tris base solution, pH 10, and the optical density was determined at 450 nm. At least 3 independent experiments were performed for each cell line.

3.2.3) Flow Cytometry

Proliferation of ESCs was evaluated by propidium iodide (PI) and bromodeoxyuridine (BrdU) incorporation followed by flow cytometry analysis. R1 and E14 cells were plated on 6 well plates (10,000 cells/cm^2) and cultured for 4 days in the presence of AA (50 nM). Medium and treatments were renewed daily. Cells were incubated with BrdU (50 μM, #B9285; Sigma-Aldrich) for 1 hour, thoroughly washed with PBS, detached, fixed with ethanol (70%) and kept overnight at -20ºC. Alternatively, after BrdU incubation, cells were washed and cultured for 4 additional hours prior to the fixation procedure. Staining protocol was preceded by DNA acidic denaturation with HCl (2N) for 15 minutes at room temperature. Both anti-BrdU mouse monoclonal primary antibody (1:250, #B2531; Sigma Aldrich) and goat anti-mouse FITC secondary antibody (1:300, #115-095-146; Jackson ImmunoResearch) were sequentially incubated for 30 minutes at room temperature in the dark. Samples were treated with PI/RNase staining buffer (#550825; BD Pharmingen) for 15 minutes at room temperature and subsequently analyzed on a Becton Dickinson FACSCalibur cytometer, using FL1 and

FL3 channels for BrdU and PI detection respectively. For the neural precursor marker nestin, fixed cells were blocked in PBT (0.5% BSA + 0.1% Tween 20 in PBS), incubated with anti-nestin mouse monoclonal antibody (1:50, #sc-58813; Santa Cruz Biotechnology) followed by staining with the previously referred secondary goat anti-mouse antibody. Data acquisition and analysis was performed in CellQuest Software (BD Biosciences). PI histogram modeling was performed in ModFit LT software (Verity Software House).

TABLE 1

Influence of AA in adenylate energy charge, adenylate pool and adenine nucleotide ratios. Energy charge was calculated as ([ATP] + 0.5×[ADP])/([ATP] + [ADP] + [AMP]) and adenylate pool as ([ATP] + [ADP] + [AMP]). Statistical analysis performed by paired sample t-student test and error = SEM.

	Energy Charge	**Adenylate Pool** *(pmol/10^6cells)*	**ATP/ADP**	**AMP/ATP**
CTR	0.87 ± 0.01	4347.79 ± 316.45	5.33 ± 0.53	0.07 ± 0.01
AA	0.83 ± 0.02*	5372.12 ± 345.04*	3.93 ± 0.41*	0.11 ± 0.03

* ***p***<0.05 vs. Control (CTR)

3.2.4) Caspase-3/7 activity:

Possible pro-apoptotic effects of AA in mESC were studied by the use of the Caspase-glo 3/7 assay (G8091; Promega). Cells were seeded in 24 well plates at a density of 10,000 cells/cm^2. AA treatment was initiated on day 0 and reapplied every day with simultaneous medium renewal. At day 4, cells were detached by accutase (#A11105-0; Invitrogen) treatment, counted and a total of 20,000 cells per condition were used. This cell number normalization was adopted to exclude possible proliferation effects what would noticeably affect total cell numbers at day 4. Cells were centrifuged (200xg for 5 minutes) and ressuspended in 100 μL of mESC proliferation medium. Equal volume of the caspase-glo 3/7 reagent was added, and samples were transferred to a white walled 96 well plate (Corning). After a gentle homogenization followed by an incubation of approximately 2 hours at room temperature, the plate was read in a LUMIstar Galaxy luminometer (BMG LABTECH).

As a positive control, cells cultured for 4 days in control conditions were incubated with H_2O_2 (0.5 mM) and caspase 3/7 activity was evaluated 4 hours later.

3.2.5) Immunoblotting Detection of HIF-1 alpha

Total cell extracts were obtained by scrapping cells with heated 2x Laemmli buffer (supplemented with DTT 350 mM) after medium aspiration and rinsing the cells in ice-cold PBS. Buffer volume was normalized by total cell number (100 μL per 1x106 cells) determined on replicate wells. Extracts were immediately heated at 95°C for 5 minutes,

submitted to 3 freeze-thaw cycles in liquid nitrogen and then kept at -80ºC or immediately processed. Subsequent to an additional denaturing step (95°C for 5 min), equal volumes of extract samples were electrophoretically separated on a 7.5 % SDS-polyacrylamide gel. Proteins were transferred to polyvinylidene fluoride (PVDF) membranes (Trans-Blot® Turbo™ Transfer Packs, Bio-Rad) using a Trans-Blot® Turbo™ Transfer System (transfer program: 30 min at 25 V constant). Membranes were blocked with 5% skim milk powder in PBS-Tween 20 (PBS-T) [0.1% (v/v)] and then incubated at RT for 2 hours with rabbit anti-HIF-1α (1:1,000, #PA1-16601; Thermo Scientific) and mouse anti-actin (1:10,000, #MAB1501; Millipore) primary antibodies. Secondary antibodies conjugated with alkaline phosphatase: goat anti-mouse (1:10,000, #155-055-003; Jackson ImmunoResearch) and goat anti-rabbit (1:3,000, #111-055-003; Jackson ImmunoResearch) were incubated for 1 hour at RT. Protein-immunoreactive bands were developed using the Enhanced Chemifluorescence (ECF) detection system (GE Healthcare) and visualized in a Molecular Imager FX System (Bio-Rad). Immunoblot results were analysed by calculation of adjusted volumes (total intensities in a given area with local background subtraction) for each immunoreactive band using Quantity One® software version 4.6 (Bio-Rad). All bands were adjusted to the loading control (actin), and normalized to the corresponding control.

3.2.6) Adenylate Energy Charge

mESCs were treated for 4 days and intracellular adenine nucleotides (ATP, ADP, and AMP) were quantified as described elsewhere (*181*). Briefly, cells extracts were

performed with 0.6 M perchloric acid supplemented with 25 mM EDTA-Na. After centrifugation, cell supernatants were neutralized with 3 M KOH in 1.5 M Tris followed by a new centrifugation step. Supernatants were assayed by separation in a reverse-phase HPLC using a Beckman-System Gold. The detection wavelength was 254 nm, and the column used was a LiChrospher 100 RP-18 (5 μM, Merck). Adenylate energy charge was calculated according to the following formula: ([ATP] + 0.5×[ADP])/([ATP] + [ADP] + [AMP]).

3.2.7) Statistical Analysis

Statistical analysis was performed by using SPSS Statistics 17.0 (SPSS Inc.). Assumptions of normality and homoscedasticity were tested and appropriate non-parametric or parametric tests were performed depending on the experimental design, as reported in the legend for each figure. Data are expressed as means ± SEM for the number of experiments indicated. Significance was considered when $p \leq 0.05$.

3.3) Results

3.3.1) Antimycin A treatment inhibits neuronal differentiation.

We have previously demonstrated that AA maintains human embryonic stem cell pluripotency under proliferative culture conditions (*72*). Our goal here was to investigate a putative AA effect in a cell differentiation context. Therefore, mESCs (E14 and R1 cell lines) were specifically differentiated into neurons with the PA6 co-culture differentiation system, consistently used for the enrichment of midbrain dopaminergic neurons (*176*).

AA treatment initiated at day 2 of the differentiation process clearly decreases differentiation efficacy (Fig. 3.1), as AA-treated cells maintain a more compact morphology resembling undifferentiated colonies until later stages of the differentiation protocol. Colony size was equally affected as AA-treated cultures exhibited reduced colony size. Furthermore, neural processes, which were present in the final stages in control (CTR) differentiations, were significantly fewer, smaller and with a lower degree of structural complexity in AA-treated cells (Fig. 3.1 and Supp. Fig. 3.1). These observations suggest that AA, when added at day 2 of ESC differentiation into neurons, inhibits or delays the process.

We further evaluated the expression of the pan-neuronal marker class III β-Tubulin (TuJ1) and the dopaminergic neuron marker tyrosine hydroxylase (TH) at the end of the differentiation protocol (day 14). For this purpose, AA treatment was initiated at different time-points (days 2, 8 and 11), resulting in distinct immunoreactivity against

the two markers. As shown in Fig. 3.2, the control group showed large colonies with intricate and complex neuronal processes, which were positive for TuJ1 (green in Fig. 3.2A, 3.2E). Treatment with AA starting at day 2 (Fig. 3.2B, 3.2F) resulted in smaller colonies with low TuJ1 labeling in cells with immature neuronal morphology. Moreover, clear TH labeling was absent in the majority of these colonies, while differentiations in the control group displayed a large numbers of cells expressing this marker. Furthermore, colonies in which AA treatment was only initiated at day 8 or 11 (Fig, 3.2C, 3.2D, 3.2G and 3.2H) revealed a disrupted morphology, with empty areas in the colonies suggestive of massive cell loss, although, still presenting reminiscent TuJ1 positive reactivity. A more objective quantification of marker expression was obtained through high resolution ELISA and manual counting of positive colonies (Fig. 3.3). ELISA quantification showed that the expression of both Tuj1 and TH was high in control condition and decreased with AA application in both cell lines, being inversely correlated with the time at which treatment was initiated (Fig. 3.3A, 3.3C). Analysis of the number of positive colonies yielded similar results, a decrease in the number of Tuj1- and TH-positive colonies after AA treatment (Fig. 3.3B, 3.3D). Although the results obtained by the ELISA assay suggest residual TH expression in AA-treated cells, our immunohistochemistry-based manual counting suggest that these were background levels, as the percentage of TH positive colonies was less than 5% (Fig. 3.3C, 3.3D).

The presence of the pluripotency marker Oct3/4 was also evaluated by ELISA. As demonstrated in Fig. 3.3E, Oct3/4 expression was significantly higher in cells that were

treated with AA earlier in the differentiation process, confirming that the inhibitor contributed to maintain the presence of this pluripotency marker in the culture, despite the differentiation process. This was further supported by the ratio between the percentage of TuJ1 and Oct3/4-positive cells (Fig. 3.3F), a good indicator of differentiation efficacy. Fig. 3.3F clearly demonstrates an inverse correlation between the time at which the inhibitor treatment was performed and the efficiency of the differentiation process, being differentiation at day 2 the lowest and at day 11 similar to control cultures.

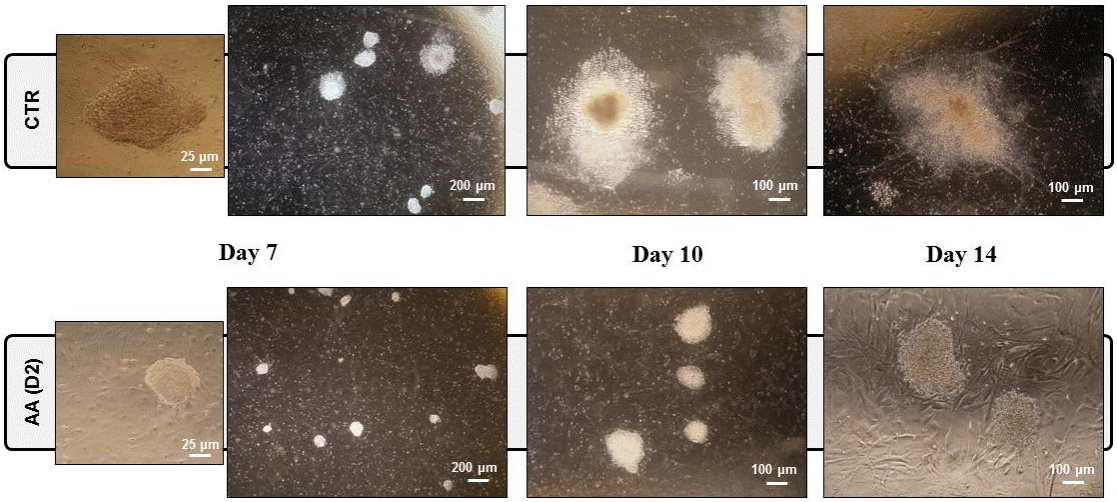

Fig. 3.1 – Antimycin A disturbs mESC neuronal differentiation. mESCs differentiated for 14 days into dopaminergic neurons using a PA6-based system were treated with AA since day 2. Representative phase contrast microscopy images were obtained at different time-points of the process (days 7, 10 and 14). AA-treated colonies were smaller and with a more compact morphology resembling undifferentiated mES cells colonies. AA-treatment also led to the absence of neuronal processes, which are easily depicted in control (CTR) colonies at later stages.

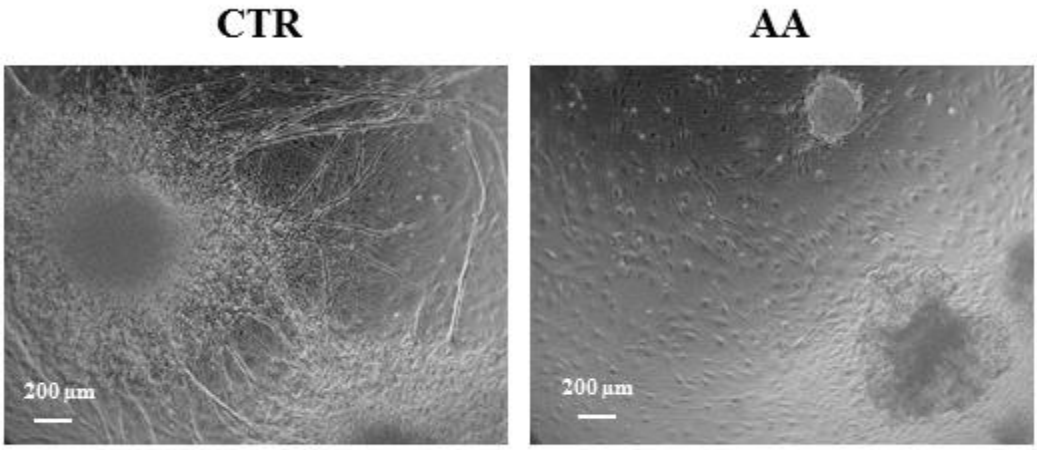

Supp. Fig. 3.1 – Antimycin A hinders the formation of complex neural processes. mESCs differentiated for 14 days using the PA6-based system were treated with AA since day 2. Control colonies presented numerous neurites forming complex structures not visible in AA-treated colonies.

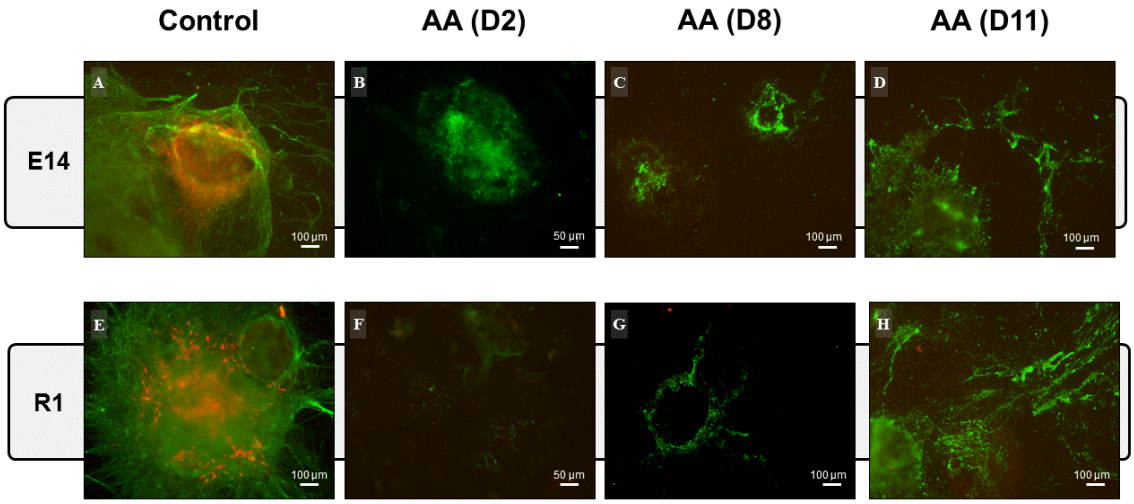

Fig. 3.2 – AA affects the mESC neuronal differentiation as seen by TuJ1 and TH labelling. At day 14 of differentiation, cells were stained for the pan neuronal marker Tuj1 (green) and the dopaminergic neuron marker TH (red) by ICC. AA treatment seems to cause stage specific effects on differentiating cell populations. Control conditions show large colonies with complex neuronal processes and consistent numbers of TH-positive cells (A and E). Cells treated with AA starting on day 2 presented colonies that were only positive for Tuj1 but with no complex neurite formations (B and F). AA treatment at later stages resulted in increased cell loss as observed by degraded colonies and loss of neuronal processes (C, D, G and H). The images are representative of at least 3 independent experiments.

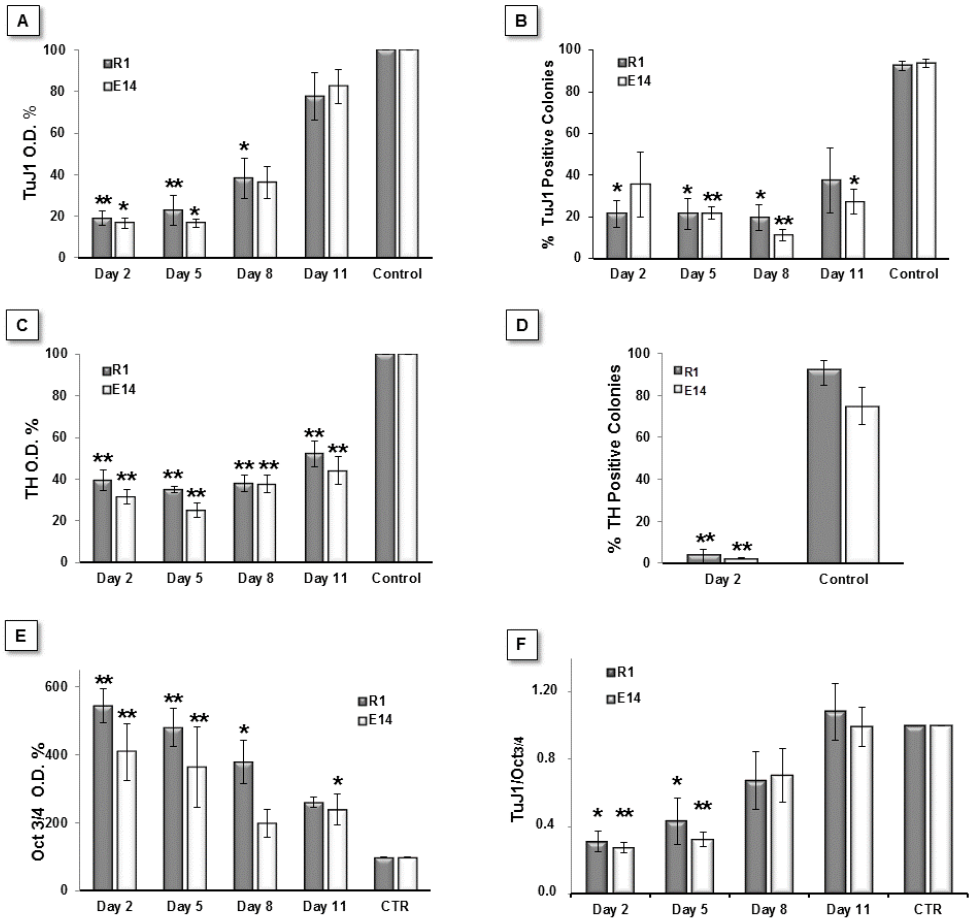

Fig. 3.3 – AA quantitatively affects mESC neuronal differentiation and maintains pluripotency. A, B, C and D - Quantification of TuJ1 and TH labeling using high resolution ELISA and manual colony counting on R1 and E14 cells differentiated for 14 days. The ELISA-based assay detected a consistent decrease on TuJ1 expression for cells treated with the inhibitor starting on day 2, 5 and 8 on both cell lines (A). This was corroborated by manual colony counting of positive colonies (B). For ELISA-based TH detection, statistical significant differences were found when comparing all treatment time-points with the control condition, for both cell lines (C). These differences were also further validated by colony counting (D). Statistical analysis on ELISA-based data was performed on raw values using a One-way Anova, followed by a Dunnett post hoc test. To maintain parametric assumptions TH data was log-transformed. On colony counting, statistical analysis was based on a One-way Anova with a Games-Howell test (homoscedasticity not verified) for TuJ1, and on a T student test for TH. E – The relative expression of the pluripotency marker Oct4, was evaluated by an Elisa-based method. Results show a clear correlation between relative Oct3/4 levels maintenance and AA treatments, with the former found more increased as treatment with AA was performed in earlier time points. Significant differences were found for all groups when compared with the control condition except for Day 8 in E14 cells. Raw data was first normalized by cell mass as assessed by SRB, and then normalized to control levels (CTR=100%). Statistical analysis was performed on O.D. values normalized by protein mass (SRB). In order to verify parametric assumptions, R1 data were log-transformed. Data were analyzed by one-way Anova followed by a Dunnett post hoc test. F – The ratio between the percentage of TuJ1-positive and Oct4-positive cells (TuJ1/Oct3/4) was used as a measure of differentiation efficiency. This ratio showed that AA treatment significantly decreased differentiation efficiency, when AA was added to cells on days 2 and 5. Statistical analysis was performed using a One-way Anova, followed by a Tukey post hoc test. Statistical significance was considered when p≤ 0.05., (* p<0.05; ** p<0.01). Error bars = SEM (calculated through error propagation formula for D). At least 3 independent experiments were performed for each experimental group.

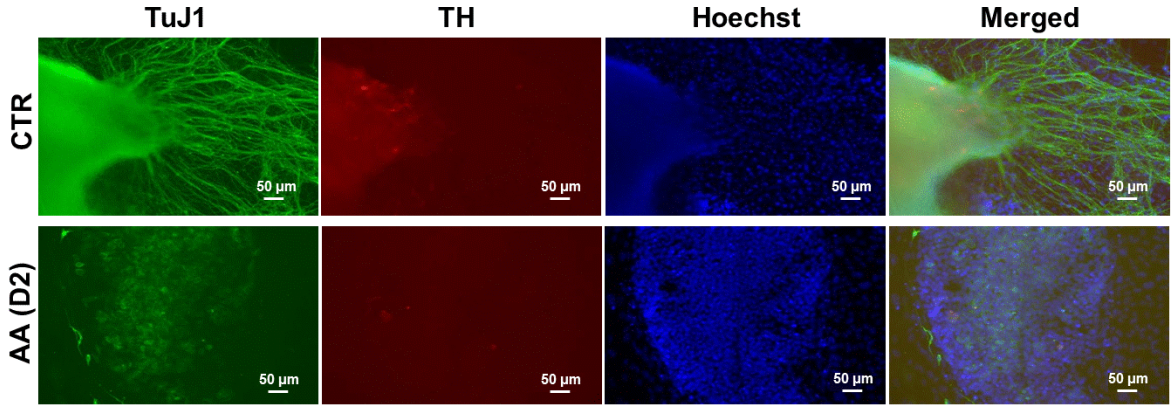

Supp. Fig. 3.2 – Immunocitochemistry for TuJ1 and TH markers. E14 cells were differentiated in the absence of PA6. After fixation at day 14 of differentiation, cells were submitted to ICC for pan neuronal marker Tuj1 (green) and TH dopaminergic neuron marker (red). Control colonies display complex neuronal processes as detected by Tuj1 staining. AA treatment starting on day 2 inhibited neuronal differentiation, confirming that AA effect does not occur through feeder cells. Control conditions presented some TH positive cells that were completely absent in treated cultures.

In order to rule out an indirect effect of AA on PA6 cells, mESC lines were also differentiated without the presence of feeder cells. Despite this being a less efficient culture condition in driving differentiation, this protocol was capable of generating a significant number of neurons. Immunocytochemistry for TuJ1 and TH revealed that AA treatment also hindered neuronal differentiation under these conditions, thus reinforcing the idea that this drug prevents the neural differentiation of mESCs (Supp. Fig. 3.2). This experiment also stressed that the inhibitory effect is not limited to the dopaminergic lineage, as the number of non-dopaminergic TUJ1^{+} cells were also reduced. We next assessed the effect of AA at an earlier stage particularly evaluating whether AA had any earlier discernible effect on the differentiation of mESC into

nestin-positive neural stem cells. As shown in Fig. 3.4, AA treatment starting on day 2 significantly reduced the numbers of nestin-positive cells, as assessed by flow cytometry. These results were observed both at days 4 and 6 using the monolayer differentiation culture system (CTR = 67.8 ± 3.7 % vs. AA = 43.5 ± 0.7 % at day 4 and CTR = 58.2 ± 6.7 % vs AA = 40.8 ± 3.3 % at day 6), confirming that AA prevents the differentiation of mES cells affecting thus their differentiation into neural stem/progenitor cells and their subsequent neuronal differentiation..

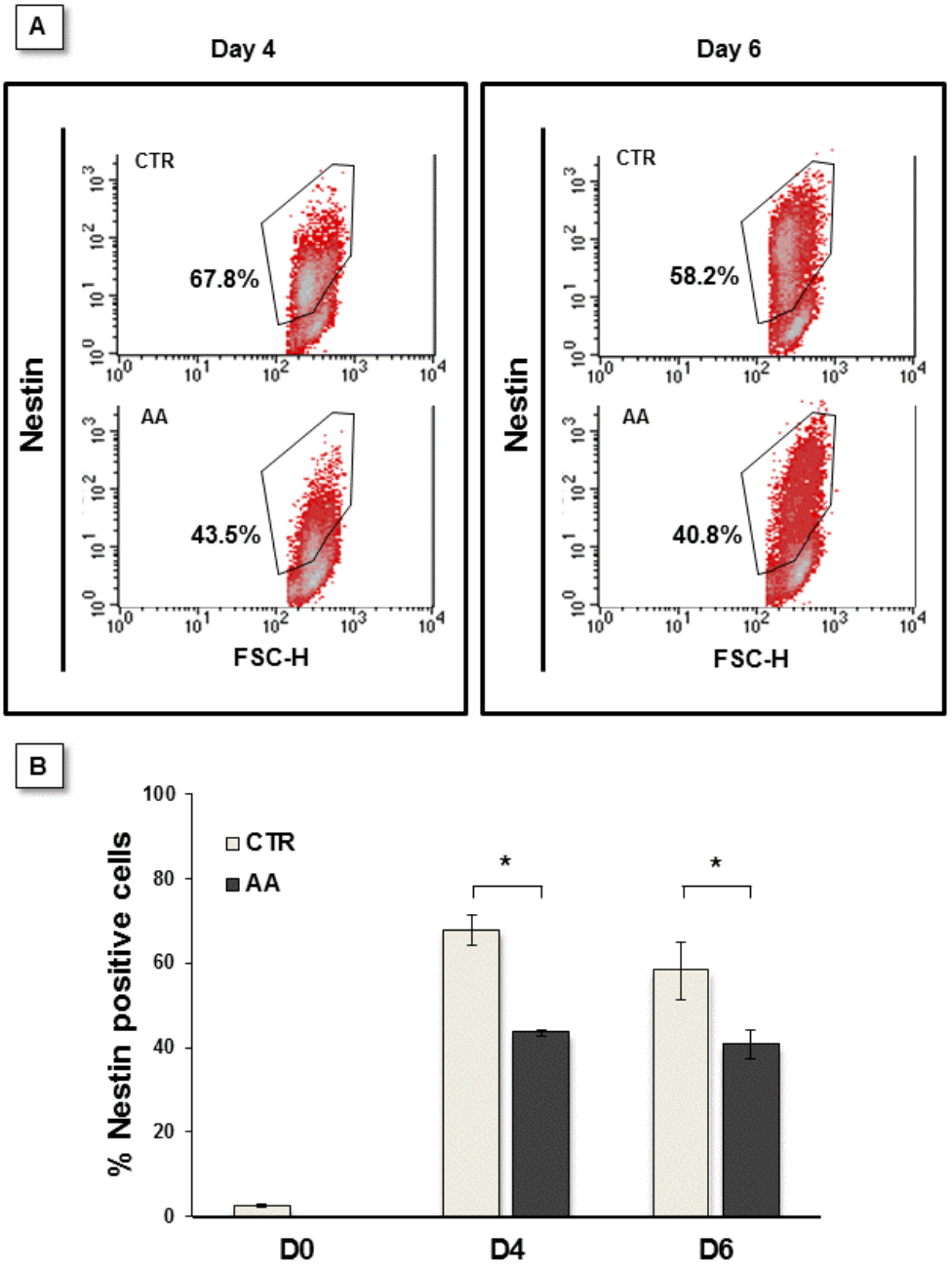

Fig. 3.4 – AA treatment causes a reduction in nestin-positive cells. E14 cells were differentiated in monolayers for 4 or 6 days in the presence of AA since day 2. Cells were analyzed by cytometry for nestin labeling (A). Nestin positive cells were reduced on treated cultures when evaluated both at day 4 and day 6. Statistically significant differences were found when comparing control and treated cultures for each time-point (B). Data were analyzed by a two-way Anova for independent samples. Error bars = SEM. Statistical significance considered when *p≤ 0.05. Results express at least 3 independent experiments.

3.3.2) Antimycin A affects the proliferation of mouse embryonic stem cells, but does not induce apoptosis

As described above, AA treatment appears to affect mESC colony size. To confirm this, we differentiated mESC in co-culture with PA6 cells and evaluated the size of the resulting colonies at days 4, 6 and 8. Fig. 3.5 shows that early AA treatment significantly prevents the increase in colony size during differentiation. When initiated at day 2, AA treatment resulted in significantly smaller colony size starting at day 4 for R1 cells and at day 6 for E14 cells, with clear differences between untreated and AA-treated cells at day 8 of differentiation for both cell lines.

These findings suggested a possible impairment in cell proliferation, or alternatively, an increase in cell death. Given that significant differences in colony size are seen as early as day 4, we examined whether AA affected early cell populations and cultured mouse embryonic stem cells under proliferating conditions for 4 days in the presence of AA. Cell proliferation-related DNA replication was monitored using the cytometric BrdU/PI assay. Although no statistically significant differences were found when comparing the percentage of BrdU positive cells following a 1 hour pulse (Fig. 3.6A) AA showed a tendency to increase the percentage of BrdU-labelled cells (70.0 ± 1.3 % for treated cells versus 62.6 ± 4.4 % for control conditions). The small tendency to increase BrdU positive cells in the AA-treated group does not necessarily correspond to a shorter and faster cell cycle as a possible S phase lengthening would also result in augmenting the BrdU positive population. When cells pulsed with BrdU and grown

for additional 4h were analyzed we found that AA-treated cells did indeed present a slower cell cycle, as the number of cells passing through S and G2/M phases and reentering G1 phase after incorporating BrdU was significantly higher in control conditions (11 ± 1.9 % in control vs 5 ± 1.2 % in AA treated cells; Fig. 3.6B).

Cell cycle analysis provided further support for the 4 h BrdU results by showing a small but significant decrease (~ 3%) in the population in G2/M phase in AA-treated cells, and a concomitant increase in cells in S phase (~ 2%; Fig. 3.6C). These results suggest that AA induces a slight S-phase arrest and decreases mitosis in mESC.

Since AA is known to be a classic mitochondrial poison, we also investigated whether AA induced apoptosis and examined the activity of the executioner caspases 3 and 7 in proliferating culture conditions by performing the Caspase-glo 3/7 luminescent assay. While cells that were incubated with H_2O_2 (0.5 mM) for 4 hours showed significant cell death (Fig. 3.6D), AA treatment for 4 days did not cause increased caspase-3/7 activity in mESCs when compared with control cells. These results thus exclude programmed cell death as responsible for the decrease in cell mass of AA-treated cells.

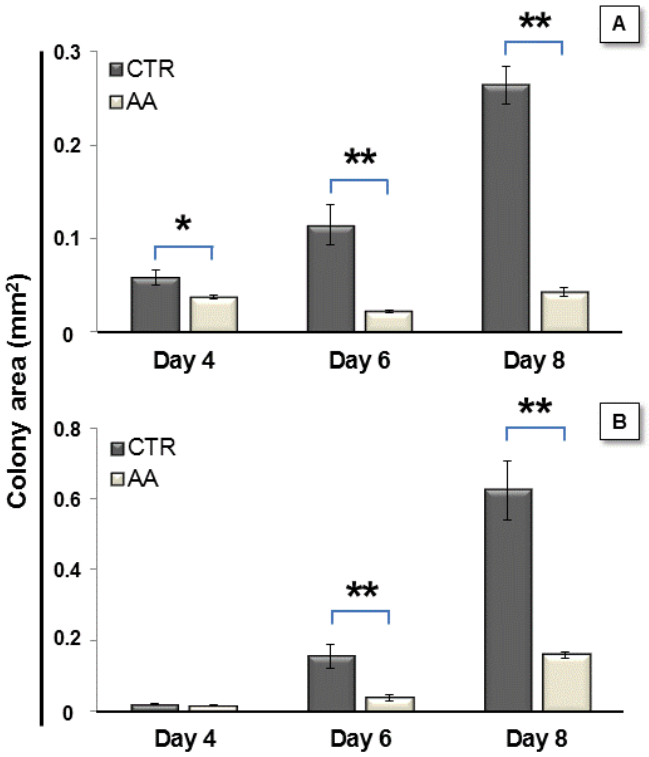

Fig. 3.5 – AA reduces colony area. Antimycin A treatments were initiated at day 2 of differentiation using both R1 (A) and E14 cells (B), and repeated every one and half days. Cells were fixed at days 4, 6 and 8 and colony areas were evaluated by processing phase-contrast microscopy photographs with Image J. For both cell lines AA treatment severely decreased the colony area. To verify parametric assumptions by Shapiro-Wilk and Levene tests, area values were submitted to a logarithm transformation. Data were then evaluated by a two-way Anova for independent samples, which revealed a significant interaction between the effects of treatment and time. Subsequent simple main effects analysis showed that the areas from treated and control colonies were significantly different at days 4 (P= 0.03), 6 (P= 0.000001) and 8 (P= 0.000002) for R1 cells and at days 6 (P= 0.0001) and 8 (P= 0.0002) for E14 cells. Error bars = SEM (* p<0.05; ** p<0.01). For better comprehension raw area values from 3 independent experiments are represented.

Fig. 3.6 – AA

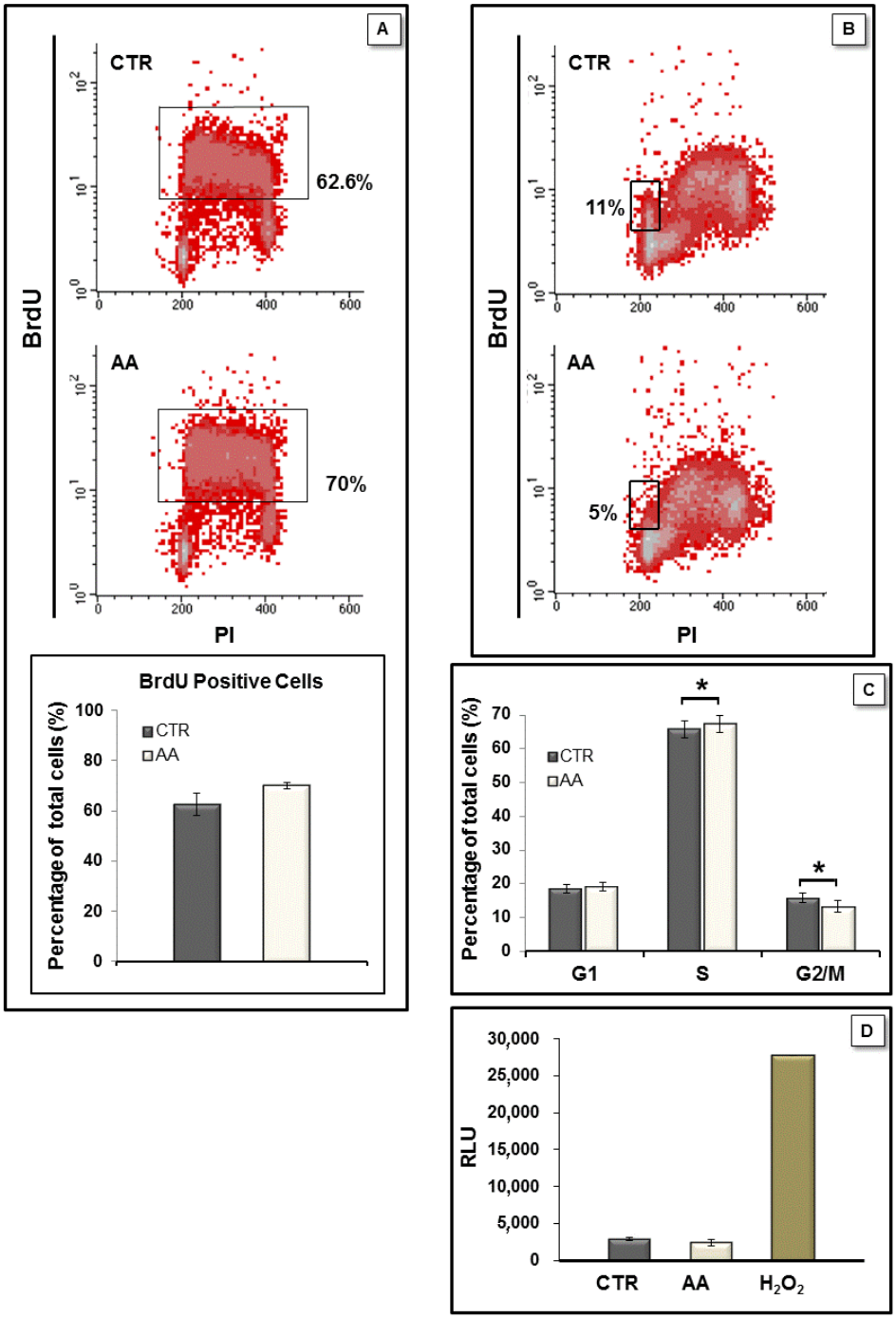

affected proliferation, cell cycle analysis but did not induce apoptosis in mESC. E14 cells were cultured for 4 days in proliferation medium in the absence or presence of AA. Cells were then pulsed with BrdU for one hour and immediately fixed (A) or further cultured for 4 more hours in the absence of BrdU prior to fixation (B). Cell cycle analysis by PI staining and analysis by flow cytometry (C). Caspase-3/7 activity was evaluated by Caspase-glo-3/7 assay (D) using H2O2 (0.5 mM) treatment for 4 hours as a positive control. Values are expressed as relative luminescence units and no significant differences were found between caspase activity in CTR and AA-treated conditions (p = 0.197). Data are normal and homoscedastic and were analyzed by paired sample Student's t tests. Error bars = SEM. Statistical significance considered when p≤ 0.05 (* p<0.05). Results express at least 3 independent experiments.

3.2.3) Antimycin A induces changes in adenine nucleotides.

As shown in Table 1 antimycin A treatment slightly decreased adenylate energy charge (CTR = 0.87 ± 0.01 and AA = 0.83 ± 0.02, p= 0.048), with a concomitant increase in the adenylate pool (CTR = 4347.79 ± 316.45 and AA = 5372.12 ± 345.04, p= 0.038). Interestingly this increase was preferentially noticed in non-energetic adenine nucleotides (AMP) resulting in a tendency for increased AMP/ATP ratio and a significant decrease in the ATP/ADP ratios (CTR = 5.33 ± 0.53 and AA = 3.93 ± 0.41, p= 0.038).

3.2.4)Antimycin A elevates HIF-1α protein content in mESCs.

Mitochondrial inhibitors have been previously shown to induce stabilization of HIF-1α (*182*, *183*), thus enhancing downstream pathways in distinct cellular contexts. To understand whether this protein is stabilized subsequently to AA treatment in mESCs, a western blot analysis using extracts from cells treated with AA for 45 min., 2 hours or 4 hours was performed. Fig. 3.7 shows that HIF-1α levels were consistently elevated after AA treatment, with both cells lines depicting a significant increase when compared to the respective control for 2 and 4 hours. HIF-1α content was particularly elevated in E14 cells, increasing up to 2.54 ± 0.4 times those of the control. R1 cells treated for 4 hours showed a 1.68 ± 0.1 times protein fold increase.

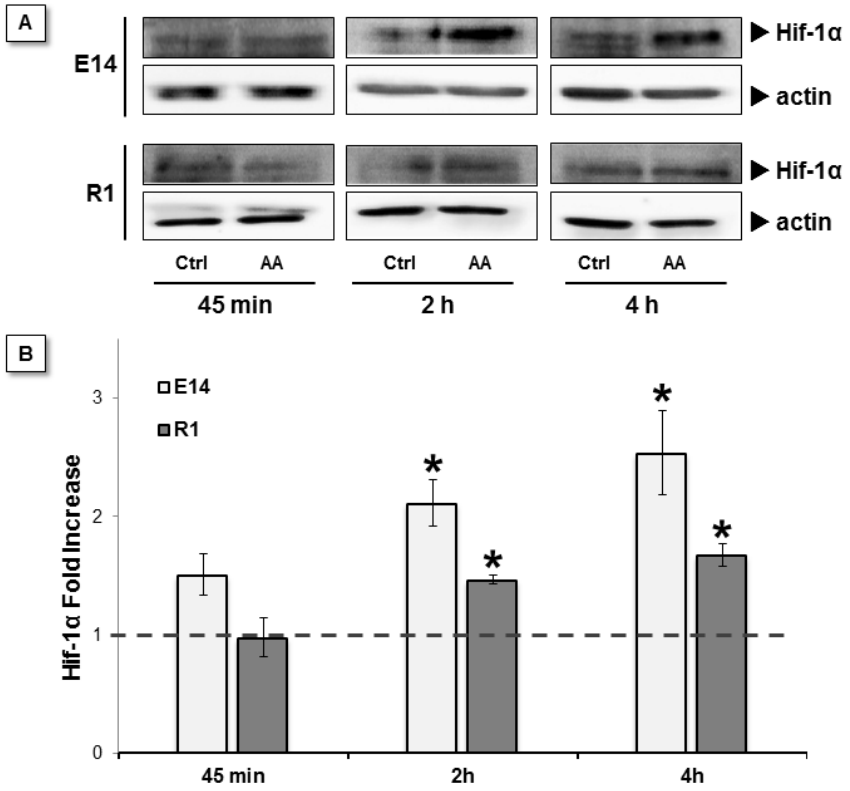

Fig. 3.7 –HIF-1α protein levels were stabilized by AA treatment. HIF-1α protein levels were evaluated by western blot at different time-points upon AA treatment. E14 and R1 cells incubated with 50 nM of AA for 45 minutes, 2 hours or 4 hours, revealed a rise in HIF-1α particularly at later time points (A). In addition, densiometric evaluation of HIF-1α and actin (loading control) bands show that a statistical significant difference exists between control and treated conditions at 2 and 4 hours (B). Data shown as protein level fold increases for each one of the AA conditions relative to the respective control (1). Data were normal and evaluated by one sample T student tests against a theoretical value of 1. Error bars = SEM and statistical significance is considered when * p<0.05.

3.4) Discussion

Many recent studies have implied metabolic mechanisms as major regulators of pluripotent stem cells properties (*184*). We have previously shown an intricate relationship between mitochondrial function modulation, as affected by antimycin A, and the maintenance of human embryonic stem cell self-renewal and pluripotency (*72*). Furthermore, structural and functional remodeling of cellular metabolism has been shown to be a hallmark of various lineage specification processes, especially when the target differentiated cells have a high-energy demand phenotype (*71*, *74*, *170*, *174*). Neurons are an example of such an energy-requiring phenotype, given that a robust metabolic performance is required to support ionic pump function and preserve membrane potential (*174*). In the present work, we studied the effects of mitochondrial inhibition by AA in the specific context of neuronal differentiation of mESC. In this work we show that AA treatment abrogated mESC differentiation, as evaluated by the reduced expression of neural (Nestin) and neuronal (Tuj-1 and TH) differentiation markers and the diminished acquisition and maturation of neuronal morphology. These results are consistent with the notion that neuronal differentiation from mESC also involves a metabolic shift towards oxidative phosphorylation, with an increased cellular reliance on mitochondrial activity (*171*, *185*).

Previous reports have addressed the use of mitochondrial modulators (inhibitors and uncouplers) during cell differentiation processes (*73*, *74*, *170*, *174*, *186*). Notably, two studies focusing on the differentiation of mESC into cardiac cells reported that application of AA affects the efficiency of the process (*74*, *170*). Although not

completely concordant, both papers draw similar conclusions, suggesting that disruption of the electron transport chain function impaired cardiomyocyte differentiation. The importance of mitochondrial activity for neuronal differentiation was also suggested in earlier studies. Vayssiére and colleagues (*174*) worked with two clonal cell lines that were derived from murine neuroblastoma submitted to a differentiation protocol based on the use of 1-methyl cyclohexane carboxilic acid (CCA) as a neurogenic inducer. Only one of the cell lines would indeed produce a neuronal-like phenotype while the other one demonstrated proliferation and differentiation arrest, and the mitochondrial uncoupler FCCP, but not oligomycin (a specific inhibitor of the ATP synthase complex), was able to hinder neuronal differentiation in this model. It was then concluded that the role of mitochondria in early neuronal differentiation was not strictly related to its function in ATP synthesis, but would rather also involve the membrane potential which is necessary for multiple physiological features including mitochondrial biogenesis, cytoskeleton organization and pyrimidine biosynthesis. Similarly, Spitkovsky et. al. suggested that energy constraint is not a major factor/player downstream of AA effects on cardiac differentiation, as immature cardiac cells still present contractile activity and differentiate in the presence of KCN (*74*).

In our study we observed that initiating AA application at distinct phases of neuronal differentiation resulted in diverse outcomes. These ranged from increased cell loss, discernible by loss of colony structure for treatments initiated at later stages, to the persistence of compact pluripotent stem cell-like colonies in the cultures, observed for

earlier treatment onsets (Fig. 3.2). These observations may be interpreted as a result of the differential effect of AA in the distinct populations present in culture, which exhibit discrete metabolic maturation and thus distinct mitochondrial dependence. Moreover, our monolayer differentiation experiments clearly showed that all neuronal lineages, and not just dopaminergic neurons, were being equally affected. This result, in conjunction with the fact that no increased cell damage was seen in those cultures after AA treatment (as evaluated by the presence of cell debris), suggested that proliferation and differentiation may be arrested at earlier neural progenitors or precursors stages. In fact, cultures treated from day 2-8 onwards presented some persistent Tuj-1^{+} cells with impaired neurite formation. Similarly, Spitkovsky et al. reported that AA treatment blocked cardiac differentiation at a precursor stage, with differentiation continuing once the AA block was removed (*74*). Indeed, AA treatment also decreased the pool of neural progenitor nestin-positive cells in our model.

AA effects during ESC differentiation seemed to involve a slight decrease in the proliferation rate, with no increased apoptosis. In contrast to what was reported for hESC (*72*), our results suggest that AA induces a slight arrest in S phase (with a consequent slight decrease of ~3% in the G2/M cell pool) which dictated a diminished proliferation rate of treated mESCs, as confirmed by a more than twofold increase in the G1 sub-population. Considering only the G2/M population, which includes cells that are indeed dividing at any given moment, it should be noted that a decrease of approximately 3% of total cells represents around 16% fewer cells in the population undergoing mitosis. Several studies have reported that interfering with mitochondrial

function may lead to changes in proliferation and the cell cycle, which may be related to a decrease in ATP or modulation of ROS signaling (*73*, *187–189*). Treatment of either hESCs or iPSCs with the mitochondrial membrane potential uncoupler CCCP decreased ATP levels on both cell types (even though the total adenylate pool and energy charge were not measured) and increased ROS formation, causing reduced proliferation, but, unlike what we report here, with a proportional slowing down in all phases of the cell cycle (*73*). Our data shows that AA treatment decreased adenylate energy charge with a concomitant increase in the adenylate pool (Table 1). This may account for the decreased proliferation observed due to AA, as it is known that an elevated AMP/ATP ratio can lead to the reduction of energy consuming processes (e.g. protein and lipid synthesis) some of which are needed for cell growth (*190*, *191*). AA induces cell type specific responses, eliciting distinct outcomes in cell cycle modulation (*187–189*, *192*). Remarkably, treatment of HeLa cells with AA (10-50 μM) also resulted in a time and dose dependent S phase arrest (*187*). Nevertheless, we cannot completely exclude the possibility that the constraint in mESC proliferation may be related to a consequent elevation of ubiquinol/ubiquinone ratio, which in turn can limit pyrimidine synthesis as oxidized ubiquinone is essential for pyrimidine synthesis (*193*).

Despite the limitation detected in mESC proliferation, AA treatment conspicuously increased Oct4 levels 4-5 fold. Simultaneously, cells in which AA was added earlier expressed lower Tuj-1 levels indicating decreased differentiation efficiency. It is worth stressing that the increment in Oct4 levels was obtained under differentiation conditions for 14 days, evidencing that AA actively supported pluripotency

maintenance. This reinforces the concept that mitochondria play a key role in the cellular processes involved in the choice between preserving stemness or engaging into differentiation. As mentioned, this notion evolved from reports that either show that the modulation of mitochondrial function in ESCs and iPSCs promoted stemness by prompting the expression of pluripotency-related markers (*72*, *73*), or by studies demonstrating that disruption of mitochondrial membrane potential or ETC complex activity hindered cell differentiation (*73*, *74*, *170*, *174*, *186*, *194*).

Some of these reports suggested that the effects were not caused by a decreased energy status due to inefficient mitochondrial function, but instead proposed alternative mechanisms downstream of AA treatment, namely the involvement of mitochondrial reactive oxygen species (ROS). Controlled elevation of mitochondrial ROS is essential for the stabilization of HIF-1α protein [58, 59, 60], and here we showed that incubation of mESCs with AA, resulted in HIF-1α stabilization under normoxia, and it is likely that this signaling pathway accounts for at least some of the results obtained. Hypoxia signaling is known to promote a metabolic shift rendering cells more reliant on glycolysis, a metabolic pattern that has been associated to stemness (*110*, *184*). Therefore, the accumulation of HIF-1α may encompass a metabolic conformation that will favor stem cell maintenance instead of differentiation, even under stringent differentiation conditions.

Further work is needed in order to elucidate the molecular basis behind these results, but it is clear that modulation of mitochondrial function can influence cell fate, and that increasing our knowledge of the stemness/differentiation-metabolic interplay may

prove an effective approach towards improving culture procedures and differentiation protocols involving pluripotent stem cells.

3.5) Acknowledgments

The authors acknowledge Rhodri Ceredig, Tara Sugrue and Isabel Nunes for the assistance in flow cytometry studies. Hugo Fôfo and Sónia Correia for inputs in the detection of HIF-1α. Maria Sancha Santos, Sandra Amaral and Ana Rodrigues for their valuable help in HPLC analysis. Gonçalo Pereira is acknowledged for supportive discussion of the results. We thank Fundação para a Ciência e a Tecnologia (FCT) for grant support (PTDC/EBB-EBI/101114/2008 co-funded by Compete/FEDER/National Funds) and a PhD scholarship attributed to S.L.P. (SFRH/BD/37933/2007). EA's work was supported by the Swedish Foundation for Strategic Research (SRL Program), Swedish Research Council (DBRM), Karolinska Institutet (SFO Thematic Center in Stem cells and Regenerative Medicine), and Hjärnfonden.

Chapter 4

Conclusions

FINAL CONCLUSIONS

ONGOING/FUTURE WORK.

REFERENCES

Final Conclusions

The work included in the present dissertation proposed the study of metabolism involvement in cellular differentiation, approaching two distinct perspectives.

The first approach was focused on the analysis and description of a possible metabolic shift accompanying the differentiation of a rat mioblastic cell line (H9c2) towards cells resembling either cardiomyocytes or skeletal muscle cells (*vide* Chapter II). The NMR-based comparative analysis of the metabolic profile of the distinct undifferentiated and differentiated populations confirmed the existence of a metabolic reprogramming supporting the considered differentiation processes. Whereas no significant differences were encountered when comparing both differentiated populations, a notorious divergence was found when comparing undifferentiated cells with more mature cells. Parental mioblast cells presented a pronounced glycolytic phenotype with high ratios of lactate production and excretion (resembling the Warburg effect). A lower coupling between the non-oxidative and oxidative metabolic machinery was also observed, denoted by the concomitant higher lactate/alanine ratio and lower O_2 consumption rates. Similar uncoupling has been recognized in several proliferating cells such as cancers (*79*), where a possible molecular basis for this uncoupling seems to be the differential regulation of pyruvate dehydrogenase kinase activity, an enzyme regulating the conversion of pyruvate to acetyl-CoA by the pyruvate dehydrogenase complex in the mitochondria (*96*, *97*). Importantly the former enzyme is a downstream target of hypoxia inducible factors (vide chapter I section

1.5.2.1). The uncoupling process may ultimately allow the cell to divert more glucose-derived carbons into biosynthetic pathways branching from glycolysis (*85*), such as the pentose phosphate pathway. Our data also point for an enhanced anaplerosis in the Krebs cycle of the undifferentiated myoblasts, which may serve to replenish the levels of intermediates that are being used for biosynthesis. Undifferentiated cells seem to adapt their metabolism to their intense biosynthetic needs.

Differentiated populations, on the other hand presented a more energy-efficient metabolic state associated with higher oxygen consumption. These efficiency-driven alterations perceived in specified cells are clearly supported by a work investigating mitochondrial biogenesis during cardiac differentiation using the same cell model (*196*). In this work, it was demonstrated that the acquisition of cardiac specific markers was concomitant to the increase in mitochondrial biogenesis and mass. Differentiated cells in this case would also present more mature mitochondria, in terms of morphology, network complexity, cristae development and energetic competence. Our study coherently merges with the growing notion referring the importance of the metabolic regulation for the differentiation processes. This is not only seen for the cardiac phenotype (*74*, *170*) but also during the specification of other lineages (*184*), representing a broader and fundamental phenomenon.

In the particular context of the application of H9c2 cells in toxicology or pharmacology-oriented projects and in line with the metabolic differences found between parental and differentiated cells our results importantly demonstrated that a proper differentiated state should be used. This is objectively justified by our work

demonstrating the distinct susceptibility that H9c2 parental and differentiated cells have to the same toxicant (*180*).

Subsequent to this first part of the thesis where we stressed the notion of metabolic remodeling during differentiation, a second approach was to understand what would be the outcome of actively modulating metabolism during cell differentiation. Therefore the third chapter of this dissertation is focused on the effects of specific inhibition of mitochondrial complex III by Antimycin A during the course of neuronal differentiation of mouse embryonic stem cells. Our results have shown that, AA is capable of consistently inhibiting neuronal differentiation and most impressively maintained the expression of pluripotency markers in cells cultured for prolonged periods under differentiation-promoting conditions. Previous work from our group also reported the AA capacity to maintain pluripotency in hESC under normal growing conditions (*72*). The observed inhibition is unlikely to be restricted to any specific neural lineage as shown from our results and even though the underlying regulatory mechanism may differ it was also shown by others that AA can inhibit other non-neural differentiation processes such as the cardiac (*74*, *170*).

In our studies, AA treatment reduced proliferation of mESC by interfering with the cell cycle inducing a slight S-phase arrest, but did not induced apoptosis in those cells. We identify a reliable HIF-1α protein level stabilization in mESC downstream the antimycin A treatment in normoxic conditions, what could at least partially account for the results observed in our experiments as hypoxia inducible factors are emerging as regulators of stem cell pluripotency. This HIF-mediated regulation of stemness can be

dually exerted by promoting a metabolic remodeling towards the Warburg effect or remarkably by directly acting on master regulators of pluripotency (*102*).

In an overall perspective the results included in the present thesis substantiate the importance of a coordinated integration of metabolism and cell processes for an adequate supply of cell's requirements and further contribute to the emerging notion that metabolism modulation can be a key instrument that must be further explored to direct stem cells differentiation and maintenance.

Ongoing/Future work.

Even though the insights brought by the reported projects were significant, new questions were also raised, some of which are already being addressed.

Regarding Antimycin A, the exact mechanism underlying the observed effects is still to be identified. From the exposed considerations in chapter I section 1.5.2.1 we find HIF as good candidates to maintain stem cell identity in mESC. We have showed an interesting stabilization of HIF-1α levels downstream the AA treatment. We believe that this effect is dependent upon the ROS produced by Antimycin A at the level of complex III. Following this line we are trying to reverse the observed effects by concomitantly applying antioxidants during the AA treatments. Moreover a more objective understanding of the role of HIF-1α would be gained recurring to specific silencing technologies or strategies to precisely decrease this protein stability, namely with specific pharmacological inhibitors.

It follows that it would similarly be valuable to evaluate the action of other HIFs.

We also observed that AA differently affected cells with distinct developmental maturity. Detailing this effect may offer some hints in possible strategies for selecting pure populations of cells or either synchronizing cultures at determined differentiation stage.

In the context of metabolic adaptation occurring to sustain cell growth, 3 studies using *in vitro* cancer models have recently demonstrated that the non-canonical reductive activity of isocitrate dehydrogenase serves as a shunt to rapidly provide the growing tumor cells with glutamine-derived anaplerotic substrates to replenish the Krebs cycle intermediates used for lipid synthesis (Chapter I section 1.5.1) (*90*–*92*). We believe that similarly to cancer cells this mechanism may be active in embryonic stem cells and we are currently undertaking experiments to answer this.

References

1. K. Hochedlinger, K. Plath, Epigenetic reprogramming and induced pluripotency., *Development* **136**, 509–23 (2009).

2. M. P. De Miguel, S. Fuentes-Julián, Y. Alcaina, Pluripotent stem cells: origin, maintenance and induction., *Stem Cell Rev* **6**, 633–49 (2010).

3. M. Evans, Discovering pluripotency: 30 years of mouse embryonic stem cells., *Nat Rev Mol Cell Biol* **12**, 680–6 (2011).

4. J. Rossant, Stem cells and early lineage development., *Cell* **132**, 527–31 (2008).

5. A. Ralston, J. Rossant, The genetics of induced pluripotency., *Reproduction* **139**, 35–44 (2010).

6. J. a Thomson *et al.*, Embryonic stem cell lines derived from human blastocysts., *Science* **282**, 1145–7 (1998).

7. L. C. Stevens, C. C. Little, Spontaneous Testicular Teratomas in an Inbred Strain of Mice., *Proc Natl Acad Sci U S A* **40**, 1080–7 (1954).

8. L. J. Kleinsmith, G. B. Pierce, Multipotentiality of single embryonal carcinoma cells., *Cancer Res* **24**, 1544–51 (1964).

9. D. Solter, From teratocarcinomas to embryonic stem cells and beyond: a history of embryonic stem cell research., *Nat Rev Genet* **7**, 319–27 (2006).

10. G. R. Martin, Isolation of a pluripotent cell line from early mouse embryos cultured in medium conditioned by teratocarcinoma stem cells., *Proc Natl Acad Sci U S A* **78**, 7634–8 (1981).

11. M. J. Evans, M. H. Kaufman, Establishment in culture of pluripotential cells from mouse embryos., *Nature* **292**, 154–6 (1981).

12. K. Takahashi, S. Yamanaka, Induction of pluripotent stem cells from mouse embryonic and adult fibroblast cultures by defined factors., *Cell* **126**, 663–76 (2006).

13. K. P. Smith, M. X. Luong, G. S. Stein, Pluripotency: toward a gold standard for human ES and iPS cells., *J Cell Physiol* **220**, 21–9 (2009).

14. A. R. Bahrami, M. M. Matin, P. W. Andrews, The CDK inhibitor p27 enhances neural differentiation in pluripotent NTERA2 human EC cells, but does not permit differentiation of 2102Ep nullipotent human EC cells., *Mech Dev* **122**, 1034–42 (2005).

15. P. J. Donovan, M. P. de Miguel, Turning germ cells into stem cells, *Current Opinion in Genetics & Development* **13**, 463–471 (2003).

16. J. Nichols, A. Smith, Naive and primed pluripotent states., *Cell Stem Cell* **4**, 487–92 (2009).

17. C. J. Lengner *et al.*, Derivation of pre-X inactivation human embryonic stem cells under physiological oxygen concentrations., *Cell* **141**, 872–83 (2010).

18. H. Hirai, P. Karian, N. Kikyo, Regulation of embryonic stem cell self-renewal and pluripotency by leukaemia inhibitory factor., *Biochem J* **438**, 11–23 (2011).

19. S. Ohtsuka, S. Dalton, Molecular and biological properties of pluripotent embryonic stem cells., *Gene Ther* **15**, 74–81 (2008).

20. R.-H. Xu *et al.*, BMP4 initiates human embryonic stem cell differentiation to trophoblast., *Nat Biotechnol* **20**, 1261–4 (2002).

21. L. Eiselleova *et al.*, Comparative study of mouse and human feeder cells for human embryonic stem cells., *Int J Dev Biol* **52**, 353–63 (2008).

22. P. J. Tesar *et al.*, New cell lines from mouse epiblast share defining features with human embryonic stem cells., *Nature* **448**, 196–9 (2007).

23. A. De Los Angeles, Y.-H. Loh, P. J. Tesar, G. Q. Daley, Accessing naïve human pluripotency., *Curr Opin Genet Dev* **22**, 272–82 (2012).

24. F. Soldner *et al.*, Parkinson's disease patient-derived induced pluripotent stem cells free of viral reprogramming factors., *Cell* **136**, 964–77 (2009).

25. K. Okita, T. Ichisaka, S. Yamanaka, Generation of germline-competent induced pluripotent stem cells., *Nature* **448**, 313–7 (2007).

26. I. Chambers, S. R. Tomlinson, The transcriptional foundation of pluripotency., *Development* **136**, 2311–22 (2009).

27. J. Nichols *et al.*, Formation of pluripotent stem cells in the mammalian embryo depends on the POU transcription factor Oct4., *Cell* **95**, 379–91 (1998).

28. H. Niwa, J. Miyazaki, a G. Smith, Quantitative expression of Oct-3/4 defines differentiation, dedifferentiation or self-renewal of ES cells., *Nat Genet* **24**, 372–6 (2000).

29. H. Niwa, How is pluripotency determined and maintained?, *Development* **134**, 635–46 (2007).

30. A. a Avilion *et al.*, Multipotent cell lineages in early mouse development depend on SOX2 function., *Genes Dev* **17**, 126–40 (2003).

31. S. Masui *et al.*, Pluripotency governed by Sox2 via regulation of Oct3/4 expression in mouse embryonic stem cells., *Nat Cell Biol* **9**, 625–35 (2007).

32. K. Mitsui *et al.*, The homeoprotein Nanog is required for maintenance of pluripotency in mouse epiblast and ES cells., *Cell* **113**, 631–42 (2003).

33. I. Chambers *et al.*, Functional expression cloning of Nanog, a pluripotency sustaining factor in embryonic stem cells., *Cell* **113**, 643–55 (2003).

34. Y.-H. Loh *et al.*, The Oct4 and Nanog transcription network regulates pluripotency in mouse embryonic stem cells., *Nat Genet* **38**, 431–40 (2006).

35. L. A. Boyer *et al.*, Core transcriptional regulatory circuitry in human embryonic stem cells., *Cell* **122**, 947–56 (2005).

36. J.-C. Yeo, H.-H. Ng, The transcriptional regulation of pluripotency., *Cell Res* **23**, 20–32 (2013).

37. J. Kim, J. Chu, X. Shen, J. Wang, S. H. Orkin, An extended transcriptional network for pluripotency of embryonic stem cells., *Cell* **132**, 1049–61 (2008).

38. X. Chen *et al.*, Integration of external signaling pathways with the core transcriptional network in embryonic stem cells., *Cell* **133**, 1106–17 (2008).

39. T. Vellai, G. Vida, The origin of eukaryotes: the difference between prokaryotic and eukaryotic cells., *Proc Biol Sci* **266**, 1571–7 (1999).

40. D. G. Searcy, Metabolic integration during the evolutionary origin of mitochondria., *Cell Res* **13**, 229–38 (2003).

41. M. W. Gray, G. Burger, B. F. Lang, The origin and early evolution of mitochondria., *Genome Biol* **2**, REVIEWS1018 (2001).

42. B. Alberts *et al.*, Energy Conversion: Mitochondria and Chloroplasts (2002).

43. M. Zick, R. Rabl, A. S. Reichert, Cristae formation-linking ultrastructure and function of mitochondria., *Biochim Biophys Acta* **1793**, 5–19 (2009).

44. I. E. Scheffler, Mitochondria make a come back., *Adv Drug Deliv Rev* **49**, 3–26 (2001).

45. C. a Mannella, Introduction: our changing views of mitochondria., *J Bioenerg Biomembr* **32**, 1–4 (2000).

46. J. Ramalho-Santos *et al.*, Mitochondrial functionality in reproduction: from gonads and gametes to embryos and embryonic stem cells., *Hum Reprod Update* **15**, 553–72 (2009).

47. R. C. Scarpulla, Transcriptional paradigms in mammalian mitochondrial biogenesis and function., *Physiol Rev* **88**, 611–38 (2008).

48. D. a Clayton, Vertebrate mitochondrial DNA-a circle of surprises., *Exp Cell Res* **255**, 4–9 (2000).

49. L. Ernster, G. Schatz, Mitochondria: a historical review., *J Cell Biol* **91**, 227s–255s (1981).

50. S. Rousset *et al.*, The biology of mitochondrial uncoupling proteins., *Diabetes* **53 Suppl 1**, S130–5 (2004).

51. C. H. Verhees *et al.*, The unique features of glycolytic pathways in Archaea., *Biochem J* **375**, 231–46 (2003).

52. D. Nelson, M. Cox, Lehninger principles of biochemistry, (2008).

53. G. C. Brown, V. Borutaite, There is no evidence that mitochondria are the main source of reactive oxygen species in mammalian cells., *Mitochondrion* **12**, 1–4 (2012).

54. M. P. Murphy, How mitochondria produce reactive oxygen species., *Biochem J* **417**, 1–13 (2009).

55. K. Wallace, Free radical toxicology, (1997).

56. T. Finkel, N. J. Holbrook, Oxidants, oxidative stress and the biology of ageing., *Nature* **408**, 239–47 (2000).

57. M. Forkink, J. a M. Smeitink, R. Brock, P. H. G. M. Willems, W. J. H. Koopman, Detection and manipulation of mitochondrial reactive oxygen species in mammalian cells., *Biochim Biophys Acta* **1797**, 1034–44 (2010).

58. A. J. Kowaltowski, N. C. de Souza-Pinto, R. F. Castilho, A. E. Vercesi, Mitochondria and reactive oxygen species., *Free Radic Biol Med* **47**, 333–43 (2009).

59. T. V Votyakova, I. J. Reynolds, DeltaPsi(m)-Dependent and -independent production of reactive oxygen species by rat brain mitochondria., *J Neurochem* **79**, 266–77 (2001).

60. M. A. Aon, S. Cortassa, B. O'Rourke, Redox-optimized ROS balance: a unifying hypothesis., *Biochim Biophys Acta* **1797**, 865–77 (2011).

61. J. F. Turrens, Mitochondrial formation of reactive oxygen species., *J Physiol* **552**, 335–44 (2003).

62. R. D. Guzy, P. T. Schumacker, Oxygen sensing by mitochondria at complex III: the paradox of increased reactive oxygen species during hypoxia., *Exp Physiol* **91**, 807–19 (2006).

63. P. S. Brookes, Mitochondrial H(+) leak and ROS generation: an odd couple., *Free Radic Biol Med* **38**, 12–23 (2005).

64. R. F. Feissner, J. Skalska, W. E. Gaum, S.-S. Sheu, Crosstalk signaling between mitochondrial Ca2+ and ROS., *Front Biosci* **14**, 1197–218 (2009).

65. a Y. Andreyev, Y. E. Kushnareva, a a Starkov, Mitochondrial metabolism of reactive oxygen species., *Biochemistry. Biokhimiia* **70**, 200–14 (2005).

66. O. Warburg, On the origin of cancer cells., *Science* **123**, 309–14 (1956).

67. D. Bonnet, J. E. Dick, Human acute myeloid leukemia is organized as a hierarchy that originates from a primitive hematopoietic cell., *Nat Med* **3**, 730–7 (1997).

68. J. C. Y. Wang, J. E. Dick, Cancer stem cells: lessons from leukemia., *Trends Cell Biol* **15**, 494–501 (2005).

69. T. Reya, S. J. Morrison, M. F. Clarke, I. L. Weissman, Stem cells, cancer, and cancer stem cells., *Nature* **414**, 105–11 (2001).

70. S. Varum *et al.*, Energy metabolism in human pluripotent stem cells and their differentiated counterparts., *PLoS One* **6**, e20914 (2011).

71. S. Chung, D. K. Arrell, R. S. Faustino, A. Terzic, P. P. Dzeja, Glycolytic network restructuring integral to the energetics of embryonic stem cell cardiac differentiation., *J Mol Cell Cardiol* **48**, 725–34 (2010).

72. S. Varum *et al.*, Enhancement of human embryonic stem cell pluripotency through inhibition of the mitochondrial respiratory chain., *Stem Cell Res* **3**, 142–56.

73. S. Mandal, A. G. Lindgren, A. S. Srivastava, A. T. Clark, U. Banerjee, Mitochondrial function controls proliferation and early differentiation potential of embryonic stem cells., *Stem Cells* **29**, 486–95 (2011).

74. D. Spitkovsky *et al.*, Activity of complex III of the mitochondrial electron transport chain is essential for early heart muscle cell differentiation., *FASEB journal : official publication of the Federation of American Societies for Experimental Biology* **18**, 1300–2 (2004).

75. C. D. L. Folmes *et al.*, Somatic oxidative bioenergetics transitions into pluripotency-dependent glycolysis to facilitate nuclear reprogramming., *Cell Metab* **14**, 264–71 (2011).

76. C. D. L. Folmes, T. J. Nelson, A. Terzic, Energy metabolism in nuclear reprogramming., *Biomark Med* **5**, 715–29 (2011).

77. H. Kondoh *et al.*, Glycolytic enzymes can modulate cellular life span., *Cancer Res* **65**, 177–85 (2005).

78. M. G. Vander Heiden, L. C. Cantley, C. B. Thompson, Understanding the Warburg effect: the metabolic requirements of cell proliferation., *Science* **324**, 1029–33 (2009).

79. O. Feron, Pyruvate into lactate and back: from the Warburg effect to symbiotic energy fuel exchange in cancer cells., *Radiother Oncol* **92**, 329–33 (2009).

80. H. Kondoh, M. E. Lleonart, J. Gil, D. Beach, G. Peters, Glycolysis and cellular immortalization, *Drug Discovery Today: Disease Mechanisms* **2**, 263–267 (2005).

81. H. Y. Ho *et al.*, Enhanced oxidative stress and accelerated cellular senescence in glucose-6-phosphate dehydrogenase (G6PD)-deficient human fibroblasts., *Free Radic Biol Med* **29**, 156–69 (2000).

82. K. E. Wellen *et al.*, The hexosamine biosynthetic pathway couples growth factor-induced glutamine uptake to glucose metabolism., *Genes Dev* **24**, 2784–99 (2010).

83. S. L. Pereira *et al.*, Metabolic remodeling during H9c2 myoblast differentiation: relevance for i*n vitro* toxicity studies., *Cardiovasc Toxicol* **11**, 180–90 (2011).

84. L. Stryer, Biochemistry , *New York* (1995) (available at http://scholar.google.pt/scholar?hl=en&q=stryer+biochemistry&btnG=&as_sdt=1%2C5&as_sdtp=#1).

85. N. M. Vacanti, C. M. Metallo, Exploring metabolic pathways that contribute to the stem cell phenotype., *Biochim Biophys Acta* **1830**, 2361–9 (2013).

86. J. W. Locasale *et al.*, Phosphoglycerate dehydrogenase diverts glycolytic flux and contributes to oncogenesis., *Nat Genet* **43**, 869–74 (2011).

87. R. J. DeBerardinis *et al.*, Beyond aerobic glycolysis: transformed cells can engage in glutamine metabolism that exceeds the requirement for protein and nucleotide synthesis., *Proc Natl Acad Sci U S A* **104**, 19345–50 (2007).

88. G. Hatzivassiliou *et al.*, ATP citrate lyase inhibition can suppress tumor cell growth., *Cancer Cell* **8**, 311–21 (2005).

89. T. G. Fernandes, A. M. Fernandes-Platzgummer, C. L. da Silva, M. M. Diogo, J. M. S. Cabral, Kinetic and metabolic analysis of mouse embryonic stem cell expansion under serum-free conditions., *Biotechnol Lett* **32**, 171–9 (2010).

90. A. R. Mullen *et al.*, Reductive carboxylation supports growth in tumour cells with defective mitochondria., *Nature* **481**, 385–8 (2012).

91. C. M. Metallo *et al.*, Reductive glutamine metabolism by IDH1 mediates lipogenesis under hypoxia., *Nature* **481**, 380–4 (2012).

92. D. R. Wise *et al.*, Hypoxia promotes isocitrate dehydrogenase-dependent carboxylation of α-ketoglutarate to citrate to support cell growth and viability., *Proc Natl Acad Sci U S A* **108**, 19611–6 (2011).

93. G. L. Semenza, Defining the role of hypoxia-inducible factor 1 in cancer biology and therapeutics., *Oncogene* **29**, 625–34 (2010).

94. I. A. Barbosa, N. G. Machado, A. J. Skildum, P. M. Scott, P. J. Oliveira, Mitochondrial remodeling in cancer metabolism and survival: potential for new therapies., *Biochim Biophys Acta* **1826**, 238–54 (2012).

95. X. Xia *et al.*, Integrative analysis of HIF binding and transactivation reveals its role in maintaining histone methylation homeostasis., *Proc Natl Acad Sci U S A* **106**, 4260–5 (2009).

96. J. Kim, I. Tchernyshyov, G. L. Semenza, C. V Dang, HIF-1-mediated expression of pyruvate dehydrogenase kinase: a metabolic switch required for cellular adaptation to hypoxia., *Cell Metab* **3**, 177–85 (2006).

97. I. Papandreou, R. a Cairns, L. Fontana, A. L. Lim, N. C. Denko, HIF-1 mediates adaptation to hypoxia by actively downregulating mitochondrial oxygen consumption., *Cell Metab* **3**, 187–97 (2006).

98. H. Kondoh, Cellular life span and the Warburg effect., *Exp Cell Res* **314**, 1923–8 (2008).

99. A. Mohyeldin, T. Garzón-Muvdi, A. Quiñones-Hinojosa, Oxygen in stem cell biology: a critical component of the stem cell niche., *Cell Stem Cell* **7**, 150–61 (2010).

100. V. Moreno-Manzano *et al.*, FM19G11, a new hypoxia-inducible factor (HIF) modulator, affects stem cell differentiation status., *J Biol Chem* **285**, 1333–42 (2010).

101. C. E. Forristal, K. L. Wright, N. a Hanley, R. O. C. Oreffo, F. D. Houghton, Hypoxia inducible factors regulate pluripotency and proliferation in human embryonic stem cells cultured at reduced oxygen tensions., *Reproduction* **139**, 85–97 (2010).

102. K. L. Covello *et al.*, HIF-2alpha regulates Oct-4: effects of hypoxia on stem cell function, embryonic development, and tumor growth., *Genes Dev* **20**, 557–70 (2006).

103. C. Hu *et al.*, Differential regulation of the transcriptional activities of hypoxia-inducible factor 1 alpha (HIF-1alpha) and HIF-2alpha in stem cells., *Mol Cell Biol* **26**, 3514–26 (2006).

104. E. Laurenti, A. Wilson, A. Trumpp, Myc's other life: stem cells and beyond., *Curr Opin Cell Biol* **21**, 844–54 (2009).

105. P. Cartwright *et al.*, LIF/STAT3 controls ES cell self-renewal and pluripotency by a Myc-dependent mechanism., *Development* **132**, 885–96 (2005).

106. C. V Dang, Rethinking the Warburg effect with Myc micromanaging glutamine metabolism., *Cancer Res* **70**, 859–62 (2010).

107. I. Samudio, M. Fiegl, M. Andreeff, Mitochondrial uncoupling and the Warburg effect: molecular basis for the reprogramming of cancer cell metabolism., *Cancer Res* **69**, 2163–6 (2009).

108. I. Samudio, M. Fiegl, T. McQueen, K. Clise-Dwyer, M. Andreeff, The warburg effect in leukemia-stroma cocultures is mediated by mitochondrial uncoupling associated with uncoupling protein 2 activation., *Cancer Res* **68**, 5198–205 (2008).

109. J. Zhang *et al.*, UCP2 regulates energy metabolism and differentiation potential of human pluripotent stem cells., *EMBO J* **30**, 4860–73 (2011).

110. G. L. Semenza, HIF-1: upstream and downstream of cancer metabolism., *Curr Opin Genet Dev* **20**, 51–6 (2010).

111. H. Lu, R. a Forbes, A. Verma, Hypoxia-inducible factor 1 activation by aerobic glycolysis implicates the Warburg effect in carcinogenesis., *J Biol Chem* **277**, 23111–5 (2002).

112. R. a Gatenby, R. J. Gillies, Glycolysis in cancer: a potential target for therapy., *Int J Biochem Cell Biol* **39**, 1358–66 (2007).

113. T. McFate *et al.*, Pyruvate dehydrogenase complex activity controls metabolic and malignant phenotype in cancer cells., *J Biol Chem* **283**, 22700–8 (2008).

114. C. M. Metallo, M. G. Vander Heiden, Metabolism strikes back: metabolic flux regulates cell signaling., *Genes Dev* **24**, 2717–22 (2010).

115. P. Madiraju, S. V Pande, M. Prentki, S. R. M. Madiraju, Mitochondrial acetylcarnitine provides acetyl groups for nuclear histone acetylation., *Epigenetics* **4**, 399–403 (2009).

116. M. J. Hitchler, F. E. Domann, Redox regulation of the epigenetic landscape in cancer: a role for metabolic reprogramming in remodeling the epigenome., *Free Radic Biol Med* **53**, 2178–87 (2012).

117. M. J. Hitchler, F. E. Domann, An epigenetic perspective on the free radical theory of development., *Free Radic Biol Med* **43**, 1023–36 (2007).

118. V. A. Sardao, P. J. Oliveira, J. Holy, C. R. Oliveira, K. B. Wallace, Doxorubicin-induced mitochondrial dysfunction is secondary to nuclear p53 activation in H9c2 cardiomyoblasts, *Cancer Chemother Pharmacol* **64**, 811–827 (2009).

119. V. A. Sardão, P. J. Oliveira, J. Holy, C. R. Oliveira, K. B. Wallace, Vital imaging of H9c2 myoblasts exposed to tert-butylhydroperoxide--characterization of morphological features of cell death., *BMC Cell Biol* **8**, 11 (2007).

120. J. P. Silva, V. A. Sardão, O. P. Coutinho, P. J. Oliveira, P. J. Olveira, Nitrogen compounds prevent h9c2 myoblast oxidative stress-induced mitochondrial dysfunction and cell death., *Cardiovasc Toxicol* **10**, 51–65 (2010).

121. Z. Liu *et al.*, Protective effect of chrysoeriol against doxorubicin-induced cardiotoxicity *in vitro*, *Chin Med J (Engl)* **122**, 2652–2656 (2009).

122. A. Cselenyák, E. Pankotai, E. M. Horváth, L. Kiss, Z. Lacza, Mesenchymal stem cells rescue cardiomyoblasts from cell death in an in vitro ischemia model via direct cell-to-cell connections., *BMC Cell Biol* **11**, 29 (2010).

123. J. C. S. T. John *et al.*, The expression of mitochondrial DNA transcription factors during early cardiomyocyte *in vitro* differentiation from human embryonic stem cells., *Cloning Stem Cells* **7**, 141–53 (2005).

124. T. Brand, Heart development: molecular insights into cardiac specification and early morphogenesis., *Dev Biol* **258**, 1–19 (2003).

125. J. J. Lehman, D. P. Kelly, Gene regulatory mechanisms governing energy metabolism during cardiac hypertrophic growth, *Heart Fail Rev* **7**, 175–185 (2002).

126. J. J. Lehman, D. P. Kelly, Transcriptional activation of energy metabolic switches in the developing and hypertrophied heart., *Clin Exp Pharmacol Physiol* **29**, 339–45 (2002).

127. A. O. Makinde, P. F. Kantor, G. D. Lopaschuk, Maturation of fatty acid and carbohydrate metabolism in the newborn heart, *Mol Cell Biochem* **188**, 49–56 (1998).

128. G. D. Lopaschuk, J. S. Jaswal, Energy metabolic phenotype of the cardiomyocyte during development, differentiation, and postnatal maturation, *J Cardiovasc Pharmacol* **56**, 130–140 (2010).

129. D. J. Fisher, M. A. Heymann, A. M. Rudolph, Myocardial consumption of oxygen and carbohydrates in newborn sheep, *Pediatr Res* **15**, 843–846 (1981).

130. J. C. Werner, R. E. Sicard, Lactate metabolism of isolated, perfused fetal, and newborn pig hearts., *Pediatr Res* **22**, 552–6 (1987).

131. J. Girard, P. Ferré, J. P. Pégorier, P. H. Duée, Adaptations of glucose and fatty acid metabolism during perinatal period and suckling-weaning transition., *Physiol Rev* **72**, 507–62 (1992).

132. G. D. Lopaschuk, M. A. Spafford, D. R. Marsh, Glycolysis is predominant source of myocardial ATP production immediately after birth, *Am J Physiol* **261**, H1698–705 (1991).

133. P. Ferré, J. F. Decaux, T. Issad, J. Girard, Changes in energy metabolism during the suckling and weaning period in the newborn., *Reprod Nutr Dev* **26**, 619–31 (1986).

134. H. Taegtmeyer, Energy metabolism of the heart: from basic concepts to clinical applications., *Curr Probl Cardiol* **19**, 59–113 (1994).

135. B. W. Kimes, B. L. Brandt, Properties of a clonal muscle cell line from rat heart., *Exp Cell Res* **98**, 367–81 (1976).

136. M. Pagano *et al.*, Differentiation of H9c2 cardiomyoblasts: The role of adenylate cyclase system., *J Cell Physiol* **198**, 408–16 (2004).

137. R. Saeedi *et al.*, AMP-activated protein kinase influences metabolic remodeling in H9c2 cells hypertrophied by arginine vasopressin., *Am J Physiol Heart Circ Physiol* **296**, H1822–32 (2009).

138. V. A. Sardão, P. J. Oliveira, J. Holy, C. R. Oliveira, K. B. Wallace, Morphological alterations induced by doxorubicin on H9c2 myoblasts: nuclear, mitochondrial, and cytoskeletal targets., *Cell Biol Toxicol* **25**, 227–43 (2009).

139. P. Mukhopadhyay *et al.*, Role of superoxide, nitric oxide, and peroxynitrite in doxorubicin-induced cell death in vivo and *in vitro*., *Am J Physiol Heart Circ Physiol* **296**, H1466–83 (2009).

140. C. Ménard *et al.*, Modulation of L-type calcium channel expression during retinoic acid-induced differentiation of H9C2 cardiac cells., *J Biol Chem* **274**, 29063–70 (1999).

141. A. P. Rolo, C. M. Palmeira, G. A. Cortopassi, Biosensor plates detect mitochondrial physiological regulators and mutations in vivo., *Anal Biochem* **385**, 176–8 (2009).

142. W.-S. Choi, S. E. Kruse, R. D. Palmiter, Z. Xia, Mitochondrial complex I inhibition is not required for dopaminergic neuron death induced by rotenone, MPP+, or paraquat., *Proc Natl Acad Sci U S A* **105**, 15136–41 (2008).

143. R. E. Swiderski, M. Solursh, Precocious appearance of cardiac troponin T pre-mRNAs during early avian embryonic skeletal muscle development in ovo., *Dev Biol* **140**, 73–82 (1990).

144. K.-M. Ng *et al.*, Exogenous expression of HIF-1 alpha promotes cardiac differentiation of embryonic stem cells., *J Mol Cell Cardiol* **48**, 1129–37 (2010).

145. E. Bettiol *et al.*, Fetal bovine serum enables cardiac differentiation of human embryonic stem cells., *Differentiation* **75**, 669–81 (2007).

146. M. Leu, E. Ehler, J. C. Perriard, Characterisation of postnatal growth of the murine heart, *Anat Embryol (Berl)* **204**, 217–224 (2001).

147. B. Künnecke, S. Cerdan, Multilabeled 13C substrates as probes in in vivo 13C and 1H NMR spectroscopy., *NMR Biomed* **2**, 274–7 (1989).

148. J. M. Facucho-Oliveira, J. C. St John, The relationship between pluripotency and mitochondrial DNA proliferation during early embryo development and embryonic stem cell differentiation., *Stem Cell Rev* **5**, 140–58 (2009).

149. S. P. Mathupala, Y. H. Ko, P. L. Pedersen, The pivotal roles of mitochondria in cancer: Warburg and beyond and encouraging prospects for effective therapies, *Biochim Biophys Acta* **1797**, 1225–1230 (2010).

150. U. Sonnewald, A. Schousboe, H. Qu, H. S. Waagepetersen, Intracellular metabolic compartmentation assessed by 13C magnetic resonance spectroscopy., *Neurochem Int* **45**, 305–10 (2004).

151. E. Olstad, H. Qu, U. Sonnewald, Glutamate is preferred over glutamine for intermediary metabolism in cultured cerebellar neurons., *J Cereb Blood Flow Metab* **27**, 811–20 (2007).

152. N. Anousis, R. A. Carvalho, P. Zhao, C. R. Malloy, A. D. Sherry, Compartmentation of glycolysis and glycogenolysis in the perfused rat heart., *NMR Biomed* **17**, 51–9 (2004).

153. A. L. Bracha, A. Ramanathan, S. Huang, D. E. Ingber, S. L. Schreiber, Carbon metabolism-mediated myogenic differentiation., *Nat Chem Biol* **6**, 202–204 (2010).

154. P. S. Green, C. Leeuwenburgh, Mitochondrial dysfunction is an early indicator of doxorubicin-induced apoptosis., *Biochim Biophys Acta* **1588**, 94–101 (2002).

155. T. Lonergan, B. Bavister, C. Brenner, Mitochondria in stem cells., *Mitochondrion* **7**, 289–96 (2007).

156. G. C. Parker, G. Acsadi, C. a Brenner, Mitochondria: determinants of stem cell fate?, *Stem Cells Dev* **18**, 803–6 (2009).

157. C. Nesti, L. Pasquali, F. Vaglini, G. Siciliano, L. Murri, The role of mitochondria in stem cell biology., *Biosci Rep* **27**, 165–71 (2007).

158. S. M. Schieke *et al.*, Mitochondrial metabolism modulates differentiation and teratoma formation capacity in mouse embryonic stem cells., *J Biol Chem* **283**, 28506–12 (2008).

159. B. Fischer, B. D. Bavister, Oxygen tension in the oviduct and uterus of rhesus monkeys, hamsters and rabbits., *J Reprod Fertil* **99**, 673–9 (1993).

160. H. Kondoh *et al.*, A High Glycolytic Flux Supports the Proliferative Potential of Murine Embryonic Stem Cells, *Antioxidants & Redox Signaling* **9**, 293–299 (2007).

161. T. Ezashi, P. Das, R. M. Roberts, Low O2 tensions and the prevention of differentiation of hES cells., *Proc Natl Acad Sci U S A* **102**, 4783–8 (2005).

162. A. Prigione, J. Adjaye, Modulation of mitochondrial biogenesis and bioenergetic metabolism upon *in vitro* and in vivo differentiation of human ES and iPS cells., *Int J Dev Biol* **54**, 1729–41 (2010).

163. L. Armstrong *et al.*, Human induced pluripotent stem cell lines show stress defense mechanisms and mitochondrial regulation similar to those of human embryonic stem cells., *Stem Cells* **28**, 661–73 (2010).

164. S. T. Suhr *et al.*, Mitochondrial rejuvenation after induced pluripotency., *PLoS One* **5**, e14095 (2010).

165. Y. Yoshida, K. Takahashi, K. Okita, T. Ichisaka, S. Yamanaka, Hypoxia enhances the generation of induced pluripotent stem cells., *Cell Stem Cell* **5**, 237–41 (2009).

166. C.-T. Chen, S.-H. Hsu, Y.-H. Wei, Upregulation of mitochondrial function and antioxidant defense in the differentiation of stem cells., *Biochim Biophys Acta* **1800**, 257–63 (2010).

167. D. K. Barnett, J. Kimura, B. D. Bavister, Translocation of active mitochondria during hamster preimplantation embryo development studied by confocal laser scanning microscopy., *Dev Dyn* **205**, 64–72 (1996).

168. T. Lonergan, C. Brenner, B. Bavister, Differentiation-related changes in mitochondrial properties as indicators of stem cell competence., *J Cell Physiol* **208**, 149–53 (2006).

169. Y. M. Cho *et al.*, Dynamic changes in mitochondrial biogenesis and antioxidant enzymes during the spontaneous differentiation of human embryonic stem cells., *Biochem Biophys Res Commun* **348**, 1472–8 (2006).

170. S. Chung *et al.*, Mitochondrial oxidative metabolism is required for the cardiac differentiation of stem cells., *Nat Clin Pract Cardiovasc Med* **4 Suppl 1**, S60–7 (2007).

171. J. M. Facucho-Oliveira, J. Alderson, E. C. Spikings, S. Egginton, J. C. St John, Mitochondrial DNA replication during differentiation of murine embryonic stem cells., *J Cell Sci* **120**, 4025–34 (2007).

172. M. J. Birket *et al.*, A reduction in ATP demand and mitochondrial activity with neural differentiation of human embryonic stem cells., *J Cell Sci* **124**, 348–58 (2011).

173. D. M. Kirby *et al.*, Transmitochondrial embryonic stem cells containing pathogenic mtDNA mutations are compromised in neuronal differentiation., *Cell Prolif* **42**, 413–24 (2009).

174. J. L. Vayssière *et al.*, Participation of the mitochondrial genome in the differentiation of neuroblastoma cells., *In Vitro Cell Dev Biol* **28A**, 763–72 (1992).

175. T. Barberi *et al.*, Neural subtype specification of fertilization and nuclear transfer embryonic stem cells and application in parkinsonian mice., *Nat Biotechnol* **21**, 1200–7 (2003).

176. H. Kawasaki *et al.*, Induction of midbrain dopaminergic neurons from ES cells by stromal cell-derived inducing activity., *Neuron* **28**, 31–40 (2000).

177. L. Cajánek *et al.*, Wnt/beta-catenin signaling blockade promotes neuronal induction and dopaminergic differentiation in embryonic stem cells., *Stem Cells* **27**, 2917–27 (2009).

178. Q.-L. Ying, M. Stavridis, D. Griffiths, M. Li, A. Smith, Conversion of embryonic stem cells into neuroectodermal precursors in adherent monoculture., *Nat Biotechnol* **21**, 183–6 (2003).

179. D. Parnas, M. Linial, Highly sensitive ELISA-based assay for quantifying protein levels in neuronal cultures., *Brain Res Brain Res Protoc* **2**, 333–8 (1998).

180. A. F. Branco *et al.*, Isoproterenol cytotoxicity is dependent on the differentiation state of the cardiomyoblast H9c2 cell line., *Cardiovasc Toxicol* **11**, 191–203 (2011).

181. S. Amaral, A. J. Moreno, M. S. Santos, R. Seiça, J. Ramalho-Santos, Effects of hyperglycemia on sperm and testicular cells of Goto-Kakizaki and streptozotocin-treated rat models for diabetes., *Theriogenology* **66**, 2056–67 (2006).

182. S. C. Correia *et al.*, Cyanide preconditioning protects brain endothelial and NT2 neuron-like cells against glucotoxicity: Role of mitochondrial reactive oxygen species and HIF-1α, *Neurobiology of Disease* **45**, 206–218 (2012).

183. N. S. Chandel *et al.*, Reactive oxygen species generated at mitochondrial complex III stabilize hypoxia-inducible factor-1alpha during hypoxia: a mechanism of O2 sensing., *J Biol Chem* **275**, 25130–8 (2000).

184. C.-T. Chen, S.-H. Hsu, Y.-H. Wei, Mitochondrial bioenergetic function and metabolic plasticity in stem cell differentiation and cellular reprogramming., *Biochim Biophys Acta* **1820**, 1–6 (2011).

185. S. Papa *et al.*, Respiratory complex I in brain development and genetic disease., *Neurochem Res* **29**, 547–60 (2004).

186. A. Carrière *et al.*, Mitochondrial reactive oxygen species control the transcription factor CHOP-10/GADD153 and adipocyte differentiation: a mechanism for hypoxia-dependent effect., *J Biol Chem* **279**, 40462–9 (2004).

187. Y. H. Han, S. H. Kim, S. Z. Kim, W. H. Park, Antimycin A as a mitochondria damage agent induces an S phase arrest of the cell cycle in HeLa cells., *Life Sci* **83**, 346–55 (2008).

188. Y. H. Han, S. H. Kim, S. Z. Kim, W. H. Park, Antimycin A as a mitochondrial electron transport inhibitor prevents the growth of human lung cancer A549 cells., *Oncol Rep* **20**, 689–93 (2008).

189. Y. H. Han, W. H. Park, Growth inhibition in antimycin A treated-lung cancer Calu-6 cells via inducing a G1 phase arrest and apoptosis., *Lung Cancer* **65**, 150–60 (2009).

190. F. I. Ataullakhanov, V. M. Vitvitsky, What determines the intracellular ATP concentration., *Biosci Rep* **22**, 501–11 (2002).

191. G. R. Steinberg, B. E. Kemp, AMPK in Health and Disease., *Physiol Rev* **89**, 1025–78 (2009).

192. H. Byun, H. Y. Kim, J. J. Lim, Y. Seo, G. Yoon, Mitochondrial dysfunction by complex II inhibition delays overall cell cycle progression via reactive oxygen species production., *J Cell Biochem* **104**, 1747–59 (2008).

193. D. R. Evans, H. I. Guy, Mammalian pyrimidine biosynthesis: fresh insights into an ancient pathway., *J Biol Chem* **279**, 33035–8 (2004).

194. C.-T. Chen, Y.-R. V Shih, T. K. Kuo, O. K. Lee, Y.-H. Wei, Coordinated changes of mitochondrial biogenesis and antioxidant enzymes during osteogenic differentiation of human mesenchymal stem cells., *Stem Cells* **26**, 960–8 (2008).

195. N. S. Chandel *et al.*, Mitochondrial reactive oxygen species trigger hypoxia-induced transcription., *Proc Natl Acad Sci U S A* **95**, 11715–20 (1998).

196. M. Comelli *et al.*, Cardiac differentiation promotes mitochondria development and ameliorates oxidative capacity in H9c2 cardiomyoblasts., *Mitochondrion* **11**, 315–26 (2011).